University of Alberta

Mapping and characterization of genetic susceptibility factors for exencephaly in *Cecr2*^{Gt45Bic} mutant mice

by

Courtney Ella Davidson ©

A thesis submitted to the Faculty of Graduate Studies and Research
in partial fulfillment of the requirements for the degree of

Master of Science
in
Molecular Biology and Genetics

Department of Biological Sciences

Edmonton, Alberta
Fall 2006

Library and
Archives Canada

Published Heritage
Branch

395 Wellington Street
Ottawa ON K1A 0N4
Canada

Bibliothèque et
Archives Canada

Direction du
Patrimoine de l'édition

395, rue Wellington
Ottawa ON K1A 0N4
Canada

Your file Votre référence
ISBN: 978-0-494-22247-8
Our file Notre référence
ISBN: 978-0-494-22247-8

NOTICE:
The author has granted a non-exclusive license allowing Library and Archives Canada to reproduce, publish, archive, preserve, conserve, communicate to the public by telecommunication or on the Internet, loan, distribute and sell theses worldwide, for commercial or non-commercial purposes, in microform, paper, electronic and/or any other formats.

The author retains copyright ownership and moral rights in this thesis. Neither the thesis nor substantial extracts from it may be printed or otherwise reproduced without the author's permission.

AVIS:
L'auteur a accordé une licence non exclusive permettant à la Bibliothèque et Archives Canada de reproduire, publier, archiver, sauvegarder, conserver, transmettre au public par télécommunication ou par l'Internet, prêter, distribuer et vendre des thèses partout dans le monde, à des fins commerciales ou autres, sur support microforme, papier, électronique et/ou autres formats.

L'auteur conserve la propriété du droit d'auteur et des droits moraux qui protège cette thèse. Ni la thèse ni des extraits substantiels de celle-ci ne doivent être imprimés ou autrement reproduits sans son autorisation.

In compliance with the Canadian Privacy Act some supporting forms may have been removed from this thesis.

While these forms may be included in the document page count, their removal does not represent any loss of content from the thesis.

Conformément à la loi canadienne sur la protection de la vie privée, quelques formulaires secondaires ont été enlevés de cette thèse.

Bien que ces formulaires aient inclus dans la pagination, il n'y aura aucun contenu manquant.

Canada

Abstract

Neural tube defects (NTDs), the second most common birth defect in humans, result from complex genetic and environmental factors. More than 100 single gene mutations cause NTDs in mice, though genetic background often influences penetrance. For instance, a homozygous *Cecr2* mutation on a BALB/c background causes an exencephaly frequency of 75%, as opposed to 0% on an FVB/N background.

Using linkage analysis I have located an exencephaly modifier region on chromosome 19. Exencephaly penetrance in *Splotch* and *shrm* mutants was not similarly reduced, indicating an effect which is specific to *Cecr2* or to a subset of NTD mutations. The modifier does not affect the location of cranial neural tube closure, a known exencephaly susceptibility factor which varies between strains. Human NTDs arise from small effect genes; therefore NTD modifiers in mice are likely candidates. Future genetic analysis will be used to narrow the modifier region, and identify the gene.

Acknowledgements

I would like to first thank Heather McDermid for giving me the chance to do this project which I have enjoyed very much, and for all the help during the research and thesis writing process. Also, thank you to Graham Banting and Tanya Ames who worked on the project before me and collected the data on which my work was based. I also want to thank everyone who assisted with the mice, including Jennifer Pockrant, Amanda Campbell, Twila Yobb, Adam Tassone, and Tanya Ames. I want to thank Lisa Rae Chisholm-Dumesnil who genotyped all of the embryos for the *shroom* experiment.

I want to thank Dr. Lucy Osborne and Guillermo Casallo for doing the genotyping for the linkage experiment, and Dr. Gary Churchill and Qian Li for help with analyzing the data. Also, thank you to Dr. Diana Juriloff and Dr. Muriel Harris, for advice in the linkage analysis, and making sense of all the penetrance data.

I received a great deal of help from Jack Scott in the microscopy unit, who made the SEM experiment possible. He was a huge help with the entire process, from advice in preparing the embryos, to taking the photographs and Photoshop to help produce the figures. I also want to thank everyone who came to the lab with me in the middle of the night while I was collecting embryos for SEM, particularly my sister, Chelsea Davidson.

Thank you to all the members of the McDermid lab who have provided experimental help and advice on everything from new techniques to presentations. I have enjoyed my time in the McDermid lab very much and I want to thank everyone for making this such a wonderful experience.

Table of Contents

Chapter 1. Introduction 1
1.1 Neural tube closure and defects in neurulation 1
1.1.1 Neurulation in the early mouse embryo 1
1.1.2 Neural tube defects (NTDs) in humans and mice 2
1.1.3 Types and causes of NTDs 5
1.1.4 Variations in cranial and caudal neural tube closure 7
1.1.5 The *Sp* mouse model of spina bifida and exencephaly 10
1.1.6 NTDs in the *shroom* mutant mouse line 14
1.2 *Cecr2* 16
1.2.1 *Cecr2* function 16
1.2.2 The role of *Cecr2* in neurulation and the *Cecr2*^{Gt45Bic} mutant phenotype 17
1.2.3 Chromatin remodeling 19
1.3 Susceptibility factors and modifiers of neural tube closure 21
1.3.1 Location of closure site 2 21
1.3.2 Female predominance of exencephaly 22
1.3.3 Other modifiers of NTD phenotypes in mice 24
1.4 Research objectives 26
Chapter 2. Materials and Methods 35
2.1 Maintaining the mouse colony 35
2.1.1 General housing conditions 35
2.1.2 Breeding and identification 35
2.1.3 Euthanasia 36
2.2 Embryo dissection and preparation 36
2.3 DNA extraction 36
2.3.1 Isolation of mouse genomic DNA 36
2.3.2 Isolation of PCR products from agarose gels 37
2.4 PCR amplification 37
2.4.1 PCR reactions 37
2.4.2 *Cecr2*^{Gt45Bic} and *Sry* genotyping 38
2.4.3 *Pax3*^{Sp} genotyping 39
2.4.4 *Shroom*^{GtROSA53Sor} genotyping PCR 40
2.5 Microsatellite genotyping and linkage analysis 41
2.5.1 Mating strategy to produce embryos for linkage analysis 41
2.5.2 Linkage analysis 42
2.6 Sequencing 43
2.7 Collection of penetrance data for *Pax3*^{Sp} and *shroom*^{GtROSA53Sor} mouse lines 44
2.8 Scanning Electron Microscopy 45
2.8.1 Embryo collection 45
2.8.2 Fixation and drying of embryos 46
2.8.3 Gold coating and Scanning Electron Microscopy 47
Chapter 3. Results 55
3.1 Mapping genetic modifiers of the exencephaly phenotype in *Cecr2*^{Gt45Bic} mutant mice 55
3.1.1 Dominant modifiers exist in the FVB/N genetic background 55

3.1.2 Collection of embryos and penetrance analysis 56
3.1.3 Microsatellite and SNP genotyping of exencephalic and unaffected embryos 57
3.1.4 Linkage analysis 59
3.1.5 Female predominance and the existence of X chromosome modifiers 60
3.1.6 Locating and analyzing candidate genes in the modifier region 62
3.2 Characterizing the effect of the FVB/N modifier(s) on two other NTD causing mutations 63
3.2.1 Penetrance analysis of exencephaly and spina bifida in C57BL/6J *Sp* mutants 64
3.2.2 Penetrance analysis of exencephaly and spina bifida in *Sp* embryos on a predominantly FVB/N genetic background 65
3.2.3 Penetrance analysis of various defects in *shroom*^{GtROSA53Sor} mutants on two genetic backgrounds 66
3.3 Characterization of normal cranial neurulation in FVB/N and BALB/c strains 68
Chapter 4. Discussion 85
4.1 A single strong dominant modifier contributes to the exencephaly penetrance variation in *Cecr2* mutants between BALB/c and FVB/N 85
4.1.1 Penetrance of exencephaly in intercross embryos resembles FVB/N 85
4.1.2 High penetrance in the backcross population suggests one strong modifier 86
4.1.3 Single region of significance found using linkage analysis 89
4.1.4 Is there a potential modifier on the X chromosome? 92
4.2 Candidate genes in the modifier region 95
4.2.1 The modifier region and potential types of modifier genes 95
4.2.2 *Smarca2* 98
4.2.3 *Cyp26a1* 101
4.2.4 *Pax2* 103
4.2.5 *Tect3* 105
4.3 Modification of the *Pax3* and *Shrm* mutant phenotypes 108
4.3.1 The frequency of spina bifida and possibly exencephaly is reduced in *Sp* mutant embryos by genes in the FVB/N background 108
4.3.2 Known modifiers of the *Pax3* mutant phenotype 109
4.3.3 Which *shrm* mutant phenotypes are affected? 112
4.3.4 How could the modifier candidates affect the *Sp* and *shrm* mutant phenotypes? 113
4.3.5 General or specific modifier 115
4.4 Closure 2 location 116
4.4.1 Closure 2 location is not a modifier of the *Cecr2* penetrance between the BALB/c and FVB/N strains 117
4.4.2 The effect of closure 2 timing on penetrance 118
4.4.3 Relevance to human neural tube defect susceptibility 119
4.5 Future directions 121
4.5.1 Narrowing the modifier region using congenic lines 121
4.5.2 Sequencing and quantitative RT-PCR the 4 candidate genes 123

List of Tables

Table 1. The penetrance of exencephaly in *Cecr2*^{Gt45Bic} mutant mice is highly dependent on modifiers in the genetic background..34

Table 2. Primer sequences used in this study..48

Table 3. The penetrance of exencephaly in *Cecr2*^{Gt45Bic} mutant mice on two pure genetic backgrounds and a heterozygous FVB/BALB background..................................70

Table 4. The p values of a subset of microsatellite markers for which the allele frequencies differed from random in the whole genome analysis of the 94 exencephalic embryos..73

Table 5. The p values of all the microsatellite and SNP markers on chromosome 19 based on comparing the expected to the unexpected genotypes in the exencephalic and unaffected control groups...75

Table 6. $\chi 2$ results for the four X chromosome markers using linkage results from a subset of 32 embryos from cross type 3...79

Table 7. The penetrance of exencephaly and spina bifida in *Sp* mutant mice on a pure C57BL/6J background and a predominantly FVB/N mixed genetic background..........82

Table 8. The penetrance of exencephaly, facial clefting, ventral closure defects and spina bifida in *shrm* mutant mice on two genetic backgrounds....................................83

4.5.3 Searching for possible X chromosome modifier 123
4.5.4 Identify the cause of NTDs in the *Cecr2* mutant line 124
4.5.5 Examine the effect of a specific FVB/N chromosome 19 region on other NTD mutant lines and teratogens which induce exencephaly 125
4.6 Significance of this work 126
Chapter 5. References 130
Appendix 150

List of Figures

Figure 1. Cross section diagram of cranial neural fold prior to fusion at the midline.....27

Figure 2. Diagram of the four closure points along the mammalian neural tube and the locations of the open neural folds in various NTDs.....29

Figure 3. NTDs in *Sp* homozygous mutant embryos.....30

Figure 4. Phenotypes of *shrm*^{GtROSA53Sor} homozygotes at E14.5.....31

Figure 5. Structure and domains of the *Cecr2* gene in mouse.....32

Figure 6. *Cecr2*^{Gt45Bic} mutant embryos which have been stained with X-gal to show the expression of the Cecr2-LacZ fusion protein.....33

Figure 7. *Cecr2*^{Gt45Bic} mutant allele and genotyping PCR.....50

Figure 8. *Pax3* wild type and *Sp* allele sequences, primer binding sites and a sample gel electrophoresis image of the *Pax3* genotyping PCR.....51

Figure 9. *Shroom*^{GtROSA53Sor} mutant allele and sample genotyping PCR image.....52

Figure 10. Mating strategy used to produce embryos for linkage analysis.....53

Figure 11. Series of crosses used to transfer the *shroom*^{GtROSA53Sor} mutation and the *Pax3*^{Sp} mutation from pure C57BL/6J backgrounds to a predominantly FVB/N mixed background.....54

Figure 12. Crossing scheme used to produce exencephalic and non-exencephalic embryos for linkage analysis.....71

Figure 13. Locations of the 112 microsatellites used to genotype the exencephalic embryos for linkage analysis.....72

Figure 14. Microsatellite and SNP markers used to define the region of a potential modifier on chromosome 19.....74

Figure 15. Graphical representation of the p values of all the microsatellite and SNP markers on chromosome 19..........76

Figure 16. Mainscan linkage results for microsatellite and SNP genotype data and the effect of the major loci on exencephaly frequency..........77

Figure 17. The variable penetrance in the backcross population of embryos used for linkage analysis based on the inheritance of the X chromosome, and the sex of the embryo..........78

Figure 18. Locations of the four modifier candidate genes on chromosome 19 relative to the linkage peak..........80

Figure 19. Conserved protein motifs and gene structure of *Smarca2*..........81

Figure 20. Normal elevation and fusion of cranial neural folds at closure point 2 in BALB/c and FVB/N mouse embryos..........84

Figure 21. Breeding strategy to make subinterval-specific congenics to narrow down the modifier region on chromosome 19..........129

List of Abbreviations

Mouse gene (Lower case, italics)
Mouse protein (Lower case)
HUMAN GENE (UPPER CASE, ITALICS)
HUMAN PROTEIN (UPPER CASE)

aa	amino acid
AAA	ATPases associated with diverse cellular activities
ACF	ATP-utilizing, chromatin assembly and remodeling complex
ASD	Apx/Shrm domain
AT Hook	Adenine/thymine hook
ATP	Adenosine triphosphate
ATRX	α-thalassemia/mental retardation syndrome X-linked
Axd	*Axial defects*
B/B	BALB/BALB
B/F	BALB/FVB
BAZ1	Bromodomain adjacent to zinc finger 1 motif
BD	Bromodomain
BMP	Bone morphogenetic protein
bp	base pair
BPTF	Bromodomain PHD finger transcription factor
BrdU	Bromodeoxyuridine
Brg1	*Brahma like gene one*
BRK	Brahma-KIS domain
BSA	Bovine serum albumin
c	cytosine
cDNA	copy DNA
CECR2/Cecr2	*Cat eye syndrome chromosome region, candidate 2 (human and mouse respectively)*
CERF	CECR2-containing remodeling factor
CHD/Mi-2	Chromodomain helicase DNA binding
CHRAC	Chromatin accessibility complex
cM	centimorgan
CO_2	carbon dioxide
CSB	Cockayne syndrome protein B
ct	*curly tail*
DDM1	DNA Methylation 1
DDT	DNA binding homeobox and different transcription factors
DEPC	Diethyl pyrocarbonate
DEXHc	DEXH-box helicases
DLHPs	Dorsolateral hinge points
DNA	Deoxyribonucleic acid
dNTPs	Deoxynucleotide triphosphates
Dpc	Days post coitus
E	Embryonic day

EDTA	Ethylene diamine tetraacetic acid
En1	*Engrailed 1*
En2	*Engrailed 2*
EtBr	Ethidium bromide
exma	*exencephaly and severe microphthalmia/anophthalmia*
FB	Forebrain
Fgf-8	*Fibroblast growth factor 8*
HB	Hindbrain
HELICc	Helicase superfamily c-terminal domain
Hh	Hedgehog
HMDS	Hexamethyldisliazane
HSA	domain in helicases and associated with SANT domains
HSF1	Heat shock factor1
HSLAS	Health sciences lab animal services
Hsp70	Heat shock promoter 70
ISWI	Imitation switch
Kb	Kilobase pairs
KCl	Potassium chloride
lacZ	β-galactosidase
lod	logarithm of the odds
m	*Gt45Bic*
M. mu	*Mus musculus*
MARCKS	myristoylated alanine rich protein kinase C substrate
Mb	Megabase pairs
MB	Midbrain
MBSU	Microbiology service unit
mct1	*modifier of curly tail 1*
$MgCl_2$	Magnesium chloride
MHP	Median hinge point
mRNA	messenger RNA
MTHFR	5,10-methylenetetrahydrofolate reductase
NaCl	Sodium chloride
NaOAc	Sodium acetate
Nap1/2	nucleosome assembly protein 1-like 2
N-cad	N-cadherin
NCAM	neural cell adhesion molecule 1
NCC	Neural crest cells
Nf1	Neurofibromin
NoRC	Nucleosome-remodeling complex
NTDs	Neural tube defects
NURF	Nucleosome-remodeling factor
Ods	*Ocular degeneration with sex reversal*
Opb	*Open brain*
Pax3	*Paired box gene 3*
PBS	Phosphate buffered saline
PCR	Polymerase chain reaction

PDZ	PSD-95/Dgl/ZO-1
PNP	Posterior neuropore
QTL	Quantitative trait loci
RA	Retinoic Acid
RARE	Retinoic acid responsive elements
RbAp48/46	retinoblastoma-associated protein 48/46
RNA	Ribonucleic acid
rpm	revolutions per minute
RSF	Remodeling and spacing factor
RT-PCR	Reverse transcription-polymerase chain reaction
SA	Splice acceptor
SANT	SWI-SNF ADA N-CoR and TFIIIB domain
SDS	Sodium dodecyl sulfate
SEM	Scanning electron Microscope
Shh	*Sonic hedgehog*
shrm	*shroom*
SNF2_N	SNF2 family N-terminal domain
Snf2h/SNF2H	*SWI/SNF related, matrix associated, actin dependant regulator of chromatin, subfamily a, member 5 (human and mouse respectively)*
Snf2l/SNF2L	*SWI/SNF related, matrix associated, actin dependant regulator of chromatin, subfamily a, member 2*
SNP	single nucleotide polymorphism
Sp	*Splotch*
Sp^{d}	*Splotch delayed*
Sp^{r}	*Splotch retarded*
Sry	sex determining region of Chromosome Y
SWI/SNF	Mating type switching/sucrose non-fermenting
t	thymine
TERC	telomerase RNA component
Tm	Melting temperature
V	Volts
WCRF	WSTF-related chromatin-remodeling factor
Wnt	Wingless-type MMTV integration site family
WSTF	Williams syndrome transcription factor
xshrm	Xenopus *shrm*
$\chi2$	chi-squared

Chapter 1. Introduction

1.1 Neural tube closure and defects in neurulation

1.1.1 Neurulation in the early mouse embryo

Neurulation is the early embryonic process that forms the neural tube, the precursor to the brain and spinal cord. During gastrulation the notochord forms, and is the source of signals which allow the neural plate to differentiate from the overlying ectoderm. The notochord signals neural plate differentiation by suppressing the BMP and Wnt signaling pathways which induce epidermal cell fate, as neural cell fate is the default state in this tissue (reviewed in Sadler 2005). The neural plate, once formed, undergoes convergent extension, where lateral cells migrate and intercalate at the midline (Schoenwolf and Alverez 1989). Convergent extension, along with the plane of cell division, causes the neural plate to elongate and become keyhole shaped, with a broad cranial region and a narrower caudal region. The neural folds then form at the lateral edges of the neural plate, due in part to the proliferation in the mesenchyme tissue located beneath the neuroepithelium (reviewed in Sadler 2005). The folds are able to converge by the induction of a median hinge point (MHP), induced by signaling from the notochord, which forms a V-shaped neural plate and brings the folds closer together **(Figure 1)** (reviewed in Sadler 2005; Smith and Schoenwolf 1989).

The elevation of the neural folds is followed by the fusion of the folds at the midline. This fusion is initially accomplished by cell surface glycoproteins at the tips of the neural folds, and eventually more permanent fusion occurs (Sadler 1978). The elevation and fusion of the neural folds begins at discrete points along the neuroaxis of the embryo (Juriloff et al. 1989) **(Figure 2)**. The initial fusion event, closure point 1, occurs at the cervical-hindbrain boundary at the 2-8 somite stage, at ~embryonic day (E) 8.5 in the mouse. Fusion proceeds both rostrally and caudally from this point, causing the neural tube to "zip up" bidirectionally. A second fusion event occurs at the forebrain-midbrain boundary at the 9-14 somite stage at ~E9, and a third occurs at the rostral most point of the forebrain at the 12-17 somite stage at ~E9-E9.5 (Macdonald et al. 1989). Closure 2 also proceeds bidirectionally, whereas closure point 3 proceeds only caudally. Through the zippering effect from these 3 points of neural fold fusion, a complete, closed neural tube is formed along the entire axis of the embryo. A fourth closure occurs in the hindbrain region; however this closure does not involve fusion of the neural folds (Golden and Chernoff 1993). In this closure event, the rhombencephalon is covered by a membrane which grows in a rostral direction.

The above events describe primary neurulation, which forms the neural tube from the rostral end to the upper sacral level (Copp and Brook 1989). Caudally, from this point, the neural tube is formed through a process called secondary neurulation. The caudal neural tube is formed from the tail bud, which is a population of stem cells in the caudal end of the embryo (reviewed in Copp et al. 2003). Mesenchymal cells in the dorsal region of the tail bud condense and undergo epithelialization. These epithelial cells reorganize around a lumen, which is continuous with the lumen formed rostrally through primary neurulation, to form the caudal end of the neural tube (Schoenwolf 1984).

1.1.2 Neural tube defects (NTDs) in humans and mice

NTDs occur in ~1/1000 live births, making them the second most common birth defect in humans (reviewed in Copp et al. 2003). Human NTDs are generally multifactorial with complex genetic and environmental causes. These defects do not show a Mendelian pattern of inheritance, though there is a 2-5% recurrence in siblings, which is up to a 50 fold increase over the occurrence risk in the general population (reviewed in Detrait et al. 2005). This indicates that there are genetic susceptibility factors. The occurrence varies with ethnic background and geographic location, and it has been found that ~70% of human NTDs can be prevented with folic acid supplements taken periconceptionally (reviewed in Detrait et al. 2005). There are several types of NTDs, which can result from defects in either primary or secondary neurulation. The failure of primary neurulation leads to open NTDs, like exencephaly and spina bifida aperta, whereas the failure of secondary neurulation leads to NTDs like spina bifida occulta, which occurs when the neural tube does not separate from the surrounding tissues (reviewed in Copp et al. 2003).

In contrast to the multifactorial inheritance of human NTDs, there are more than 100 single gene mutations in mice which lead to NTDs (Boyles et al. 2005). These mutant lines are a valuable resource for studying neurulation and identifying the underlying processes which occur to allow the elevation and fusion of the neural folds. These mutant lines may also be a good tool for predicting the types of genes which are involved in human neurulation, and are therefore potential human candidate genes for NTD susceptibility. There is a large variety in the types of genes which are associated with NTDs in mice, including transcription factors, tumor suppressors and factors involved in signal transduction (reviewed in Harris and Juriloff 1999). Some of the processes which can be affected in the mouse models of NTDs are apoptosis, as in *Cited2* mutants (Bamforth et al. 2001), neural patterning, as in *Shh* mutants (Echelard et al.

1993), proliferation defects in adjacent tissues like the mesenchyme and ventral tail bud, as in *Twist* and *ct* mutants respectively (Chen and Behringer et al. 1995; van Straaten and Copp 2001), convergent extension, as in *loop-tail* mutants (Murdoch et al. 2001), and actin organization, as in *shroom* mutants (Hildebrand and Soriano 1999). There has been much debate over the use of mouse models to study human NTDs, due to the variation in the genetic cause and possible differences in the mechanism of neural tube closure.

One possible problem in using mouse models to study exencephaly is that the existence of closure 2 is controversial in humans, and therefore cranial neurulation may have some significant differences between the species. There are also a variety of differences between the mouse models of NTDs, including the inheritance patterns and the effects on other tissues. There are syndromic mouse models, which have a variety of other defects and may die midgestation, including *Splotch (Sp)* and *Twist* (Auerbach 1954; Chen and Behringer 1995). There are also many non-syndromic models, which show no other abnormalities and often live at least until the time of birth, including the *Cecr2*$^{m/m}$ mice (Banting et al. 2005). Most human NTDs are non-syndromic and therefore these models may be the most useful in the study of human NTDs. Some mutant mouse lines are multifactorial and depend on more than one gene to cause the NTD phenotype, including the SELH/Bc strain, which is predicted to have ~3 genes that contribute to the exencephaly phenotype, and the *curly tail* strain, which depends on the *ct* gene and at least one other strong modifier, the *mct1* gene, for its phenotype (Juriloff et al. 2001; Letts et al. 1995). These models may be useful in studying human NTDs, which also have a multifactorial inheritance pattern. In addition, many of these mouse mutants are highly susceptible to genetic background and incomplete penetrance is very common.

This means that many single gene mutant lines depend on other genetic factors to cause NTDs.

Compounding the understanding of the genetic factors involved in NTDs, there are also various environmental causes which vary the penetrance of NTDs, both to increase and decrease their frequency. The environmental factors associated with mouse NTDs, in many cases, are common to human environmental factors involved in NTD frequency, including the protective effect of folic acid supplementation. This supports the usefulness of mouse models of NTDs for studying how various environmental and chemical factors are causing or rescuing NTDs in human cases, and for locating new supplements and treatments for NTD prevention. There are enough similarities between neurulation in mice and humans that that the mouse models of NTDs are likely a good tool for understanding the process of neural tube closure, and the effects of various environmental factors. Certain mouse models, such as the SELH/Bc strain, are particularly similar to human NTDs, as they are non-syndromic and multifactorial. The usefulness of mouse NTD models for determining the genetic causes of human NTDs remains to be proven, as relatively few of these genes have been thoroughly examined in human NTD cases. The underlying similarity of the neurulation process makes it likely that there is some underlying genetic similarity as well.

1.1.3 Types and causes of NTDs

There are several types of open NTDs that can occur depending on which region of the neural tube fails to close **(Figure 2)**. A failure of closure point 1 leads to craniorachischisis, in which the entire spinal region remains open as well as the cranial region up to the rostral portion of the midbrain. This defect is seen in mice with mutations in components of the planar cell polarity pathway, including *circletail*, *loop-tail*, *crash* and *disheveled 1/2* double knockouts (Curtin et al. 2003; Murdoch et al. 2001; Murdoch et al. 2003; Hamblet et al. 2002). These mutations lead to defective convergent extension and produce a broad neural plate in which the neural folds are too far apart to converge at the midline.

Defects in closure site 2 formation, or fusion of the neural folds in the midbrain region, lead to exencephaly. Anencephaly is the human equivalent of exencephaly, though the human defect includes a more pronounced degradation of exposed brain tissue, likely due to the longer gestation (reviewed in Copp 2005). Exencephaly is the most common NTD in single mutant mice and it can affect a variable extent of the cranial region. The SELH/Bc strain, for example, develops exencephaly at a penetrance of 17% due to a complete absence of closure 2 (Macdonald et al. 1989). Exencephaly also occurs in the Sp^{2H} mutant line which has a deletion in the *Pax3* gene, though in this line closure 2 does form and exencephaly occurs because the neural folds in the midbrain region fail to fuse (Fleming and Copp 2000). Exencephaly in SELH/Bc mutant embryos includes the entire developing brain, whereas in Sp^{2H} mutants, exencephaly does not extend into the forebrain region.

Defects in closure point, 3 at the rostral most point in the neural tube, result in facial clefting which often occurs in conjunction with exencephaly, as in *Hes1* and *Ski* knockout mice (Ishibashi et al. 1995; Berk et al. 1997). Spina bifida aperta results from the failure of the posterior neuropore to fuse at the caudal end of the neural tube (Harris and Juriloff 1999). The posterior neuropore is the final region of the neural tube to complete closure, at ~E10. Very few mouse mutants specifically disrupt this process, and it is not associated with a closure point. Some mutants which do specifically affect this process are *Wnt3a* and *Axd* (*Axial defects*) (Takada et al. 1994; Essien 1992).

1.1.4 Variations in cranial and caudal neural tube closure

There are characteristics of neural tube closure which are common to primary neurulation along the entire rostrocaudal axis, and there are also significant variations. Many mouse mutants result in exencephaly alone, and many result in exencephaly and spina bifida (reviewed in Harris and Juriloff 1999). Many teratogens also specifically affect neural tube closure in the cranial region (Copp 1990). Some mutations result in spina bifida alone, though the relatively small number of such mutants supports the prediction that there are either less mechanisms specifically involved in caudal neurulation, or that the mechanisms are more highly redundant.

The formation of the MHP occurs along almost the entire length of the neural tube due to signaling from the notochord, likely involving Sonic hedgehog (Shh) **(Figure 1)** (reviewed in Sadler 2005; Smith and Schoenwolf 1989). This process forms a V shaped neural plate, which is the first step in bringing the neural folds together. Many of the further steps in neural fold convergence at the midline vary between the cranial and caudal regions. In the upper spinal region, around closure point 1 **(Figure 2)**, the MHP is the only hinge point and the narrow lumen is formed by a bulging out of the tips of the neural folds (reviewed in Sadler 2005). As closure proceeds rostrally and caudally from this initial site, two additional hinge points begin to form symmetrically in the neural plate, adjacent to the junction with the surface ectoderm. These dorsolateral hinge points (DLHPs) occur in addition to the MHP in the cranial and intermediate spinal regions of the neural tube **(Figure 1)** (Ybot-Gonzalez and Copp 1999). A decrease in Shh signaling likely permits the DLHPs to form in the intermediate and lower spinal regions, and this mechanism may also allow DLHPs to form in the cranial region (Ybot-Gonzalez et al. 2002). The lower spinal region has been suggested to lack the MHP and be formed by DLHPs alone (Ybot-Gonzalez and Copp 1999). The closure of the cranial and caudal regions of the primary neural tube likely have many common mechanisms, as both can be affected by folic acid supplementation, and have a similar dependence on methionine (reviewed in Harris and Juriloff 1999). In addition, some mutations which affect apoptosis and retinoic acid signaling affect cranial and caudal neurulation, indicating that they are required at multiple points along the neural tube.

Some cranial specific processes exist, based on the fact that mutations in some neurulation genes cause exencephaly only, or cranial specific expression is seen for these genes. For instance, proliferation of the cranial mesenchyme allows the initial elevation of biconvex neural folds (reviewed in Copp 2005). *Twist* and *Cart1* mutants show defects in this process and specifically develop exencephaly (Chen and Behringer 1995; Zhao et al. 1996). In the spinal region, removal of paraxial mesoderm does not prevent neural tube closure, so a parallel mechanism is not occurring (van Straaten et al. 1993). As well, the role of the actin cytoskeleton is variable between the cranial and caudal regions of the neural tube. The use of cytochalasins, drugs which disassemble actin microfilaments, demonstrates this as cranial neurulation is extremely sensitive to the drug, and neurulation in the spinal region is relatively resistant (Wiley 1980). Several mouse mutants which affect the cytoskeleton recapitulate this by developing only exencephaly, including vinculin, an actin binding protein, and MARCKs, which crosslinks actin microfilaments (Xu et al. 1998; Stumpo et al. 1995).

Another difference between cranial and caudal neural tube closure is the relation to neural crest emigration. In the cranial region, the neural crest cells (NCCs) emigrate very near to the time of neural tube closure, at the point when the folds are becoming concave (reviewed in Copp 2005). It has been speculated that this release of NCCs allows this change in neural fold morphology. Several mutations, including a *connexin 43* mutation, as well as treatment with chondroitinase ABC which dissolves chondroitin sulfate, show neural crest cell defects as well as exencephaly (Ewart et al. 1997; Morriss-Kay and Tuckett 1989). In the spinal region, neural crest cell emigration occurs several hours after the neural tube closes, so this relationship is not seen (reviewed in Copp 2005). The fusion of the neural folds also uses different cell surface receptors along the axis of the neural tube. Ephrin-A5 is a glycosylphosphatidylinositol-linked cell surface Eph ligand, which along with the EphA7 receptor, is expressed only in the cranial neural tube (Holmberg et al. 2000). Mutants for these genes undergo normal cranial neural fold elevation, but fusion is defective. Both of these mutants cause exencephaly only.

The use of mouse models must take into account the differences between primary neurulation in the cranial and caudal regions. By determining if closure along the entire neural tube is disrupted or if it is only disrupted in a specific region, the underlying cause of the defect can be narrowed down. For instance, a mutant mouse strain that specifically develops exencephaly is likely defective for a cranial-specific process. As well it would be interesting to determine whether a gene or background which modifies neurulation in one region of the neural tube, has a similar effect elsewhere along the axis of the neural tube. This will begin to explain how a modifier is affecting neurulation.

The use of mouse models to uncover human susceptibility genes is an ongoing process, though there has been little success. Many homologs of mouse candidate genes have been sequenced in human cases of NTDs, including *NCAM*, *MTHFR*, *noggin*, and *TERC*. Linkage analysis has focused on regions of some mouse NTD genes in human NTD cases, including some genes in the retinoic acid pathway (Deak et al. 2005a; Viera et al. 2005; Bauer et al. 2002; Benz et al. 2004; Deak et al 2005b). Many of these studies have focused on spina bifida patients, due to greater availability, even when examining genes which specifically lead to exencephaly in the mouse mutant. Knowing whether a gene affects a cranial specific process will determine the likelihood that these screens will prove successful. A failure to take this into account may be one explanation for the lack of success in the human genetic analysis of NTDs. Understanding the differences between neurulation in the cranial and caudal regions of the neural tube will allow the most effective screening of human homologs of mouse NTD mutations in human cases.

1.1.5 The *Sp* mouse model of spina bifida and exencephaly

The *Sp* mutation is one of the best studied mouse models of NTDs. This mutant line exhibits spina bifida as well as exencephaly, and has been studied extensively in terms of interacting genes, environmental and chemical effects, and underlying causes for the defects (reviewed in Machado et al. 2001).

Sp (*Sp*) is one of several mouse lines containing a mutation in the *Pax3* gene; others include Sp^{2H}, Sp^{r} and Sp^{d} (Goulding et al. 1993). The various *Sp* mutant lines have served as models for both NTDs and neural crest cell defects. The *Sp* line is presumed to be a null, and has a mutation in a splice acceptor in intron 3 which causes 4 non-functional mRNA species to be produced (Epstein et al. 1993). The *Sp* homozygotes develop spina bifida at 100% penetrance and exencephaly to a lesser extent (Auerbach 1954) **(Figure 3)**. The homozygotes also develop a number of defects in neural crest derived structures, including the cardiac outflow tracts, dorsal root ganglia, Schwann cells, and melanocytes (Auerbach 1954; Franz 1989; Franz 1990). *Sp* homozygotes die at ~E14, presumably from heart defects (Conway et al. 1997). *Sp* heterozygotes are normal, except for a minor defect involving melanocytes which causes a white belly spot and a lack of pigmentation in the feet and the tip of the tail (Auerbach 1954). The precise cause of the NTDs in the *Sp* line is still unclear, as is the relationship between neural tube closure and the emigration of the NCCs.

In *Sp* homozygous mutant embryos, delays in neural crest cell emigration and a decrease in the number of cells which migrate, have been reported (Moase and Trasler 1990; Serbedzija and McMahon 1997). These defects worsen along the rostrocaudal axis, and at the caudal end it has been reported that no NCCs emigrate and the caudal NCC derived structures are completely absent. This likely is not a causative factor in the development of spina bifida, however, as the caudal region of the neural tube closes before NCC emigration. NCC defects often occur in conjunction with neural tube closure defects, which implies either a common regulatory mechanism or a direct dependence of neural tube closure on neural crest cell emigration. It has been suggested, for instance, that the release of NCCs may allow bending of the cranial neural folds by reducing the rigidity of the neural plate (reviewed in Copp et al. 2003). If NCC emigration is causative in exencephaly, this implies some difference in the underlying cause of NTDs at various regions of the neural tube. It has not been determined whether the neural crest cell defect is due to a defect in the neuroepithelium which prevents NCC emigration, or a defect in the environment that the NCCs migrate through. If it is a defect in the neuroepithelium, it is more likely relevant to the closure of the neural tube. Some experiments have been designed to test this, including a transgenic *Pax3* construct which rescues only neural crest and neural tube expression of *Pax3*, and not expression in the somites (Li et al. 1999). The rostral somites are part of the pathway traveled by migrating NCCs, so by rescuing the neuroepithelial expression and not the expression in the migratory pathway, the role of Pax3 in NCC emigration can be more precisely determined. In this case, the NTDs were rescued as well as NCC emigration and migration defects, suggesting a cell autonomous role for Pax3 in NCC migration. Other experiments have shown that transplanting the neural tube from a *Sp* mutant embryo onto a chick neural tube rescued the emigration and migration of NCCs, as did growing neural tube explants from *Sp* mutants in culture (Serbedzija and McMahon 1997; Moase and Trasler 1990). This suggests that a wild type environment can rescue the neural crest defects. These experiments are contradicting in that the former suggests that Pax3 is required only in the neuroepithelium to allow NCCs to emigrate, and the latter suggests that the NCCs in *Sp* mutant mice can emigrate normally, but that Pax3 is required for normal NCC migration. It is likely that Pax3 is required in the environment for migration of NCCs and in the neuroepithelium for correct emigration of NCCs.

Several common molecules and processes are likely involved in both neural tube closure and neural crest cell emigration. These processes are the most likely candidates for the underlying defect in the *Sp* mutant line. Pax3 is a transcription factor and some of its potential targets include *N-CAM*, *N-cad*, *versican*, and *Pax7* (Chalepakis et al. 1994; Edelman and Jones 1995; Henderson et al. 1997; Borycki et al. 1999). Many variations in other proteins and in the process of neurulation exist between wild type and *Sp* mutant embryos. The neural tube in *Sp* homozygotes is deformed along the entire rostrocaudal axis and the lumen is collapsed in some regions, with a disorganized neuroepithelium (Auerbach 1954). Also, there are gap junction vesicles along the neural groove indicating a possible change in cellular adhesion or interaction, and the cell cycle is lengthened (Wilson and Finta 1979). *Sp* mutants overexpress the chondroitin sulphate proteoglycan, versican, in the neural crest cell migration pathway, which is known to be non-permissive for migration (Henderson et al. 1997). This may explain the environmental, non-autonomous effect of the *Pax3* mutation on neural crest cell migration. Another difference in *Sp* mutant mice is that they express a modified form of N-CAM with α-2,8 linked polysialosyl units at the time of neural tube closure, E9 (Neale and Trasler 1994). N-CAM is a cell adhesion molecule, which is not normally sialylated until E11 in wild type mouse embryos. It is known that an increase in sialylation causes a decrease in the adhesive capacity of N-CAM, and that N-CAM is normally unsialylated as the neural tube is bending and closing and is sialylated at the time of caudal neural crest cell emigration. This is presumed to be because adhesive N-CAM is required for stability of the neural plate as it undergoes the mechanical stress of bending, and removing the adhesive property allows the NCCs to leave the neural tube. The premature sialylation may be responsible for NTDs by decreasing cell communication and contact. Another important difference between *Sp* mutant and wild type embryos is related to apoptosis. *Sp* mutants have increased apoptosis in the neuroepithelium and somites, and increased p53 protein levels (Pani et al. 2002). A *p53* knockout completely rescues NTDs in the *Sp* mutant embryos.

The *Sp* mutation, which arose spontaneously more than 60 years ago and was conclusively mapped to the *Pax3* gene in 1993, has long been a model of neural crest cell migration and neural tube closure defects. Mutations in the human *PAX3* gene have been found in Waardenberg Syndrome Type I, which is associated with pigmentation defects, defects in hearing, and occasional NTDs, which makes an understanding of the defects and the genes and chemicals which affect them even more critical (Baldwin et al. 1992; Tassabehji et al. 1992). The study of genes which modify NTDs in *Sp* mutants would be interesting in understanding neural tube closure and in understanding the relationship between two critical embryonic processes, neurulation and neural crest cell migration.

1.1.6 NTDs in the *shroom* mutant mouse line

The *shroom* (*shrm*) gene was discovered during an analysis of a recessive lethal genetrap mutation (Hildebrand and Soriano 1999). The *shrm* homozygous mutant embryos ($shrm^{GtROSA53Sor/GtROSA53Sor}$) develop three types of NTDs: exencephaly, which is completely penetrant, and facial clefting and spina bifida which are incompletely penetrant **(Figure 4)**. The neural folds in *shrm* mutant embryos "mushroom" out and fail to converge at the midline. The *shrm* homozygotes also show a low penetrance of defects in ventral closure, which results in the herniation of the liver and intestines. The Shroom protein contains a PDZ domain, which facilitates protein-protein interactions, and two ASD domains. Shrm is expressed in the neuroepithelium, and following neural tube closure, it is expressed in the roof and floor plate of the neural tube.

Shrm localizes to actin stress fibers and Adherens junctions, which are involved in cell-cell adhesion, in cultured epithelial cells (Hildebrand and Soriano 1999). The role of the Shrm protein was further examined, to determine its role in neural tube closure.

Shrm was found to bind F-actin via the ASD1 domain and was able to cause apical constriction of neuroepithelial cells in culture, which also required the ASD2 domain. During apical constriction, the apical region of a polarized epithelial cell contracts to form a wedge shaped cell with a reduced apical surface area, which allows bending of the epithelium. The *shrm* homozygous mutant embryos lacked the high concentration of apically localized actin in their neural folds, which is typical in wild type embryos. These embryos also show a diffuse pattern of non-muscle myosin II, as compared to the apically localized myosin II in wild type embryos (Hildebrand 2005).

The *Xenopus laevis* shrm protein (xshrm) is also required for cranial neural tube closure, and for the closure of the posterior neural tube and to a lesser degree (Haigo et al. 2003). Xshrm is expressed in the neural plate overall, but most robustly in two stripes along the anterior-posterior axis which may represent the forming hinge points. This provides some evidence that Shrm functions at the hinge points, and it is known that apical constriction occurs during neurulation at these regions of the neural tube which are responsible for bending. This bending allows the neural folds to meet at the midline, and therefore the Shrm protein is likely to be required for the cellular architecture of neural tube closure. Shrm is believed to regulate the formation of a contractile actomyosin network which allows the apical constriction of cells at the hinge points. The injection of mouse Shrm into *Xenopus* blastulae shows that Shrm is sufficient to cause apical constriction in naïve epithelial cells, but only in cells which have apical-baso polarity.

While it appears that Shrm functions at the hinge points, some evidence exists that the hinge points are not actin-dependent, as they can form in mouse embryos cultured in cytochalasin D which disrupts actin polymerization (Ybot-Gonzalez and Copp 1999). It has also been suggested rather that cytochalasins affect cranial neural tube closure because actin is required for the rigidity of non-bending regions of the neural plate.

1.2 *Cecr2*

1.2.1 *Cecr2* function

The *Cecr2* gene, which is now known to be associated with exencephaly, was originally chosen for study based on its location in the 2 Mb Cat Eye critical region on chromosome 22q11, which is duplicated in humans with Cat Eye Syndrome (Footz et al. 2001). *Cecr2* was considered a likely candidate for dosage sensitivity based on an initial analysis of its domains. *Cecr2* contains a bromodomain, which binds acetylated lysine on histone H4 tails, as well as a nuclear localization signal, a DDT domain and an A/T hook, which binds DNA at the minor groove **(Figure 5)** (Banting et al. 2005). These motifs suggest a role in transcriptional regulation. The *Cecr2* gene contains 19 exons, and many potential and confirmed splice variants. In mouse, a common variant lacks exon 8, and this transcript has been confirmed in adult brain and liver and embryonic tissue at E12.5 and E15.5 (Ames 2006).

Orr Barak in Ramein Sheikhattar's lab, found human CECR2 in a complex with SNF2L in HEK293 cells, though this has not been confirmed in mouse (Banting et al. 2005). This CERF (CECR2-containing remodeling factor) complex has ATP-dependent chromatin remodeling activity. The Cecr2 motifs support this role in chromatin remodeling, as they predict nuclear localization, and are similar to the motifs found in other proteins which interact with SNF2L and SNF2H. For example, the DDT domain is necessary for the Acf1 protein to bind ISWI in *Drosophila*, which is an SNF2L homolog (Fyodorov and Kadonaga 2002).

1.2.2 The role of *Cecr2* in neurulation and the *Cecr2*^{Gt45Bic} mutant phenotype

The function of the *Cecr2* gene was examined by creating a mutant mouse line with an intron 7 splice trap containing the β-gal gene. This produced a truncated protein consisting of the first 7 exons of Cecr2 fused to LacZ (Banting et al. 2005). This truncated version of Cecr2 does not contain the bromodomain, which is located in exons 12 and 13, so it should presumably lack the ability to bind histones and therefore to remodel chromatin. RT-PCR, however, has shown that some readthrough occurs, meaning that in some cases transcription continues past the transcription stop site in the splicetrap (Banting 2003). The splicetrap may then be spliced out to create a wild type transcript. RNA past the genetrap is decreased 17-25X in *Cecr2*$^{m/m}$ embryos at E15.5 as compared to wild type littermates, indicating that the mutant line is hypomorphic for Cecr2 rather than a complete knockout (Ames 2006; Adam Tassone, unpublished data). For this reason "*m*" (mutation) is used to represent the *Gt45Bic* allele, as "–" implies a complete knockout.

The expression of the Cecr2 protein was analyzed using LacZ staining in *Cecr2*^{Gt45Bic} mutant mice, as the Cecr2-LacZ fusion protein is expressed from the endogenous *Cecr2* promoter. The Cecr2 protein is expressed at the time of neurulation, ~E9.5, in a generalized pattern with enrichment in the neural tube (Banting et al. 2005). By E12.5 and E13.5 the expression pattern is more specific, and is strong in the brain, spinal column, spinal ganglia, eyes, nasal cavities and mesenchyme of the limbs **(Figure 6)**.

Homozygous mutant embryos on the original mixed genetic background of 129P2/ola and BALB/c, developed the neural tube defect exencephaly at a penetrance of

67% (24/36) (Banting et al. 2005) **(Table 1)**. The mutants display open neural folds in the entire cranial region, implying a failure of closure point 2. No other phenotypes have been associated with the mutant allele, and homozygous mutants that manage to close their neural tubes appear to develop normally. It is therefore likely that the CERF complex, or another Cecr2-containing complex, may remodel chromatin to control transcription of genes involved in cranial neurulation. It is also possible that Cecr2 is involved in other developmental processes as it is widely expressed. A full knockout may uncover these other functions.

The penetrance of the exencephaly phenotype was found to be highly dependent on the genetic background, based on an early observation that crossing the BALB/129P2 $Cecr2^{Gt45Bic}$ mutant mice to the FVB/N strain decreased the penetrance from 67% to 36% (21/58) **(Table 1)** (Banting et al. 2005). This background effect was confirmed after breeding the *Cecr2* mutation onto three pure genetic backgrounds for 5-6 generations. At this point the penetrance was reexamined and found to be highly variable between the lines. The low number of embryos collected on the 129P2/ola background makes it difficult to accurately estimate the penetrance, though it is predicted to be ~63% (5/8) (data not shown). The most striking observation was the variation between BALB/c *Cecr2* mutants, which develop exencephaly at a penetrance of 74% (35/47), and the FVB/N *Cecr2* mutants which did not develop exencephaly (0/42). Another interesting aspect of the phenotype is the female predominance of exencephaly. On the BALB/c background, 66% (23/35) of exencephalic embryos were female (Ames 2006). There is also a low penetrance of exencephaly in $Cecr2^{+/m}$ embryos for the two mixed backgrounds studied, of 3.5% on the BALB/129P2 background and 4% on the BALB/129P2/FVB background (Banting et al. 2005).

1.2.3 Chromatin remodeling

CECR2 has been found in a complex which shows chromatin remodeling activity in vitro, though the in vivo role of Cecr2 in remodeling chromatin remains unknown. The structure of chromatin, besides being a means of packaging DNA into the nucleus, plays a role in regulating transcription activation and repression, replication, DNA repair, and recombination (reviewed in Eberharter and Becker 2004). Several multiprotein complexes exist which modify chromatin, and in turn modify these processes. These complexes have two main effects on chromatin: covalent modification of histones and ATP-dependent remodeling of the nucleosome arrangement. Within the ATP-dependent chromatin remodeling complexes, 7 subgroups exist which differ based on the type of ATPase protein they contain. These 7 groups are ISWI, SWI/SNF, CHD/Mi-2, INO80, RAD54, CSB and DDM1 (reviewed in Eberharter and Becker 2004; Fazzio et al. 2005). Chromatin can be remodeled in a number of ways, including the sliding of nucleosomes along DNA, changing the path of DNA over the nucleosomes (for example, looping out of the DNA), exchanging histones within existing nucleosomes, and removing nucleosomes from a specific region (Fazzio and Tsukiyama 2003). The two best studied classes of chromatin remodeling complexes are ISWI and SWI/SNF. In mice and humans there are two ATPases in the ISWI family, Snf2l/SNF2L and Snf2h/SNF2H (Lazzaro and Picketts 2001). These ATPase proteins, as well as the components of the complexes they form, are well conserved in *Drosophila melanogaster* and *Saccharomyces cerevisiae*.

CECR2 has been found to complex with SNF2L, a human ISWI homolog, in HEK293 cells (Banting et al. 2005). The CERF complex, of CECR2 and SNF2L, is the second SNF2L containing complex to be purified from mammalian cells. The first complex purified was NURF, which consists of SNF2L, BPTF, and RbAp48/46 (Barak et al. 2003). Both SNF2L complexes, as is the case for other ISWI complexes, are stimulated by nucleosomes and act by sliding intact nucleosomes. Snf2l in mice is expressed in the embryo as early as E9.5, but at a low level (Lazarro and Picketts 2001). The expression of Snf2l is upregulated in the postnatal brain, particularly the hippocampus and cerebellum. It is also strongly expressed in the ovaries. Snf2l is most strongly expressed in differentiated neurons, as well as differentiated cells in the ovaries. While the role of the CERF complex remains unknown, some functions of the mammalian NURF complex have been determined. It is known that the NURF complex binds upstream of the *engrailed-1* and *engrailed-2* genes, and regulates their expression (Barak et al. 2003). Engrailed is a homeotic protein involved in development of the mid-hindbrain. The human NURF complex is also able to potentiate neurite outgrowth in culture.

In contrast to the limited number of Snf2l complexes isolated, several complexes containing Snf2h have been isolated and characterized including WSTF-related chromatin-remodeling factor (WCRF), ATP-utilizing chromatin assembly and remodeling factor (ACF), remodeling and spacing factor (RSF), WSTF-ISWI chromatin-remodeling complex (WICH), nucleosome-remodeling complex (NoRC), chromatin assembly complex (CHRAC), and SNF2H-cohesin (reviewed in Barak et al. 2003). Many of the Snf2h containing complexes play a role in the replication of heterochromatin

(Stopka and Skoultchi 2003). Snf2h is expressed in the early embryo and in the testes, and is prevalent in proliferating cells (Lazzaro and Picketts 2001). A null *Snf2h* mutant is periimplantation lethal, likely dying between E5.5 and E7.5 (Stopka and Skoultchi 2003). The null embryos show an arrest in cell division and massive apoptosis.

1.3 Susceptibility factors and modifiers of neural tube closure

The penetrance of NTDs in many mouse models, including the *Sp*, *ct*, *Ski* and *Cecr2* mutant lines, is very often affected by the genetic background (Moase and Trasler 1987; Neumann et al. 1994; Colmenares et al. 2002; Banting et al. 2005). While these background effects suggest that neural tube closure is highly susceptible to modifier genes, this area has not been well studied. A few of the factors which can affect neural tube closure, like sex and closure site 2 location, have been determined, though these factors fail to explain all the background effects observed, and likely there are many unknown factors. Even these known susceptibility factors are not well understood. The underlying cause of sex specific penetrance is still unknown; as well no causative genes which affect closure site 2 location have been determined.

1.3.1 Location of closure site 2

A genetic susceptibility factor for the development of exencephaly is the location of closure site 2. The locations of closure points 1 and 3 are uniformly located in all strains examined to date, whereas significant variation has been seen in closure 2 location (Juriloff et al. 1991). Several mouse strains close their cranial neural tube at the boundary between the forebrain and the midbrain, including LM/Bc, AEJ/RkBc, ICR/Bc and CD1 random bred mice (Juriloff et al. 1991; Fleming and Copp 2000). This is the most common closure 2 location, but the SWV/Bc and NZW strains both have a more rostral closure 2 location within the forebrain region (Juriloff et al. 1991; Fleming and Copp 2000). The DBA/2 strain has been reported to have a more caudal closure 2 location, within the midbrain (Fleming and Copp 2000).

This inherent variability in closure 2 location has been presumed to affect penetrance in relation to environmental and genetic causes of exencephaly. The SVW/Bc strain is more susceptible to exencephaly induced by hyperthermia and exposure to valproic acid than other strains, including the LM/Bc strain (Finnell et al. 1986; Finnell et al. 1988). As well the NZW strain exhibits a higher than normal level of spontaneous exencephaly (Vogelweid et al. 1993). The penetrance of exencephaly in *Sp*^{2H} mutant mice has been examined on genetic backgrounds with variable closure 2 locations (Fleming and Copp 2000). The mutation was originally on a mixed background of C3H/He, 101 and CBA/Ca, and all the embryos within the *Sp*^{2H} line, regardless of genotype, have a rostral closure 2 site. The penetrance was reexamined after 4 generations of crossing to the caudally closing DBA/2 strain and the closure 2 location was examined following each generation. After 4 generations, closure site 2 had moved to a caudal location within the midbrain, as in DBA/2 mice, and the penetrance of exencephaly had dropped from 75% to 35.7%. Therefore, changing the location of closure site 2 was correlated to a decrease in the penetrance of exencephaly.

1.3.2 Female predominance of exencephaly

Many mouse mutants which display exencephaly have a variable penetrance between male and female embryos. This includes the SELH/Bc strain, as well as the *curly tail*, *p53*, *exencephaly* and *Cecr2* mutant lines (MacDonald et al. 1989; Embury et al. 1979; Armstrong et al. 1995; Wallace et al. 1978). Environmental effects, including hyperthermia, also cause exencephaly in a female predominant manner (Webster and Edwards 1984). Though female predominance of exencephaly is a consistent observation between many mouse strains, as well as in human fetuses, it has still not been explained. In human embryos, primary neurulation defects occurring in the cranial and upper spinal regions show female predominance whereas lower spinal defects in primary and secondary neurulation show an equal occurrence or a slight male predominance (Hall 1986; Seller 1995). It is clear that the cause of this female predominance is chromosomal rather than hormonal, as neurulation occurs before gonadal differentiation, and several hypotheses have been formed based on this fact. For instance, female cells have ~2% more DNA, which could slow replication and cause a decrease in growth rate (Seller 1995). This could cause the female embryos to be at a more immature developmental stage at the time of neural tube closure. It had been thought that if females grow more slowly they may spend longer in the period of neural tube closure, and therefore be more susceptible to closure defects, in particular to teratogens, for a longer period. This effect was disproved in the *curly tail* strain, where although females were developmentally at an earlier stage than males as neurulation was beginning, the growth rate was the same for all embryos between E8.5 and E10 (Brook et al. 1994).

Another of the hypotheses which attempts to explain the female predominance is that males with exencephaly are selectively lost early in gestation, though mouse mutants with female predominant exencephaly all seem to show a 1:1 male to female ratio (reviewed in Harris and Juriloff 1997). It is also thought that as females grow more slowly, they may sometimes lack a sufficient number of cells in the neuroepithelium or mesoderm to undergo normal neural tube closure (Brook et al. 1994). This also seems unlikely, as males and females tend to have a comparable somite number at the time of closure site 2 formation. It is also possible that males and females may close their neural tubes in slightly different manners, or that some maternal factor is present at the time males close their neural tube which favors its successful completion. One other possibility is that the process of X inactivation in the neural folds may take away methyl groups which are required in some other aspect of cranial neural tube closure (reviewed in Harris and Juriloff 1997). While the female predominance of exencephaly in mice and anencephaly in humans has been studied extensively, the cause is still not understood.

1.3.3 Other modifiers of NTD phenotypes in mice

Modifier genes can affect the phenotypes in mutant strains in a number of ways, including affects on the penetrance, dominance, expressivity or pleiotropy of a trait (reviewed in Nadeau 2001). The phenotypes can be enhanced or decreased, and in some cases, novel phenotypes can arise. A modifier does not necessarily act in the same pathway as the gene it is modifying; a modifier can affect the phenotype produced by a mutant gene in a number of ways. A modifier can alter the expression of the modified gene, it can interact with, or act in the same pathway as the gene it is affecting, or it may simply correct or enhance the underlying defects in an indirect manner which affects the phenotype at a cellular or tissue level.

Neural tube closure is known to be highly susceptible to genetic modifiers, which is apparent when examining the strain-dependent penetrance seen in several NTD causing mutations. The *curly tail* strain, which develops spina bifida, tail flexion defects and less frequently exencephaly, develops NTDs at a frequency of 18.5% when backcrossed to C57BL/6J and at a frequency of only 2.2% when backcrossed to DBA/2 mice (Neumann et al. 1994). A strong background effect is also seen for the *jumonji* gene, which causes cranial neurulation defects at a frequency of ~40% on a mixed background of 129/ola and BALB/cA (Takeuchi et al. 1999). When this mutation was crossed onto the BALB/cA, C57BL/6J and DBA/2J strains, no NTDs were seen. An opposite effect was seen when the *jumonji* mutation was crossed onto the C3H/He strain, as all homozygous mutants developed NTDs. Therefore in this mutant line the penetrance can range from 0 to 100% based on genetic background. Another interesting example of strain dependent penetrance occurs for the *Ski* gene, which causes exencephaly and facial clefting. On a mixed 129/P2 and Swiss black background, 88% of *Ski*$^{-/-}$ embryos develop exencephaly and the remaining 12% develop facial clefts (Colmenares et al. 2002). When this mutation was crossed onto a C57BL/6J background, the exencephaly penetrance dropped to only 5%, whereas the penetrance of the facial clefting defect rose to 93%. This is an example in which neurulation is affected differently along the axis of the neural tube by the same genetic background.

While these genetic background effects are prevalent among NTD mouse models, they have not been studied in many cases. One of the few modifiers which has been mapped is the *mct1* gene on chromosome 17, which modifies the NTD frequency in the *curly tail* strain, though no gene has been identified to date (Letts et al. 1995). Mapping of more NTD modifiers will help answer questions regarding the strength of single gene modifiers, and the number of modifiers responsible for strain dependent penetrance effects. Identification of modifiers will also help determine whether single modifiers can have variable effects in different regions of the neural tube.

Neurulation follows the pattern of a threshold trait, meaning that there is some tolerable biological time limit, or threshold, beyond which the neural tube cannot completely close (MacDonald et al. 1989). This fits well with the observation of variable and incomplete penetrance in NTD mouse models, as several genes in a different genetic background may each contribute to a delay or increase in the timing of neural tube closure, allowing the threshold to be exceeded in some cases. Small effect genes are difficult to map, and the use of highly penetrant mutations to uncover their effects may allow identification of some of these susceptibility factors. The etiology of human NTDs makes the identification of low penetrance or minor effect genes even more interesting, as human NTDs are multifactorial and likely result from a summation of gene variants with minor effects, and environmental factors, which cause the threshold to be exceeded. One interesting question that may be answered by determining the identity of mouse modifiers, is whether gene variants of highly penetrant mouse NTD mutations can modify penetrance between normal mouse strains. It is also possible that a unique set of genes which has yet to be identified is responsible for modifying the penetrance of NTDs between mouse strains.

1.4 Research objectives

The main objective of my project was to map and characterize the modifiers of the exencephaly phenotype in *Cecr2*^{Gt45Bic} mutant mice. The specific goals used to address this objective were as follows:

1. To intercross *Cecr2*^{Gt45Bic} mutants from the exencephaly-resistant FVB/N strain and the exencephaly-susceptible BALB/c strain and characterize the modifier(s) as dominant or recessive.

2. To collect ~100 exencephalic and ~100 non-exencephalic $Cecr2^{m/m}$ embryos from a population of FVB/BALB F1 $Cecr2^{m/m}$ mice backcrossed to BALB/c $Cecr2^{+/m}$ mice and use whole genome microsatellite and SNP genotyping to find linkage to the regions of potential modifiers.
3. To examine the region(s) of the potential modifier(s) for candidate genes and use sequence analysis to begin looking for variations in these candidates.
4. To analyze the effect of the FVB/N genetic background on the penetrance of exencephaly and spina bifida in the $Pax3^{Sp}$ mutant line.
5. To analyze the effect of the FVB/N genetic background on the penetrance of exencephaly, spina bifida, facial clefting and ventral closure defects in the $shrm^{GtROSASor}$ mutant line.
6. To characterize the location of closure 2 in wild type FVB/N and BALB/c embryos to determine if variability in the closure site correlates with susceptibility to exencephaly in these two strains.

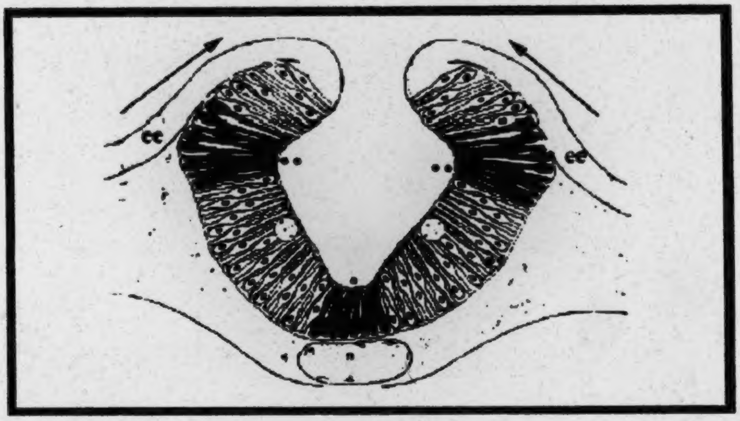

Figure 1. Cross section diagram of cranial neural fold prior to fusion at the midline. The notochord (n) signals the bending at the MHP * which creates a V-shaped neural plate. The bending at the dorsolateral hinge points ** brings the tips of the neural folds together at the midline. The overlying ectoderm (ee) also plays a role in closure and in signaling to the developing neural tube. Am. J Med. Genet. C Semin. Med. Genet, Sadler 2005.

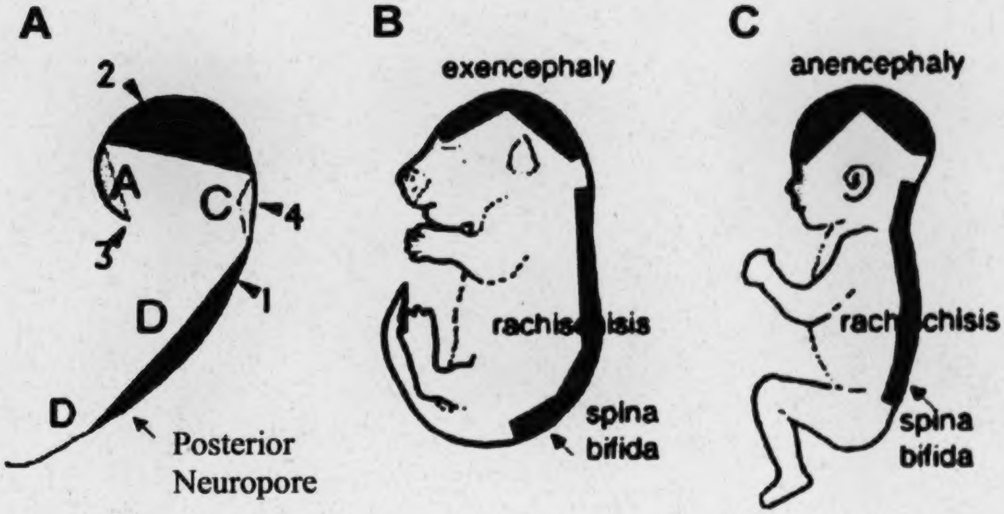
A
2
A
C
4
3
1
D
D
Posterior
Neuropore
B
exencephaly
rachischisis
spina
bifida
C
anencephaly
rachischisis
spina
bifida

Figure 2. Diagram of the four closure points along the mammalian neural tube and the locations of the open neural folds in various NTDs. A) The rostrocaudal location of the four closure points are indicated by arrowheads on the schematic diagram of the neural tube. If the neural tube in the red area at the top of the head fails to fuse, exencephaly (B) or anencephaly (C) develops. In craniorachischisis, the blue region is open, in addition to a portion of the cranial region in red. If the posterior neuropore fails to close in the red region at the caudal end of the embryo, spina bifida develops. Human Molecular Genetics, Juriloff and Harris 2000.

Figure 3. NTDs in a *Sp* homozygous mutant embryo. The phenotype of *Pax3*$^{Sp/Sp}$ embryos compared to control *Pax3*$^{+/+}$ embryos at E12.5. *Sp* homozygotes develop spina bifida (between the white arrows), and exencephaly involving the hindbrain region (red arrow).

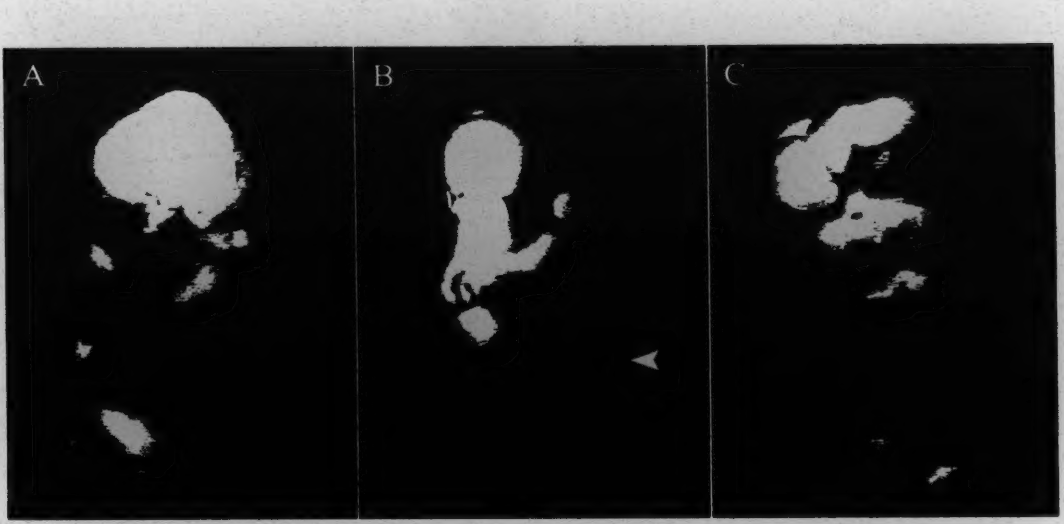

Figure 4. Phenotypes of *shrm*^{GtROSA53Sor} homozygotes at E14.5. A) Side view of a wild type embryo showing no defects. B) Front view of a *shrm* homozygous mutant embryo showing exencephaly (red arrow), a defect in ventral closure leading to herniation of the liver and intestines (white arrow), and facial clefting (green arrow). C) Side view of a different *shrm* homozygous mutant embryo showing exencephaly (red arrow) and spina bifida (blue arrow).

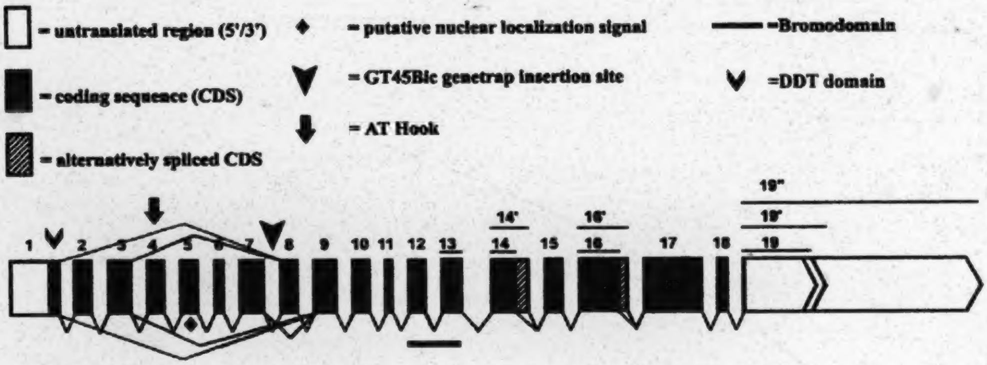
= untranslated region (5'/3')
= coding sequence (CDS)
= alternatively spliced CDS
= putative nuclear localization signal
= GT45Bic genetrap insertion site
= AT Hook
=Bromodomain
=DDT domain
1
2
3
4
5
6
7
8
9
10
11
12
13
14
14'
15
16
16'
17
18
19
19'
19"

Figure 5. Structure and domains of the *Cecr2* gene in mouse. The exons, but not the introns, are drawn to scale. Conserved protein domains are included, in addition to the location of the splicetrap insertion site in intron 7. The alternative splicing which removes exon 8 as well as the alternative 3' end of exon 14 has been confirmed in mouse. The other splice variants are predicted based on RT-PCR in human tissues. Adapted from Banting 2003.

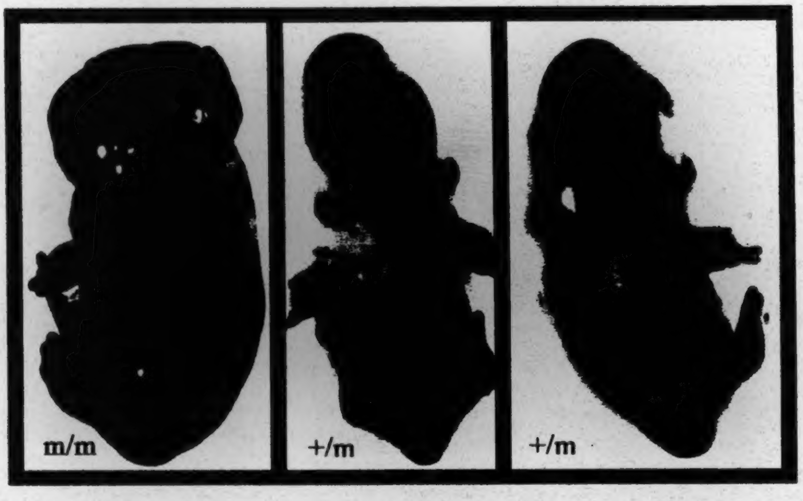

Figure 6. ***Cecr2*$^{\mathit{Gt45Bic}}$ mutant embryos which have been stained with X-gal to show the expression of the Cecr2-LacZ fusion protein.** The homozygous mutant 13.5 dpc embryo (*m/m*) shows the exencephaly phenotype. Heterozygous mutant 13.5 dpc embryos display no abnormal phenotype. The X-gal staining shows expression of the Cecr2-LacZ fusion protein in the brain, and developing neural tube, as well as in the eyes, nasal epithelium, spinal ganglia and mesenchyme of the limbs. Human Molecular Genetics, Banting et al. 2005.

Table 1. The penetrance of exencephaly in *Cecr2*^{Gt45Bic} mutant mice is highly dependent on modifiers in the genetic background (Banting et al. 2005).

	Balb/129P2			Balb/129P2/FVB			FVB/N			Balb/c		
	m/m[1]	+/m	+/+	m/m	+/m	+/+	m/m	+/m	+/+	m/m	+/m	+/+
Exencephaly	24	4	0	21	7	1	0	0	0	35	0	0
Normal	12	113	38	37	166	82	42	99	59	12	110	70
Penetrance (%)	67	3.5	0	36	4	1	0	0	0	74	0	0

Exencephaly penetrance for FVB/N and BALB/c was scored in incipient congenic strains at generation F5 or F6.

[1]. *m = Gt45Bic*

Chapter 2. Materials and Methods

2.1 Maintaining the mouse colony

2.1.1 General housing conditions

Mice were housed at the Health Sciences Laboratory Animal Services (HSLAS) facility. The mice were kept on a 14 hour light/10 hour dark cycle at 22±2°C. Mice were housed up to five per cage in standard filter top cages. Mice were fed Laboratory Rodent Diet 5001 (LabDiet) which contained 4% fat, with the exception of breeding females which were fed a 9% fat diet from the start of mating until pups were weaned (Mouse diet 9F 5020 from LabDiet).

2.1.2 Breeding and identification

Breeding was done in two ways. The first method used individual breeder pairs which were not separated before litters were born, allowing post partum mating in order to increase the frequency of litters produced. The second method was harem mating, of one male with up to four females. In harem mating cages, females were removed to individual cages once they became visibly pregnant. To examine embryos at a specific gestational age, a male mouse was placed in a cage with 1-4 females in the afternoon, and the following morning females were tested by an HSLAS technician for the presence of a vaginal plug, which indicated that mating had occurred. Females were removed to individual cages when a plug was found. Mice ovulate approximately midway through the dark cycle and therefore noon of the plug date was considered 0.5 days gestation (Brook et al. 1994). Mice were weaned three weeks after birth by HSLAS staff, at which point male and female progeny were separated into separate cages. At the time of weaning, mice were given ear notches for identification, and tail biopsies were taken for DNA extraction and genotyping.

2.1.3 Euthanasia

Mice were euthanized in a standard CO_2 chamber. Mice were monitored for five minutes after breathing ceased and death was thought to have occurred. A toe pinch test was done to confirm death and mice were dissected or immediately stored at -20°C until incineration.

2.2 Embryo dissection and preparation

The uterus was removed into 1x PBS (137 mM NaCl, 2.7 mM KCl, 10 mM Na_2HPO_4, 2 mM KH_2PO_4, pH 7.4) and embryos were dissected out under a dissecting microscope. A sample of extraembryonic membrane or a small piece of the embryo was removed and stored at -20°C for genotyping. Embryos were put into 1.5 ml Eppendorf tubes, and in the case of embryos being collected for microsatellite genotyping, the embryos were cut in half and put into two separate tubes at -20°C. Embryos being kept for long term storage were fixed overnight at 4°C in ~1 ml of 4% paraformaldehyde in 1x PBS. Fixed embryos were washed twice in 1x PBS for five minutes before being dehydrated. This was done using a methanol gradient, consisting of a five minute wash in each of 25%, 50%, and 75% methanol in 1x PBS and 2 five minute washes in 100% methanol. Embryos were stored at -20°C in 100% methanol.

2.3 DNA extraction

2.3.1 Isolation of mouse genomic DNA

Genomic DNA was extracted from mouse tail biopsies, extraembryonic membranes, and embryo biopsies, using the following protocol. Tissue samples were digested overnight at 60°C, using 300 μg of proteinase K (Invitrogen) in 350 μl of proteinase K digestion buffer (50 mM Tris pH 8, 100 mM EDTA pH 8, and 0.2% SDS) (Banting 2003). Samples were then placed on ice for five minutes, followed by the addition of 125 μl of 5 M NaCl (final concentration of 1.7 M NaCl) and then an additional five minutes on ice. Samples were centrifuged at 14,000 rpm for 15 minutes in a microcentrifuge with a fixed angle rotor. The supernatant was added to 500 μl of isopropanol and 0.75 μl of 2% dextran blue. The samples were precipitated at -20°C for 20 minutes and then centrifuged for 15 minutes at 14,000 rpm. The isopropanol was removed, and 500 μl of 70% ethanol was added to the pellet, followed by a 15 minute centrifugation at 14,000 rpm. Finally, the DNA pellet was dried and resuspended in 20 μl of water.

2.3.2 Isolation of PCR products from agarose gels

PCR products were excised from a 1-2% agarose gel in 1x TAE (40 mM Tris-acetate, 1 mM EDTA, pH 8.4) for purification. DNA was isolated using the manufacturer's instructions with a QIAquick gel extraction kit (Qiagen). To determine the approximate concentration of the purified DNA sample, 5 μl of the 30 μl sample was electrophoresed on a 1% agarose gel.

2.4 PCR amplification

2.4.1 PCR reactions

In general, PCR reactions were done in 25 μl reaction volumes using a PTC-200 thermal cycler (MJ Research). Reactions contained 1 μl of DNA template (~0.5 μg), 1x PCR buffer (25 mM Tris pH 9, 50 mM KCl, 1.5 mM $MgCl_2$ and 0.02 mg/ml bovine serum albumin [BSA] dissolved in water), 0.2 mM dNTPs, 20 pmol of each primer and 1

U of recombinant *Taq* DNA polymerase (purified by Dr. Pickard, Department of Biological Sciences, University of Alberta). Reactions were done in PCR plates, and mineral oil was used to prevent evaporation. The cycling conditions were: a 90 second "hotstart" at 94°C, followed by the addition of *Taq* polymerase while the samples remain at 80°C, 35 cycles of 94°C for 20 seconds, 72°C for 60 seconds per Kb, 30 seconds at the appropriate annealing temperature for the primer chosen **(Table 2)**, and a 72°C extension for 5 minutes following the final cycle. The annealing temperature of primers was determined by calculating the melting temperature (Tm= 67.5 + 34(%G+C) - 395/#bases) and subtracting 5-10°C (Ames 2006). PCR products were stored at 4°C until gel electrophoresis on a 1-2% agarose gel in 1x TAE at ~125 V. Samples were mixed with 1x loading dye (50% glycerol, 10 mM Tris pH 7.5, 100 mM EDTA, 0.1% bromophenol blue, 0.1% xylene cyanol, and 0.1% orange G), and run on a gel with a 1 Kb plus DNA ladder (Invitrogen) to allow size determination of the bands produced.

2.4.2 *Cecr2*^{Gt45Bic} and *Sry* genotyping

A 20 μl reaction volume was used, containing 1 μl of undiluted genomic DNA (~0.5 μg), 1x PCR buffer, 0.25 mM of dNTPs, 20 pmol of each of the Cecr2 7iF4, Cecr2 7iR4, pGT1 R4, SRYfor and SRYrev primers, and 1 U of recombinant *Taq* polymerase which was added following a 90 second hotstart at 94°C **(Table 2)**. This is a multiplex PCR, in which the Cecr2 7iF4 and Cecr2 7iR4 primers produce a 376 bp band from the normal *Cecr2* allele, and the Cecr2 7iF4 and pGT1 R4 primers produce a 573 bp fragment from the *Cecr2*^{Gt45Bic} allele **(Figure 7)**. The SRYfor and SRYrev primers amplify a 266 bp band from the *Sry* gene on the Y chromosome in male mice, allowing the samples to be scored for sex as well as for the *Cecr2* genotype **(Figure 7)**. Each

Cecr2^{Gt45Bic} genotyping PCR included normal, heterozygous and homozygous mutant DNA samples, as well as water, to act as PCR controls. The cycling conditions of the PCR reaction following the hotstart are: 35 cycles of 94°C for 15 seconds, 62°C for 20 seconds, and 72°C for 40 seconds. Following this, a final extension of 72°C for five minutes was done, and the samples remained at 4°C until gel electrophoresis on a 2% agarose gel at 125 V for 50 minutes.

2.4.3 *Pax3*^{Sp} genotyping

The *Pax3*^{Sp} mutant allele differs from the wild type allele due to point mutations in 4 adjacent base pairs, and a single nucleotide deletion which disrupts the splice acceptor of intron 3 **(Figure 8)**. The mice were genotyped for the presence of both alleles using two separate PCR reactions. To amplify the wild type *Pax3* allele, a 20 µl reaction containing ~0.5 µg of genomic DNA, 1x PCR buffer, 1x High Fidelity PCR buffer (Invitrogen), 0.25 mM dNTPs, 20 pmol of the SpWTFwd primer, 20 pmol of the SpWTRev primer and 1 U of recombinant *Taq* polymerase was used **(Table 2)**. A PCR product of 1301 bp was produced, indicating that the mouse had either 1 or 2 copies of the wild type *Pax3* allele **(Figure 8)**. The mutant *Pax3*^{Sp} allele was amplified using the same reaction conditions with the exception of the SpWTRev primer, which was replaced with the SpMUTRev primer, which differs from the SpWTRev primer by 4 bp at the 3' end. The presence of the *Pax3*^{Sp} allele is indicated by a 1300 bp band in this PCR reaction, due to the fact that the SpWTRev and SpMUTRev primers bind at the same genomic position on the two different *Pax3* alleles, and there is a single nucleotide deletion in the *Sp* allele **(Figure 8)**. The cycling conditions for both PCR reactions are as follows: a 90 second hotstart at 94°C, 94°C for 2 minutes, 67°C for 2 minutes, 72°C for 5 minutes and then 35 cycles of 94°C for 30 seconds, 67°C for 30 seconds and 72°C for 1 minute, followed by a final cycle of 94°C for 1 minute, 67°C for 1 minute and 72°C for 10 minutes (Machado et al. 2001). Each genomic DNA sample was amplified twice using each PCR reaction (wild type and mutant). *Pax3*$^{+/+}$ and *Pax3*$^{Sp/Sp}$ DNA samples were included with each genotyping PCR, in addition to water, as PCR controls.

To confirm any unclear PCR genotyping results, a 352 bp PCR fragment was amplified which contained the base pairs which vary in the mutant allele. A 25 µl reaction volume, containing ~0.5 µg of genomic DNA, 1x PCR buffer, 0.2 mM dNTPs, 20 pmol of the Spl F1 primer, 20 pmol of the Spl R1 primer, and 1 U of *Taq* Polymerase, was used to PCR the fragment **(Table 2)**. The PCR cycling conditions were as follows: a 94°C 90 second hotstart, 35 cycles of 94°C for 20 seconds, 72°C for 45 seconds, 59°C for 30 seconds and then a final extension of 72°C for 5 minutes. The PCR product was run on a 1% agarose gel, purified, and sequenced using the Spl F1 primer. The sequence at the variable base pairs was examined to determine the genotype, and double peaks on the chromatograph at the variable region indicate a heterozygous genotype.

2.4.4 *Shroom*^{GtROSA53Sor} genotyping PCR

The GtROSA53 genetrap is located in intron 3 of the *shroom* gene (Jeff Hildebrand, personal communication). A multiplex PCR was used to amplify fragments from the wild type and the mutant *shroom* alleles. A 25 µL reaction volume was used, containing 20 pmol of each of the following primers, ShrmFor2, ShrmR1 and ShrmRevLD, as well as 1 µl of undiluted genomic DNA (~0.5 µg), 1x PCR buffer (Invitrogen), 1x PCRx enhancer (Invitrogen), 1.5 mM $MgSO_4$, 0.25 mM of dNTPs and 1 U of recombinant *Taq* polymerase (Primers designed by Jeff Hildebrand, Jennifer

Pockrant, and Lisa Rae Chisholm-Dumesnil) **(Table 2)**. The ShrmFor2 and ShrmRevLD primers produce an 837 bp band from the wild type *shrm* allele and the ShrmFor2 primer amplifies a ~950 bp band from the *shroom*^{GtROSA53Sor} allele with the ShrmR1 primer **(Figure 9)**. Each *shroom*^{GtROSA53Sor} genotyping PCR included normal, heterozygous and homozygous mutant DNA samples, as well as water, to act as PCR controls. The cycling conditions were as follows: a 94°C 90 second hotstart, 35 cycles of 94°C for 45 seconds, 62°C for 30 seconds and 72°C for 1 minute, and then a final extension of 72°C for 7 minutes (Lisa Rae Chisholm-Dumesnil, personal communication).

Initially, before the above PCR was developed, a PCR was used which amplified a fragment within the GtROSA53 genetrap. This PCR is able to distinguish mice which have the mutant allele from wild type mice, but cannot distinguish heterozygotes from homozygous mutants. This PCR was therefore used to genotype the weaned mice. A 25 µl reaction volume containing ~0.5 µg of genomic DNA, 1x PCR buffer, 0.2 mM dNTPs, 5 pmol of the GTL primer, 5 pmol of the GT-LacZ-R1' primer, and 1 U of *Taq* Polymerase, was used **(Table 2)**. The PCR cycling conditions were as follows: a 94°C 90 second hotstart, 35 cycles of 94°C for 20 seconds, 60°C for 20 seconds and 72°C for 30 seconds and then a final extension of 72°C for 5 minutes (Angela Keuling, personal communication). A ~350 bp band indicates the presence of the mutant allele by amplifying a fragment from the GtROSA53 genetrap. A wild type DNA sample as well as a *shroom*$^{+/GtROSA53Sor}$ sample was included, along with water, as a PCR control with each *shroom*^{GtROSA53Sor} genotyping PCR reaction.

2.5 Microsatellite genotyping and linkage analysis

2.5.1 Mating strategy to produce embryos for linkage analysis

A large sample of exencephalic and non-exencephalic *Cecr2* mutant embryos on a mixed FVB/N and BALB/c genetic background was required for linkage analysis. To produce F1 FVB/BALB *Cecr2*$^{m/m}$ mice, congenic FVB/N *Cecr2*$^{m/m}$ males, in which the *Cecr2*^{Gt45Bic} mutation has been mated onto the FVB/N background for at least 10 generations, were mated to BALB/c *Cecr2*$^{+/m}$ congenic females (*m*=*Gt45Bic*) **(Figure 10A)**. The reciprocal cross was done as well, in which the BALB/c *Cecr2*$^{+/m}$ males were mated to FVB/N *Cecr2*$^{m/m}$ females **(Figure 10B)**. The resulting F1 FVB/BALB mice were genotyped, and male and female *Cecr2*$^{m/m}$ mice were selected and crossed to BALB/c *Cecr2*$^{+/m}$ mice. Embryos from this backcross were collected between E13.5 and E15.5, because mice are visibly pregnant by this point and exencephaly is easily phenotyped. The bodies of 94 exencephalic embryos and 94 non-exencephalic embryos were sent on dry ice to Dr. Lucy Osborne's laboratory at the University of Toronto for DNA extraction and microsatellite and SNP genotyping. As well, tail biopsies from pure FVB/N and BALB/c mice were sent as parental DNA controls to confirm microsatellite and SNP genotypes for the two strains. The embryo heads were kept in the McDermid lab at -20°C, in case the initial samples were lost in transport or additional DNA was required

2.5.2 Linkage analysis

To determine the significance of the linkage, the microsatellite data from the markers which were tested on both the exencephalic and non-exencephalic samples, was combined. The analysis method combined the "expected genotypes" and the "unexpected genotypes" from both groups, to allow an analysis of the data which took into account the mirror image effect expected between the two groups. The "expected genotype" in the exencephaly group is BALB/BALB (B/B) because this is the susceptible genotype, so for a modifier, more B/B individuals should develop exencephaly than F/B individuals. The "expected genotype" in the non-exencephaly group is therefore FVB/BALB (F/B) in the region of a potential modifier, because this resistant genotype should be enriched in the subset of *Cecr2*$^{m/m}$ embryos which do not develop exencephaly. To analyze the data, the "expected genotypes" were added together and the "unexpected genotypes" were added together. The following formulas used were: Expected genotypes=B/B (exencephaly group) + F/B (unaffected group) and Unexpected genotypes=F/B (exencephaly group) + B/B (unaffected group). A chi-squared goodness-of-fit test was used to look for a significant difference between the expected and unexpected genotypes for each microsatellite. A p value of $\leq$0.001 was considered significant because only 50 independent tests are possible due to the size of the mouse genome, and an effective p value of 0.05 requires an observed p value of 0.001 (0.5/50) (Juriloff et al. 2001). This observed p value was determined using the Bonferroni correction, which is a multiple comparison correction used when several independent statistical tests are being performed (reviewed in Shaffer 1995). For example, if 100 microsatellite genotypes are being analyzed throughout a genome, there are likely to be 5 false positives if a genome wide p value of $\leq$0.05 is used. The Bonferroni correction avoids false positives by considering that 50 independent tests are being undertaken for the 50 independent linkage regions in the mouse genome, rather than considering the linkage as a single statistical test.

2.6 Sequencing

Sequencing PCR reactions were done using the DYEnamic ET terminator cycle sequencing kit (Amersham). The reactions were done based on the manufacturer's instructions, but the reaction volume was modified from 20 µl to 10 µl. The reaction contained 4 µl of the sequencing premix, 2 pmol of the appropriate primer, and between 40 ng and 60 ng of the DNA template, which was gel extracted. Reactions went through 30 cycles of: 96°C for 30 seconds, 60°C for 1 minute, and 50°C for 1 minute. To precipitate the samples, 1 µl of 1.5 M NaOAc/250 mM EDTA, pH 7.8 was added, in addition to 40 µl of cold 95% ethanol. Samples were incubated at -20°C for 30 minutes and then centrifuged for 15 minutes at 14,000 rpm. The ethanol was removed and 200 µl of 70% ethanol was added. The samples were centrifuged for 5 minutes at 14,000 rpm and the pellet was dried and stored at -20°C. Samples were taken to the Microbiology Service Unit (MBSU) for the remainder of the sequencing, where they were dissolved in formamide loading dye and loaded into an ABI 377 automated sequencer (Applied Biosystems). GeneTool v2.0 (Biotools) was used to analyze chromatographs obtained from the automated sequencer.

2.7 Collection of penetrance data for *Pax3*^{Sp} and *shroom*^{GtROSA53Sor} mouse lines

Pax3^{Sp} heterozygous mice, as well as wild type C57BL/6J mice from the colony, were provided by Dr. Underhill, Department of Medical Genetics, University of Alberta. Two male and two female *shroom*$^{+/GtROSA53Sor}$ mice were purchased from Jackson Laboratories from a cryopreserved stock. In addition, two male and two female wild type controls from the *shroom*^{GtROSA53Sor} colony were provided. Both mutations were originally on a pure C57BL/6J background. The change in the NTD penetrance for the *shroom*^{GtROSA53Sor} allele and the *Pax3*^{Sp} allele on a predominantly FVB/N background, as compared to a pure C57BL/6J background, was examined by crossing heterozygous males for each of these mutations to wild type FVB/N females. The F1 progeny were genotyped, using PCR, for the appropriate mutation, and heterozygous males were backcrossed to wild type FVB/N females. The F2 progeny from this cross are ~75% FVB/N in terms of genetic background (http://www.jax.org/imr/controls.html). Heterozygous males and females from the F2 progeny were mated together and plug tested, to obtain timed pregnancies in order to collect embryos **(Figure 11)**.

Between 100 and 150 embryos were collected on this mixed background for each mutation, of which 25% should be homozygous mutant. Embryos from intercrosses of *Pax3*^{Sp} heterozygotes were examined at E12.5, due to lethality of homozygotes at mid-gestation, and were genotyped using PCR. Embryos from intercrosses of *shroom*^{GtROSA53Sor} heterozygotes were collected between E12.5 and E15.5, and were genotyped using the multiplex *Shrm*^{GtROSA53Sor} genotyping PCR. Collection of embryos on the original C57BL/6J background was done by intercrossing C57BL/6J *shroom*$^{+/GtROSA53Sor}$ mice or intercrossing C57BL/6J *Pax3*$^{+/Sp}$ mice and collecting embryos as described above, with the exception of the C57BL/6J *shroom*^{GtROSA53Sor} embryos as only 31 were collected. Only a small number of embryos were collected in this case because a recent and complete penetrance analysis was completed on this line by Hildebrand and Soriano (1999).

2.8 Scanning Electron Microscopy

2.8.1 Embryo collection

Wild type BALB/c males were mated to 1-4 wild type BALB/c females, and wild type FVB/N males were mated to 1-4 wild type FVB/N females, and plug tested the following morning. BALB/c and FVB/N embryos were harvested at various times between E8.5 and E9.5 to determine the approximate time of closure 2, which can vary depending on the strain. Closure 2 fusion occurred at ~E9.25 in BALB/c mice, and therefore these embryos were harvested between 5:00 am and 7:00 am on day 9 of gestation. Closure 2 fusion in FVB/N embryos occurred earlier in gestation, at ~E8.75, and embryos of this strain were collected between 5:00 pm and 7:00 pm on day 8 of gestation. Embryos were removed from the uterus under a dissecting microscope at 25X magnification, and the cranial region was examined under 50X magnification to determine the status of closure 2. At this point the somites were also counted using 50X magnification. Any embryos that were at a developmental stage immediately before or after the fusion of the neural folds at closure point 2 were chosen for fixation. Any embryos that were slightly later in development, but in which the anterior neuropore and the hindbrain neuropore remained open, were also fixed.

2.8.2 Fixation and drying of embryos

Embryos were fixed in 2.5% gluteraldehyde in 1x PBS at 4°C for 1-3 days. Following fixation, embryos were dehydrated using an ethanol gradient. Initially two 5 minute washes in 1x PBS were done, followed by one 5 minute wash in each of the following: 20%, 40%, 60%, and 80% ethanol in 1x PBS. Next the embryos were washed twice for 5 minutes in 95% ethanol in 1x PBS and four times for 10 minutes in 100% ethanol. The neural folds of fixed embryos were photographed using a Wild M8 Dissecting Microscope with a Nikon LM CCD Digital Camera. Embryos were stored for up to 3 months in 100% ethanol at -20°C. Embryos were chemically dried using hexamethyldisilizane (HMDS). Embryos that were initially stored in 100% ethanol were transferred to 100% HMDS through a graded series of ethanol-HMDS mixtures. The embryos were washed once for 10 minutes each in the following mixtures: 2 ethanol:1 HMDS, 1 ethanol:1 HMDS, 1 ethanol:2 HMDS. Embryos were then washed twice for 10 minutes in 100% HMDS and stored in 100% HMDS at room temperature until being mounted onto stubs.

2.8.3 Gold coating and Scanning Electron Microscopy

From the BALB/c strain, 12 embryos were collected that were at the appropriate developmental stage to illustrate closure 2, as described above, and 8 were collected from the FVB/N strain. These embryos were mounted onto adhesive aluminum SEM stubs. The embryos were positioned on their backs, so that the forebrain is facing upwards, to view closure 2. The embryos were sputter coated with gold using a Hummer sputtering system (Anatech Ltd.). Following coating, the stubs were inserted into a Philips/FEI LaB6 Environmental Scanning Electron Microscope to be photographed.

Table 2. Primer sequences used in this study.

Primer Name	Primer Location	Sequence 5’-3’
*Cecr2 7iF4	*M. mu Cecr2* gene	ccc cat tta ttt gct tga gct g
*Cecr2 7iR4	*M. mu Cecr2* gene	cac gaa caa tgg aag gaa tga
*Sry Fwd	*M. mu Sry* gene	gag agc atg gag ggc cat
*Sry Rev	*M. mu Sry* gene	cca ctc ctc tgt gac act
*pGT1 R4	pGT1 genetrap vector	acg cca tac agt cct ctt cac atc
**SpWT Fwd	*M. mu Pax3* gene	aca acg cct gac gtg gag aa
**SpWT Rev	*M. mu Pax3* gene	ggc tga tag aac tca ctg ga
**SpMut Rev	*M. mu Pax3* gene	ggc tga tag aac tca cac ac
Spl F1	*M. mu Pax3* gene	acc tct ctg gcc ttt cac ttg
Spl R1	*M. mu Pax3* gene	tac gtt agc tgg gcc ttt gag
GTL	GTROSA53 genetrap vector	ctc gcg gtt gag gac aaa ct
GTLacZR1	GTROSA53 genetrap vector	ccg tgc atc tgc cag ttt ga
ShrmFor2	*M. mu shroom* gene	ggc ccc aga ctc acc ata atc
ShrmR1	GTROSA53 genetrap vector	gag ttt gtc ctc aac cgc gag c
ShrmRevLD	*M. mu shroom* gene	tgg cta tcc tct ggc tac aca
Smarca2 I7Fwd	*M. mu Smarca2* gene	cta ggc tta cag tca gtc at
Smarca2 I8Rvs	*M. mu Smarca2* gene	gca ggt tat ctt ctc agt ct
Smarca2 I8Fwd	*M. mu Smarca2* gene	gct tgg ctc atg gtc tgt tg
Smarca2 I9Rvs	*M. mu Smarca2* gene	ctt cgt gtc tgt gta tac ttg g
Smarca2 I10Fwd	*M. mu Smarca2* gene	aga gcc tcc tat gac aca ag
Smarca2 I12Rvs	*M. mu Smarca2* gene	ctt cag agc cta ccc aaa tg
Smarca2 I13Fwd	*M. mu Smarca2* gene	atg cgt agt gtg gcc ctg at
Smarca2 I14Rvs	*M. mu Smarca2* gene	cca gga tga caa cag acc ag
Smarca2 I14Fwd	*M. mu Smarca2* gene	ggg aca ctc agc ata cag ca
Smarca2 I15Rvs	*M. mu Smarca2* gene	ccc atg cca cta ttc tgt ct
Smarca2 I15Fwd	*M. mu Smarca2* gene	gcc tct tac ctg cat agc tt
Smarca2 I17Rvs	*M. mu Smarca2* gene	tcc aat gac caa atg ata ctg tt
Smarca2 I17Fwd	*M. mu Smarca2* gene	gga agc cac tgt acg tct gt
Smarca2 I18Rvs	*M. mu Smarca2* gene	atc cca ccc act gag caa ac
Smarca2 I18Fwd	*M. mu Smarca2* gene	agg agc tga gac ata gac ac
Smarca2 I19Rvs	*M. mu Smarca2* gene	acc tgc cat gat ttc act tg
Smarca2 I19Fwd	*M. mu Smarca2* gene	atg gtg ctc ctg tcc tca ag
Smarca2 I21Rvs	*M. mu Smarca2* gene	gcc ttc cta act agc aca ct
Smarca2 I21Fwd	*M. mu Smarca2* gene	cgc ttt gaa gat gcc cta ga
Smarca2 I22Rvs	*M. mu Smarca2* gene	caa gga ggc tgg cta tgt gt
Smarca2 I22Fwd	*M. mu Smarca2* gene	cgc atg gtt tag gag ctg gt
Smarca2 I23Rvs	*M. mu Smarca2* gene	tgc agg ccc act tct caa ca
Smarca2 I23Fwd	*M. mu Smarca2* gene	ggg tgc aca tct aaa gga ac
Smarca2 I24Rvs	*M. mu Smarca2* gene	ggg cag aac aca gaa ata gc
Smarca2 I24Fwd	*M. mu Smarca2* gene	agc cca gac ttc ctc att ag
Smarca2 I25Rvs	*M. mu Smarca2* gene	acc gtt aga ttt ccc aag tc
Smarca2 I27Fwd	*M. mu Smarca2* gene	ctc ctt cgt tga tga ctg tt
Smarca2 I28Rvs	*M. mu Smarca2* gene	gca cat cct ctc aag tcc ta

Smarca2 I28Fwd	*M. mu Smarca2* gene	gct ttc act cca ctc cca ga
Smarca2 I30Rvs	*M. mu Smarca2* gene	tgg cag gaa gca cga gta ga
Smarca2 I30Fwd	*M. mu Smarca2* gene	gga agc cag tga cta agg ag
Smarca2 I31Rvs	*M. mu Smarca2* gene	gga tgg agc ctc aca gtc ta

*Banting et al. 2005

**Machado et al. 2001

I/i designates that the primer is in an intron. The number of the intron follows the I in the primer name.

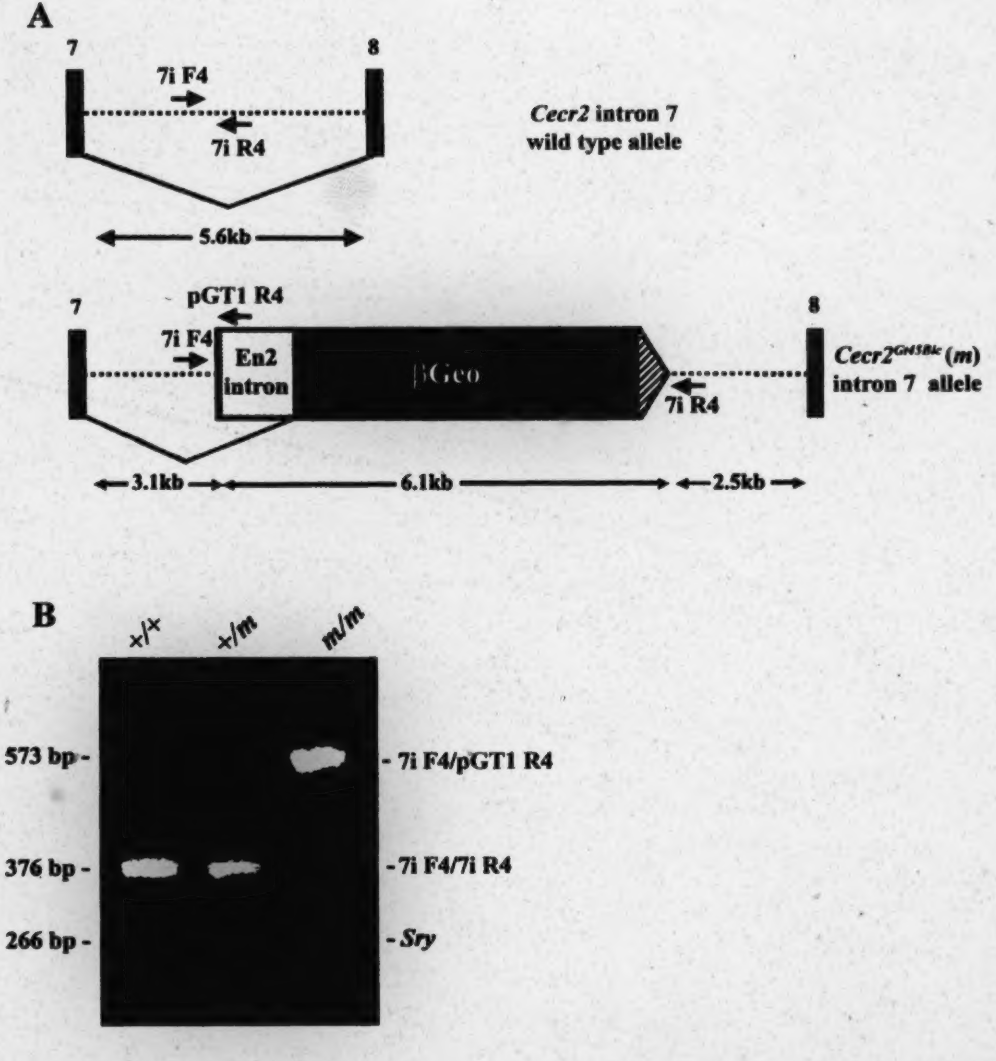
A
7
8
7i F4
7i R4
Cecr2 intron 7
wild type allele
5.6kb
7
pGT1 R4
7i F4
En2
intron
βGeo
7i R4
8
Cecr2^Gt45Bic (m)
intron 7 allele
3.1kb
6.1kb
2.5kb
B
+/+
+/m
m/m
573 bp
376 bp
266 bp
7i F4/pGT1 R4
7i F4/7i R4
Sry

Figure 7. ***Cecr2*^{Gt45Bic} mutant allele and genotyping PCR.** (A) The binding sites of the three *Cecr2* genotyping primers in intron 7 are shown on the wild type *Cecr2* allele, and on the *Cecr2*^{Gt45Bic} mutant allele. (B) Sample genotyping PCR gel electrophoresis image of the three potential bands produced. The 573 bp band is produced from the mutant allele, and the 376 bp band is produced from the wild type *Cecr2* allele. The 266 bp band is amplified from the *Sry* gene in male mice (Adapted from Banting et al. 2005).

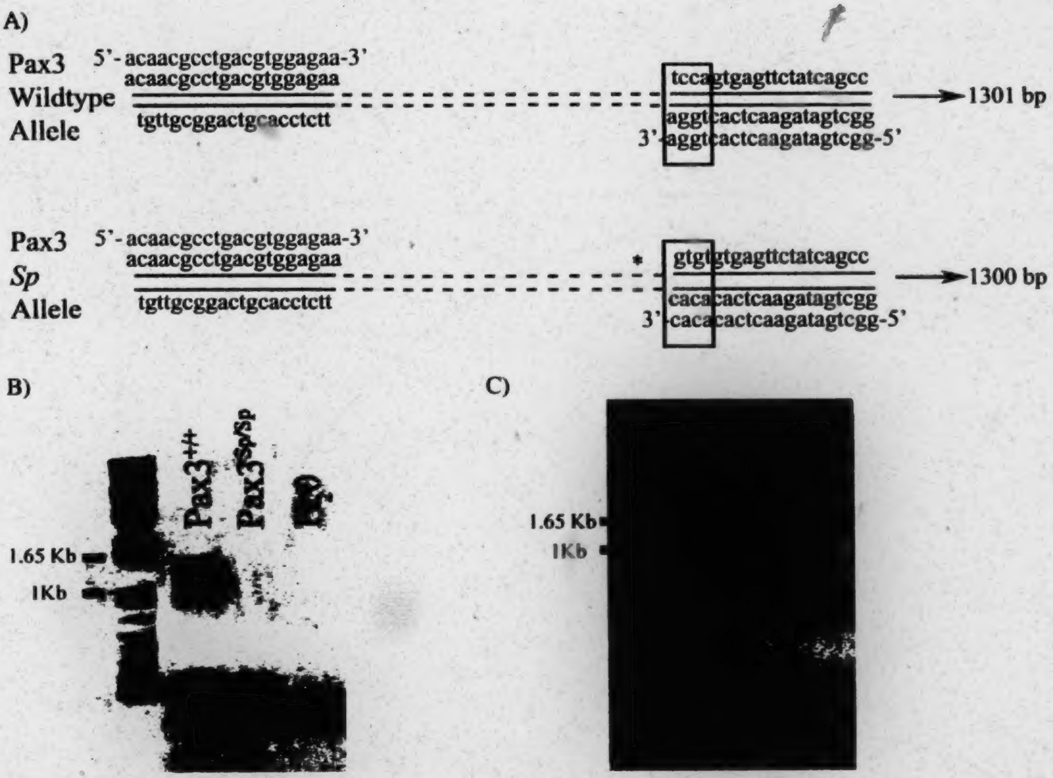
A)
Pax3 Wildtype Allele
5'- acaacgcctgacgtggagaa-3'
acaacgcctgacgtggagaa
tgttgcggactgcacctctt
tccagtgagttctatcagcc
aggtcactcaagatagtcgg
3'-aggtcactcaagatagtcgg-5'
1301 bp
Pax3 Sp Allele
5'- acaacgcctgacgtggagaa-3'
acaacgcctgacgtggagaa
tgttgcggactgcacctctt
*
gtgtgtgagttctatcagcc
cacacactcaagatagtcgg
3'-cacacactcaagatagtcgg-5'
1300 bp
B)
Pax3+/+
Pax3Sp/Sp
1.65 Kb
1Kb
C)
1.65 Kb
1Kb

Figure 8. *Pax3* wild type and *Sp* allele sequences, primer binding sites, and a sample gel electrophoresis image of the *Pax3* genotyping PCR. Diagrams of the *Pax3* wild type and *Sp* alleles, showing the location of the SpWTFWD primer (red), which is common to both alleles. (A) The SpWTREV primer (blue) binds specifically to the wild type allele, and the SpMUTREV primer (green) binds specifically to the *Pax3*^{Sp} allele. The boxed sequence represents the 4 bp which vary between the two alleles and the * represents the deletion. SpWTREV and SpMUTREV primers can amplify 1301 bp, and 1300 bp bands respectively, with the SpWTFWD primer, depending on the allele. Shown below is a sample picture of a genotyping PCR for the wild type allele, containing SpWTFWD and SpWTREV primers (B), and for the *Sp* allele, containing SpWTFWD and SpMUTREV primers (C).

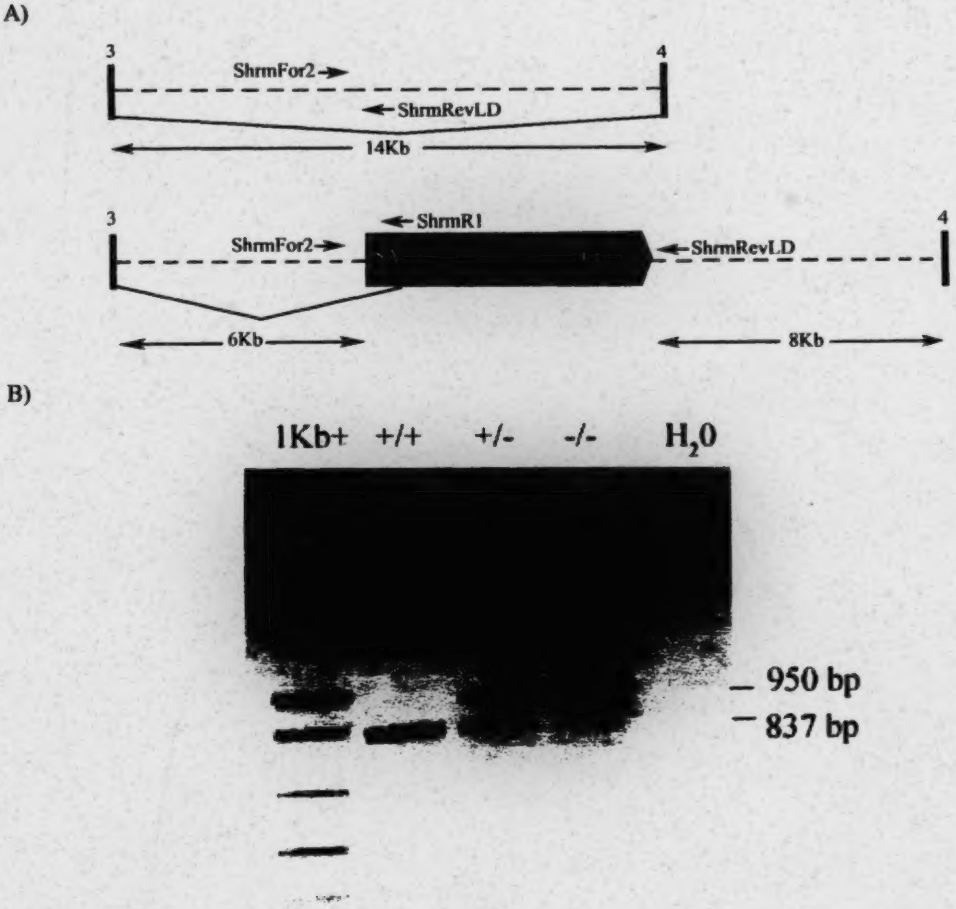
A)
3
4
ShrmFor2
ShrmRevLD
14Kb
3
ShrmR1
4
ShrmFor2
ShrmRevLD
6Kb
8Kb
B)
1Kb+
+/+
+/-
-/-
H$_2$0
950 bp
837 bp

Figure 9. *Shroom*^{GtROSA53Sor} mutant allele and sample genotyping PCR image. (A) The binding sites of the ShrmFor2, ShrmRevLD, and ShrmR1 primers on the wild type and *GtROSA53Sor* alleles of the *shroom* gene. (B) Gel electrophoresis image of the *shroom*^{GtROSA53Sor} genotyping PCR showing the wild type band at 837 bp and the band produced from the mutant allele at ~950 bp (genotyping performed by Lisa Rae Chisholm-Dumesnil).

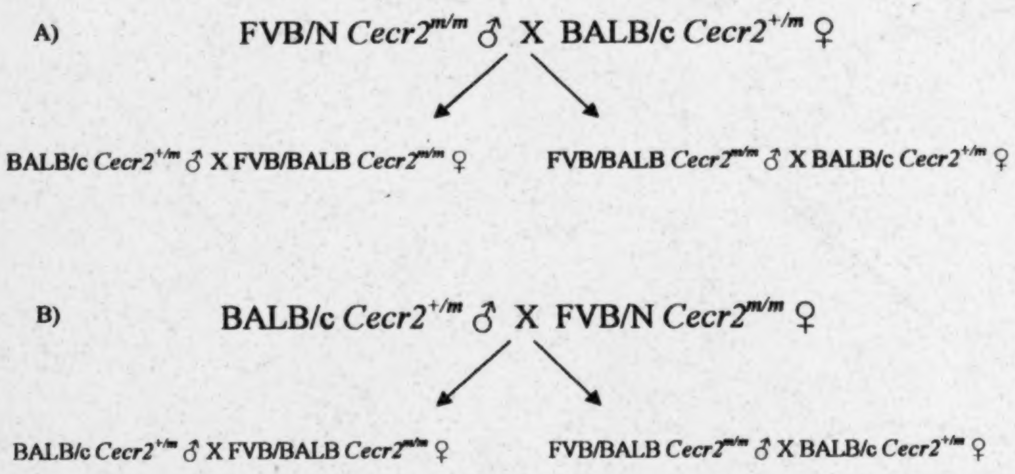
A)
FVB/N *Cecr2*$^{m/m}$ ♂ X BALB/c *Cecr2*$^{+/m}$ ♀
BALB/c *Cecr2*$^{+/m}$ ♂ X FVB/BALB *Cecr2*$^{m/m}$ ♀
FVB/BALB *Cecr2*$^{m/m}$ ♂ X BALB/c *Cecr2*$^{+/m}$ ♀
B)
BALB/c *Cecr2*$^{+/m}$ ♂ X FVB/N *Cecr2*$^{m/m}$ ♀
BALB/c *Cecr2*$^{+/m}$ ♂ X FVB/BALB *Cecr2*$^{m/m}$ ♀
FVB/BALB *Cecr2*$^{m/m}$ ♂ X BALB/c *Cecr2*$^{+/m}$ ♀

Figure 10. Mating strategy used to produce embryos for linkage analysis. (A) FVB/N *Cecr2* mutant males were crossed to BALB/c *Cecr2* heterozygous females, and the resulting male and female *Cecr2*$^{m/m}$ progeny were crossed to BALB/c *Cecr2*$^{+/m}$ mice to collect embryos. (B) The reciprocal cross was done using BALB/c *Cecr2* heterozygous males and FVB/N *Cecr2*$^{m/m}$ females. Both the male and female FVB/BALB *Cecr2*$^{m/m}$ progeny from this reciprocal cross were backcrossed to BALB/c *Cecr2*$^{+/m}$ mice to collect embryos.

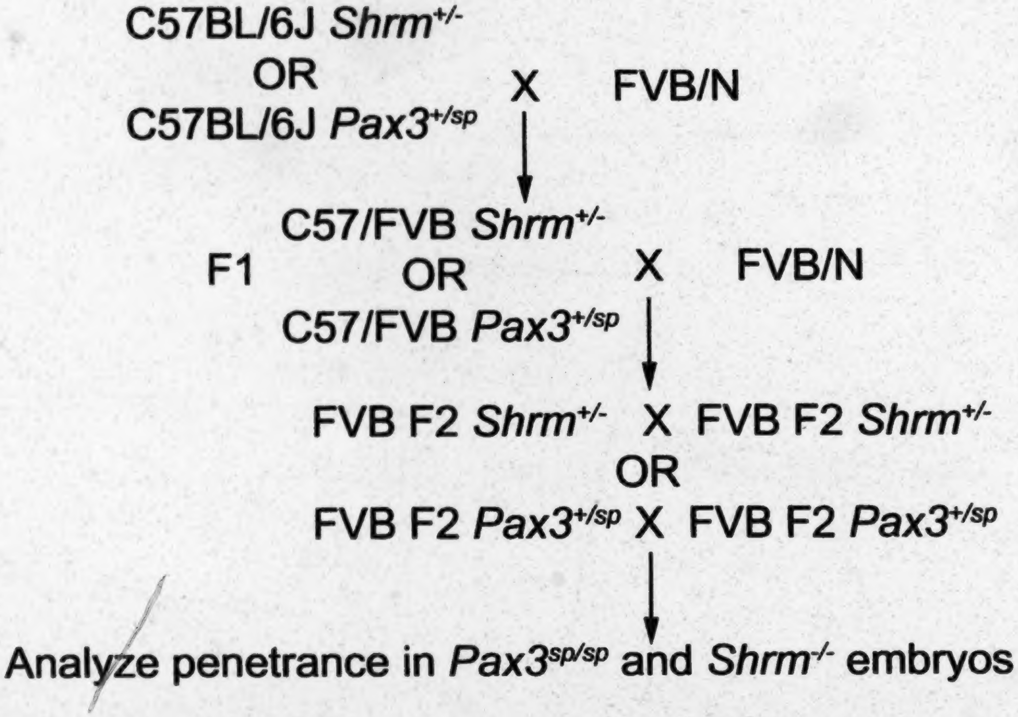
C57BL/6J *Shrm*$^{+/-}$
OR
C57BL/6J *Pax3*$^{+/sp}$
X
FVB/N
F1
C57/FVB *Shrm*$^{+/-}$
OR
C57/FVB *Pax3*$^{+/sp}$
X
FVB/N
FVB F2 *Shrm*$^{+/-}$ X FVB F2 *Shrm*$^{+/-}$
OR
FVB F2 *Pax3*$^{+/sp}$ X FVB F2 *Pax3*$^{+/sp}$
Analyze penetrance in *Pax3*$^{sp/sp}$ and *Shrm*$^{-/-}$ embryos

Figure 11. Series of crosses used to transfer the *shroom*^{GtROSA53Sor} mutation, and the *Pax3*^{Sp} mutation, from pure C57BL/6J backgrounds to a predominantly FVB/N mixed background. C57BL/6J heterozygotes for the *shrm* and *Pax3* mutant alleles were crossed to pure FVB/N females and the resulting progeny were crossed again to pure FVB/N females to ensure the X chromosome was derived from the FVB/N strain (- = *GtROSA53Sor*). At the F2 generation, in which the genetic background is ~75% FVB/N, *Pax3* heterozygotes were intercrossed, and *shrm* heterozygotes were intercrossed, and a penetrance analysis of the various phenotypes for each mutation was done.

Chapter 3. Results

3.1 Mapping genetic modifiers of the exencephaly phenotype in *Cecr2*^{Gt45Bic} mutant mice

3.1.1 Dominant modifiers exist in the FVB/N genetic background

The *Cecr2*^{Gt45Bic} mutation has been examined on various backgrounds, including two pure genetic backgrounds, FVB/N and BALB/c. Originally the *Cecr2*^{Gt45Bic} mutation was on a BALB/129P2 mixed background, and the penetrance of exencephaly in homozygous mutants was determined by Graham Banting to be 67% (24/36) (Banting et al. 2005). Mice on a BALB/129P2/FVB mixed background that were heterozygous for the *Cecr2*^{Gt45Bic} allele were crossed and backcrossed to pure BALB/c and pure FVB/N mice for 5 or 6 generations and a penetrance analysis was repeated on these incipient congenic backgrounds, which were ~96.9% BALB/c and ~96.9% FVB/N respectively for the F5 generation, and ~98.4% BALB/c and ~98.4% FVB/N respectively for the F6 generation. Tanya Ames found the penetrance of exencephaly in *Cecr2* homozygous mutant embryos to be 74% on the BALB/c background and 0% on the FVB/N background **(Table 3)**. This observation strongly indicated the presence of genetic modifier(s) that differ between the BALB/c and FVB/N strain, and affect the frequency of exencephaly in *Cecr2*$^{m/m}$ mutant mice.

To examine the effect of modifiers in a heterozygous state (FVB/BALB) on the penetrance of exencephaly in *Cecr2*^{Gt45Bic} mutants, I intercrossed the two strains. *Cecr2*$^{m/m}$ and *Cecr2*$^{+/m}$ mice from an FVB/N incipient congenic line at generation F7, at which point 99.2% of alleles are FVB/N, or F8, at which point 99.6% of alleles are FVB/N, were crossed to BALB/c *Cecr2*$^{+/m}$ mice, which were also at generation F7 or F8.

This was done while continuing to produce congenic lines for linkage analysis. The genetic background in female embryos collected from this cross is almost completely heterozygous for all alleles, including the X chromosome. Male embryos, however, inherit the X chromosome from the maternal strain, and therefore the cross was done reciprocally. The embryos collected from these crosses were observed for exencephaly, and genotyped using the *Cecr2*^{Gt45Bic} and *Sry* multiplex PCR. Of the 35 *Cecr2*$^{m/m}$ embryos examined, 1 female with exencephaly was found (2.9%), and of the 39 *Cecr2*$^{+/m}$ embryos examined, 1 exencephalic female was found which also displayed facial clefting (2.6%) **(Table 3)**. Facial clefting has only been found in one other embryo during the study of the *Cecr2*^{Gt45Bic} mutation, and therefore is likely a spontaneous effect, though it could be a background dependent effect with extremely low penetrance. The FVB/N modifier(s) are therefore able to produce an almost complete resistance to exencephaly in a heterozygous state and can be considered dominant or semi-dominant. This observation helped determine the mapping strategy which would allow modifier region(s) to be located using linkage analysis.

3.1.2 Collection of embryos and penetrance analysis

A sample set of embryos for linkage analysis was collected and scored for the presence of exencephaly. The genomes of these embryos were a mixture of heterozygous FVB/BALB regions, and homozygous BALB/c regions. Both the BALB/c and FVB/N lines used in this experiment were now congenic, meaning they were at generation F10 or greater and that 99.9% of the alleles in the background were derived from the BALB/c and FVB/N genomes respectively. The embryos were collected from an intercross of FVB/N *Cecr2*$^{m/m}$ mice with BALB/c *Cecr2*$^{+/m}$ mice, followed by a backcross of resulting

Cecr2$^{m/m}$ F1 FVB/BALB progeny to BALB/c *Cecr2*$^{+/m}$ mice **(Figure 10)**. To produce a sample size of ~100 exencephalic embryos from this cross, 706 total embryos were collected. Of the embryos collected, 339 were *Cecr2*$^{+/m}$, one of which was exencephalic (0.29%), and 360 were *Cecr2*$^{m/m}$, 101 of which were exencephalic (28.1%) **(Figure 12)**. A sample of 94 exencephalic *Cecr2*$^{m/m}$ embryos was used for linkage analysis in addition to 94 non-exencephalic *Cecr2*$^{m/m}$ embryos, which were chosen to represent samples from all the types of reciprocal crosses done **(Figure 10)**. The samples were used to correlate the exencephaly phenotype to region(s) of the genome which were homozygously derived from the susceptible BALB/c strain significantly more frequently than expected through random segregation. The non-exencephalic embryos were used to cancel the effect of segregation distortion, where the allele frequency differs from random due to some non-related cause, and to create a sample of embryos which should be enriched for the resistant F/B genotype in the region of a potential modifier. To complete the linkage analysis, these samples were sent to Dr. Lucy Osborne's laboratory at the University of Toronto for microsatellite genotyping throughout the entire genome.

3.1.3 Microsatellite and SNP genotyping of exencephalic and unaffected embryos

Dr. Osborne's lab used 112 microsatellites that differ between the FVB/N and BALB/c strains to genotype the 94 exencephalic embryos, and used parental DNA samples from pure FVB/N and BALB/c mice as controls. The 112 microsatellites were spread throughout the genome ~20 cM apart, including on the X chromosome **(Figure 13)**. The allele ratios (FVB/BALB: B/B) were examined for all of the microsatellites, and any which varied from the random inheritance pattern of 47 F/B: 47 B/B, were also tested on the unaffected embryo samples. An allele ratio of ~55:39 (alleles with $p<0.1$)

in either direction for the exencephalic embryos was considered significant enough to test the unaffected embryos. The subset of these 112 microsatellites that showed this degree of variation were located on chromosomes 2, 14, 15 and 19. The microsatellites tested on both exencephalic and non-exencephalic samples were: D2Mit92, D2Mit249, D2Mit101, D2Mit395, D14Mit60, D15MIT270, D15Mit209, D17Mit51, D19Mit31, D19MIT63 and D19Mit88. No unaffected embryos were genotyped for microsatellites on the X chromosome. These 11 microsatellites were analyzed by combining the "expected genotypes" and the "unexpected genotypes" from both groups, which allows the mirror image effect between the two groups to be analyzed and corrects for any segregation distortion (Materials and Methods, 2.6.2). The only significant region found, based on a level of significance of $p \leq 0.001$, was on chromosome 19 in the region of D19MIT63 and D19Mit88 **(Table 4)**. The region on chromosome 2, with a peak at D2Mit249, had a p value of 0.00558, which was not considered significant based on this analysis, but may be suggestive of a weaker modifier. .This region, however, showed an opposite effect to that expected, meaning that the F/B genotype, rather than the B/B genotype, was seen more frequently than expected in the exencephalic embryos.

In order to confirm the chromosome 19 linkage region, define the significance levels of various points along the chromosome, and chart a "peak" area, 16 SNPs were chosen on chromosome 19 **(Figure 14)**. The exencephalic and non-exencephalic embryos were all tested for these SNPs, which allowed an examination of markers spaced ~3 Mb apart along the entire chromosome. All of the markers between rs3090325 and rs13483654 were found to be significant as well as rs3709671 **(Table 5)**. The peak of significance is at the marker rs3677115 **(Figure 15)**. The region of significance is from

~23 Mb to ~58 Mb on chromosome 19 with the peak at ~40.1 Mb. This 35 Mb region was scanned for possible candidate genes (See section 3.1.6).

3.1.4 Linkage analysis

A further analysis of the microsatellite and SNP data was done by Qian Li in Dr. Gary Churchill's lab at Jackson Laboratories. This analysis confirmed the chromosome 19 linkage and the possible linkage on chromosome 2 which were found using the statistical methods mentioned above. The analysis was done using Rqtl 1.02-26 software, R version 2.3.1. Mainscan results, using the model y=QTL, located two regions with lod scores above the significance level of 37%, which is considered the suggestive threshold **(Figure 16A)**. Lod scores representing significance thresholds of 37%, 90% and 95% were determined using 1000 permutation tests for the mainscan analysis using the y=QTL model. The 37% significance threshold was considered because it is the standard level of suggestive linkage which is reported for a whole genome QTL analysis which uses a permutation based method to determine the significance thresholds (Lander and Krugylak 1995). QTL regions which exceed this suggestive linkage threshold, but not the 95% threshold, are generally reported for complex traits, although these values are likely to occur once in a genome scan due to chance. This standard for reporting linkage results for complex traits is designed to avoid overlooking minor effect genes which may be significant when combined with the data from multiple studies of the same complex trait. This analysis scans the genotype and phenotype data to produce a graph of the lod scores for all the markers against their location in the genome. The y=QTL model does not take into account other data, like the sex of the embryo. The first region, which is the rs3677115 marker at ~40.1 Mb on chromosome 19, shows the strongest linkage and has a lod score of 4.4 which places it above the 95% significance level, which is represented by a lod score of 2.1129 **(Figure 16B)**. The second region is located on chromosome 2 at ~48 cM or 103 Mb, and has a lod score of 1.5 which is slightly above the suggestive threshold. The X chromosome could not be included in this analysis as very few samples represented recombination on the X chromosome, due to the backcross method used for embryo collection. An effect plot for the rs3677115 marker on chromosome 19 shows that a B/B genotype in this location increases the frequency of exencephaly by ~30-35% from a B/F genotype **(Figure 16C)**. In an effect plot, individuals with exencephaly are scored as 0 and unaffected individuals were scored as 1, and the mean scores for each genotype group are plotted. This shows the effect of each genotype on the frequency of exencephaly. The chromosome 2 region is far less significant, as indicated by the lod score. In the case of the chromosome 2 linkage region, the B/F genotype, as opposed to the B/B genotype, is linked to the exencephaly phenotype. The chromosome 2 region is therefore having an effect in the opposite direction, and the B/F phenotype appears to be the susceptible genotype in this region.

3.1.5 Female predominance and the existence of X chromosome modifiers

The *Cecr2*$^{m/m}$ backcross embryos, which were on a mixed FVB/BALB background, developed exencephaly in a female predominant manner, as was seen for other backgrounds examined. Female embryos developed exencephaly at a penetrance of 37% whereas only 19% of males developed exencephaly **(Figure 17)**. This sex specific penetrance varied depending on the inheritance of the X chromosome. The difference in penetrance between males and females, as well as the total penetrance, varied based on the genotype of the X chromosome **(Figure 17)**. In cross type 1, the X chromosome is derived from the BALB/c strain in male and female embryos, and the total penetrance is 34.7%. In this cross the penetrance variation is very small between males (32.8%) and females (36.7%). In cross type 2, in which females are heterozygous for the X chromosome and males have a BALB/c X chromosome, 27.1% of females are exencephalic and 15.6% of males, giving a total penetrance of 21.5%. Finally, in cross type 3, females which have one BALB/c derived X chromosome and one that is derived from recombination between BALB/c and FVB/N, develop exencephaly at a penetrance of 43.8%. Males from this cross have an X chromosome which is also a mixture of BALB/c and FVB/N alleles, and develop exencephaly at a penetrance of 9.6%, giving a total penetrance of 26.7%. These penetrance rates might be useful in assessing the contribution of any potential modifiers on the X chromosome. The pattern of these variations, however, is complex and does not clearly indicate that modifiers exist on the X chromosome. Linkage analysis, done by Gary Churchill's Lab, could also not confirm the existence of any X chromosome modifiers **(Figure 16A)**. The X chromosome data was excluded from further analysis due to the small sample size and the lack of data for unaffected controls, which led to artificial peaks in the preliminary analysis.

The linkage results for the X chromosome were analyzed using only the 32 exencephalic embryos produced from cross type 3. These 32 embryos are the only samples which represent a potential crossover on the X chromosome which is inherited from the FVB/BALB mother. For these 32 exencephalic embryos, the total number of X^B/X^B genotypes was combined with the number of X^B/Y genotypes, and the X^B/X^F genotypes were combined with the X^F/Y genotypes for each of the four markers on the X chromosome **(Table 6)**. The unaffected embryos were not genotyped for these markers, so a $\chi 2$ analysis comparing expected genotype ratios (1:1) to the observed frequencies was used. The DXMit140 marker showed the largest deviation from the expected genotypic frequency, with a p value of 0.077. This was not below the $p \leq 0.05$ level of significance, but this may be due to the small sample size available. These results suggest, but cannot confirm, a potential modifier on the X chromosome.

3.1.6 Locating and analyzing candidate genes in the modifier region

Four interesting candidate genes within this 35 Mb region were noted after an initial analysis, based on known functions of genes in the region, though ~260 known genes and ~280 more predicted genes are in this region (See Appendix). These genes were *Cyp26a1*, a gene encoding a retinoic acid catabolizing enzyme (Abu-Abed et al. 2001; Sakai et al. 2001), *Pax2*, which is involved in neural patterning in the midbrain/hindbrain (MB/HB) region (Favor et al. 1996), *Smarca2*, which encodes an ATP dependent chromatin remodeling protein (Reyes et al. 1998), and *Tect3*, which is closely related to the *Tectonic* gene, which is involved in neural tube patterning (Reiter and Skarnes 2006) **(Figure 18)**. Both the *Cyp26a1* and *Pax2* genes have been knocked out in mice and the mutant lines develop exencephaly (Abu-Abed et al. 2001; Sakai et al. 2001; Torres et al. 1996). *Tect3* was noted because of a potential role in neural tube development, and because it contains a known SNP between the BALB/c and FVB/N strains which results in a non-synonymous change in a conserved residue. *Smarca2* was noted because it is involved in chromatin remodeling, as is the SNF2L protein which interacts with CECR2 in human cells (Banting et al. 2005). Preliminary sequence analysis was done on the *Smarca2* gene. *Smarca2* contains 6 conserved protein motifs: an HSA domain (domain in helicases and associated with SANT domains), a BRK domain (Brahma-KIS domain), an SNF2_N domain (SNF2 family N-terminal domain), a DEXHc domain (DEXH-box helicases), a HELICc domain (Helicase superfamily c-terminal domain) and a Bromodomain **(Figure 19)**. Sequencing was begun on these conserved motifs, by PCR amplifying fragments from BALB/c and FVB/N genomic DNA which contained exons flanked by splice acceptor and donor sequences. Two different genomic samples were used for each strain and the sequence was confirmed using 4 individual sequencing reactions.

Exons 14 and 19, which encode part of the SNF2_N domain, were sequenced and one nucleotide polymorphism was found at position 3020 in exon 19 (gi:51593083). The FVB/N strain contains a C at this position, whereas the BALB/c strain has a T. This nucleotide variation, however, conserves the proline residue at this position. Exon 15, which is in the region of the DEXHc and SNF2_N domains, had no polymorphisms. Exons 22, 24 and 25, within the HELICc domain, were sequenced and one polymorphism was found in exon 24 at position 3465. This nucleotide was a T in BALB/c and a C in FVB/N, but both sequences encode a leucine at this position. Exon 28 and 31, within the bromodomain, were also sequenced and no polymorphisms were found. Of the initial 8 exons sequenced, no variation in the protein sequence was found between BALB/c and FVB/N and no mutations existed in splice acceptor or donor sequences.

3.2 Characterizing the effect of the FVB/N modifier(s) on two other NTD causing mutations

To begin to determine whether the modifier(s) in the FVB/N strain that reduce the penetrance of exencephaly in the *Cecr2*^{Gt45Bic} mutant line can also reduce penetrance in other NTD mutant lines, two other mutations were bred onto predominantly FVB/N backgrounds. This might indicate whether the modifier is specific to the *Cecr2* pathway, or if it affects some general aspect of neurulation. Mutants for the *Pax3* and *shroom* genes were chosen because the pathways of these genes, and their causative roles in neurulation, are fairly well established, and because they result in multiple types of NTDs. This allows a possible determination of the types of pathways which can be affected by the modifier(s) and allows the effect of the modifier(s) on closure of multiple regions along the neural tube to be examined.

3.2.1 Penetrance analysis of exencephaly and spina bifida in C57BL/6J *Sp* mutants

The *Sp* mutation in the *Pax3* gene arose spontaneously on a C57BL/6J background. The *Sp* homozygous mutant embryos develop two types of NTDs, exencephaly and spina bifida. Spina bifida was originally characterized as being completely penetrant, whereas the penetrance of exencephaly was 56% (Auerbach 1954). The *Sp* mutants also have cardiac outflow tract defects and consequently die at ~E14. Heterozygous *Sp* mutants are generally normal, with the exception of a white belly spot due to a defect in melanocyte development, which is 100% penetrant (Auerbach 1954). The *Sp* mutation has been maintained on a C57BL/6J background for >50 years, and mutations may have arisen during this period which modify the phenotype. This idea is supported by an observation that the penetrance of exencephaly in the *Sp* mouse line is well below the previously reported penetrance of 56% (4th International NTD conference, September 10-13, 2005). The penetrance was therefore reanalyzed in the C57BL/6J *Sp* mice within our mutant line at the HSLAS facility. Adult mice were genotyped using the presence or absence of the belly spot, and embryos were genotyped using the *Sp* genotyping PCR. Embryos were collected at E12.5 to avoid any effects of lethality in homozygotes. The embryos collected, fit the Mendelian ratio expected from a cross of two heterozygotes, 1:2:1, indicating that there was no significant loss of *Sp/Sp* embryos ($\chi 2$ goodness-of-fit test, p=0.286). The penetrance of spina bifida was 100% (35/35) in homozygous mutants as previously reported, and 1/63 heterozygotes developed spina bifida **(Table 7)**. Exencephaly, however, differed from the reported penetrance of 56%. Of the 35 homozygotes examined, only 9 developed exencephaly (25.7%) **(Table 7)**.

3.2.2 Penetrance analysis of exencephaly and spina bifida in *Sp* embryos on a predominantly FVB/N genetic background

The C57BL/6J *Sp* heterozygotes were crossed to FVB/N mice for two generations to produce a ~75% FVB/N genetic background. The FVB/N F2 mice were then intercrossed and the penetrance of spina bifida and exencephaly were reexamined. C57BL/6J mice have a black coat, on which the white belly spot is visible and could be used to genotype the heterozygotes. FVB/N mice have a white coat, and the FVB/C57 F1 mice have an agouti coat, however the agouti mice do not develop the belly spot. All adult mice and embryos were therefore genotyped using the *Sp* genotyping PCR. The penetrance of spina bifida on this predominantly FVB/N background dropped significantly from 100% (35/35) to 73.1% (19/26) ($\chi 2$ goodness-of-fit test, p=0.001) **(Table 7)**. Exencephaly also dropped from 25.7% (9/35) to 11.5% (3/26) **(Table 7)**. The decrease in the exencephaly phenotype, however, is not statistically significant due to the small number of embryos which develop exencephaly on either background ($\chi 2$ goodness-of-fit test, p=0.168). This produced a much smaller sample size to examine as compared to spina bifida. The Mendelian inheritance of the *Sp* mutation on this background also conformed to a 1:2:1 ratio (χ2 goodness-of-fit test, p=0.101)

3.2.3 Penetrance analysis of various defects in *shroom*^{GtROSA53Sor} mutants on two genetic backgrounds

The *shroom*^{GtROSA53Sor} mutation, which is a genetrap insertion, was originally characterized on a C57BL/6J background (Hildebrand and Soriano 1999). The homozygous mutants develop 4 defects: exencephaly at 100% penetrance (93/93), facial clefting at 87% penetrance (68/78), spina bifida at 23% penetrance (21/93), and defects in ventral closure, which allow herniation of the liver and intestine, at 12% penetrance (7/59) (Hildebrand and Soriano 1999). To confirm the approximate penetrance of these defects in the cryopreserved C57BL/6J line purchased from Jackson Labs, 31 total embryos were examined on the original background. Embryos collected from this line were genotyped by Lisa Rae Chisholm-Dumesnil using the *shroom*^{GtROSA53Sor} multiplex genotyping PCR. Of these 31 embryos, 8 were homozygous for the *shroom*^{GtROSA53Sor} mutation **(Table 8)**. The penetrance of exencephaly was 100% (8/8), the penetrance of craniofacial clefting was 62.5% (5/8) and the penetrance of ventral closure defects was 25% (2/8). The penetrance for these 3 defects was approximately the same as that observed by Hildebrand and Soriano (1999). The 8% (1/12) exencephaly seen in the heterozygotes was also similar to data collected by Hildebrand and Soriano, who observed exencephaly in 8% (21/279) of heterozygotes. The spina bifida penetrance, however, did significantly differ from that observed previously. In my analysis, 87.5% (7/8) of homozygous mutants developed spina bifida, as opposed to the 23% observed by Hildebrand and Soriano (1999).

The C57BL/6J *shrm* heterozygotes were crossed to FVB/N mice for two generations to produce a ~75% FVB/N genetic background. The FVB/N F2 mice were then intercrossed, and the penetrance of the four defects was reexamined. The exencephaly phenotype was completely penetrant on this predominantly FVB/N background (23/23), as on the original background **(Table 8)**. The penetrance of facial clefting was found to be 100% (23/23) and ventral closure defects occurred at a frequency of 13% (3/23) on the mixed background. These penetrance values were not significantly different from the penetrance values seen on the C57BL/6J background, which were 87% and 12% respectively ($\chi 2$ goodness-of-fit test, p=0.07 and p=0.43). No exencephaly was seen in the heterozygotes on this background, which differed from the results seen for the C57BL/6J background in my analysis and the analysis done by Hildebrand and Soriano, which both found 8% penetrance in heterozygotes (1999). The only other difference seen between the two backgrounds was in the penetrance of spina bifida. The penetrance of spina bifida on the predominantly FVB/N background was 8.7% (2/23), which was significantly lower than the penetrance on the C57BL/6J background seen in my analysis, which was 87.5% (7/8) ($\chi 2$ goodness-of-fit test, p=0.000023). The variation between the spina bifida penetrance on the FVB/C57 mixed background (8.7%) and the C57BL/6J background as observed by Hildebrand and Soriano (23%), however, did not differ significantly ($\chi 2$ goodness-of-fit test, p=0.13). The C57BL/6J penetrance seen for spina bifida was not consistent between the previous work, and what was seen in this analysis. The comparison between the two backgrounds using data collected in my analysis is more relevant in this case, as it eliminates most environmental effects, though it is flawed due to the low number of embryos examined.

3.3 Characterization of normal cranial neurulation in FVB/N and BALB/c strains

Exencephaly occurs when the neural folds in the cranial region of the neural tube do not fuse, usually because closure point 2 does not form for one of a variety of reasons. Because the failure of closure 2 occurs in 74% of BALB/c *Cecr2*$^{m/m}$ mice, and closure 2 never fails to occur in FVB/N *Cecr2*$^{m/m}$ mice, closure point 2 in wild type embryos of both strains was examined. To locate ~5-10 embryos from each strain which were undergoing closure site 2 fusion, 130 BALB/c embryos and 85 FVB/N embryos were examined. Within a single litter, embryos varied from immediately following elevation of the cranial neural folds, to being zippered up to the posterior hindbrain region. Embryos within a single litter were observed that were at variable developmental stages, up to 5 somites pairs different. Embryos which were at a developmental stage preceding closure 2 were seen at approximately the same frequency as embryos which had already fused in the forebrain/midbrain (FB/MB) region and zippered up too far for the initial fusion location to be determined. This indicated that this was the most favorable time for observing closure site 2 fusion, though only ~4% of BALB/c and ~7% of FVB/N embryos examined were currently undergoing, or immediately preceding closure 2 fusion. Closure 2 likely occurs over a very short period of time, and therefore is difficult to characterize.

BALB/c embryos undergo closure 2 at ~E9.25, which differs from FVB/N embryos which undergo closure 2 earlier, at ~E8.75. In BALB/c embryos, closure 2 occurred most frequently at the 9 somite stage, but varied between 8 and 10 somites. The point of fusion of the neural folds in the cranial region in BALB/c embryos is at the boundary between the forebrain and the midbrain **(Figure 20)**. Three embryos were found with a small area of fusion in this region, indicating that closure had occurred very recently, and 2 were found which immediately preceded fusion. All of these embryos clearly showed the location of the closure point to be at the FB/MB boundary. In FVB/N embryos closure 2 occurs at the same developmental stage as in the BALB/c strain, which is between 8 and 10 somites, even though this is at an earlier time point in gestation. The neural folds in the cranial region of FVB/N embryos fuse at the same location as in BALB/c embryos, at the FB/MB boundary **(Figure 20)**. This observation was consistent in all 3 embryos found which were immediately following fusion of the neural folds, and in 3 embryos which were collected slightly prior to closure 2. The developmental stage and the location of fusion at closure point 2 did not vary between the two strains.

Table 3. The penetrance of exencephaly in *Cecr2*^{Gt45Bic} mutant mice on two pure genetic backgrounds and a heterozygous FVB/BALB background. The penetrance is highly dependent on the genetic background, and the FVB/N background causes resistance to exencephaly even in a heterozygous state.

	FVB/N			BALB/c			FVB/BALB		
	m/m	+/m[a]	+/+	m/m	+/m	+/+	m/m	+/m	+/+
Exencephaly	0	0	0	35	0	0	1	1	0
Normal	42	99	59	12	110	70	34	38	3
Penetrance (%)	0	0	0	74	0	0	2.9	2.6	0

[a] m=*Cecr2*^{Gt45Bic}, and += wild type *Cecr2* allele

Embryos were collected from incipient congenic BALB/c and FVB/N *Cecr2*^{Gt45Bic} lines at generations F5 to F8.

FVB/N and BALB/c data, collected by Tanya Ames and Amanda Burnham, was published in Banting et al. 2005.

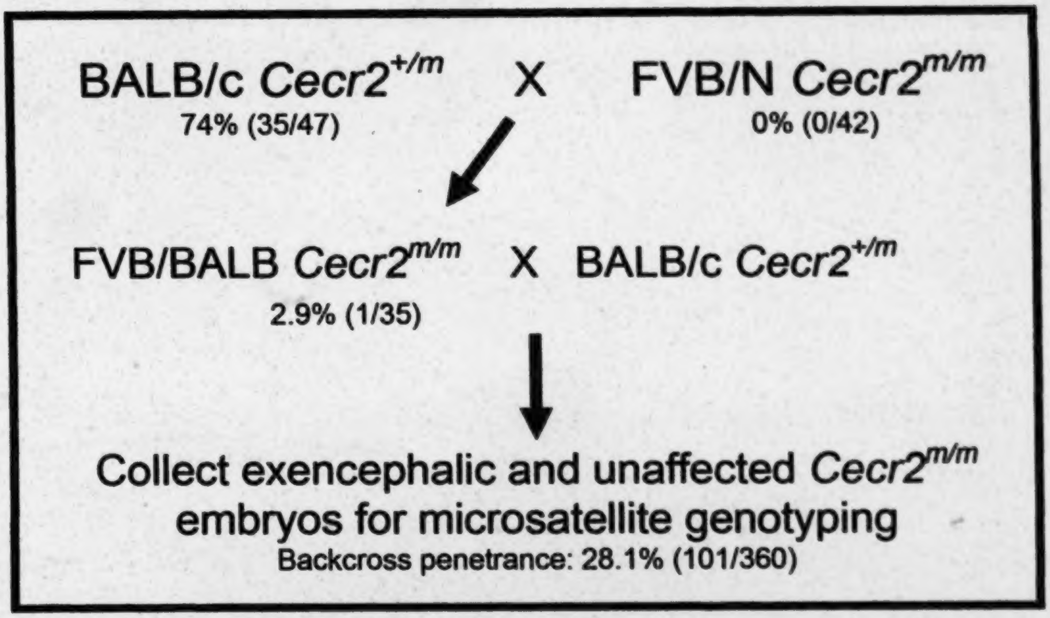
BALB/c $Cecr2^{+/m}$ X FVB/N $Cecr2^{m/m}$
74% (35/47)
0% (0/42)
FVB/BALB $Cecr2^{m/m}$ X BALB/c $Cecr2^{+/m}$
2.9% (1/35)
Collect exencephalic and unaffected $Cecr2^{m/m}$ embryos for microsatellite genotyping
Backcross penetrance: 28.1% (101/360)

Figure 12. Crossing scheme used to produce exencephalic and non-exencephalic embryos for linkage analysis. Heterozygotes from the susceptible strain, BALB/c, were crossed to homozygous *Cecr2* mutants from the resistant strain, FVB/N, and the resulting non-penetrant $Cecr2^{m/m}$ mice were backcrossed to BALB/c $Cecr2^{+/m}$ mice. This produced a sample of embryos with a mixture of F/B and B/B alleles throughout the genome. From this sample, 94 exencephalic and 94 unaffected $Cecr2^{m/m}$ embryos were used for microsatellite genotyping and linkage analysis.

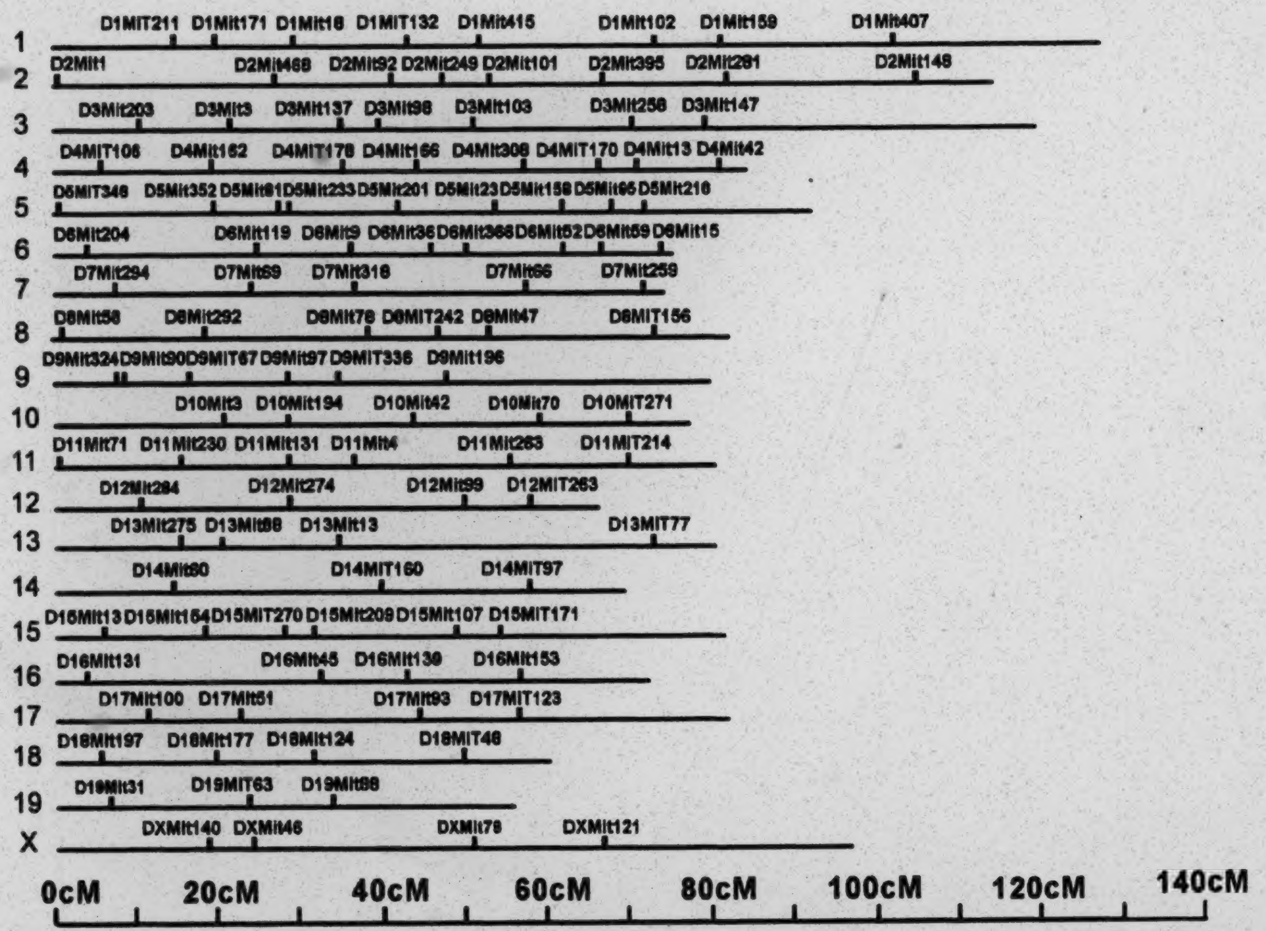

Figure 13. Locations of the 112 microsatellites used to genotype the exencephalic embryos for linkage analysis. The microsatellites, which all vary between the BALB/c and FVB/N strains, are spread at ~20 cM distances throughout the genome.

Table 4. The p values of a subset of microsatellite markers for which the allele frequencies differed from random in the whole genome analysis of the 94 exencephalic embryos.

Marker	Exencephaly group		Unaffected control group		p value
	F/B	B/B	F/B	B/B	
D2Mit92	53	41	41	53	0.080052802
D2Mit249	61	33	42	52	0.005580985
D2Mit101	59	35	44	50	0.028671435
D2Mit395	55	39	41	53	0.041140637
D14Mit60	33	61	43	51	0.144661542
D15MIT270	59	35	48	46	0.10860063
D15Mit209	58	36	47	47	0.10860063
D17Mit51	35	59	49	45	0.041140637
D19Mit31	36	58	49	45	0.057927678
D19MIT63	34	60	60	34	0.000149144
D19Mit88	35	59	61	33	0.00014914

The unaffected embryos were also genotyped for these markers and the "expected genotypes" and "unexpected genotypes" were compared to determine the p value. The two markers which varied significantly from random ($p \leq 0.001$ level of significance) were D19MIT63 and D19Mit88 on chromosome 19. The p values in red represent a significant difference between the expected and unexpected genotype group. The D2Mit249 marker, though it is not significant at a $p \leq 0.001$ level of significance, is suggestive of a possible modifier region, though the F/B genotype rather than the expected B/B genotype is enriched in the exencephalic samples.

Chromosome 19

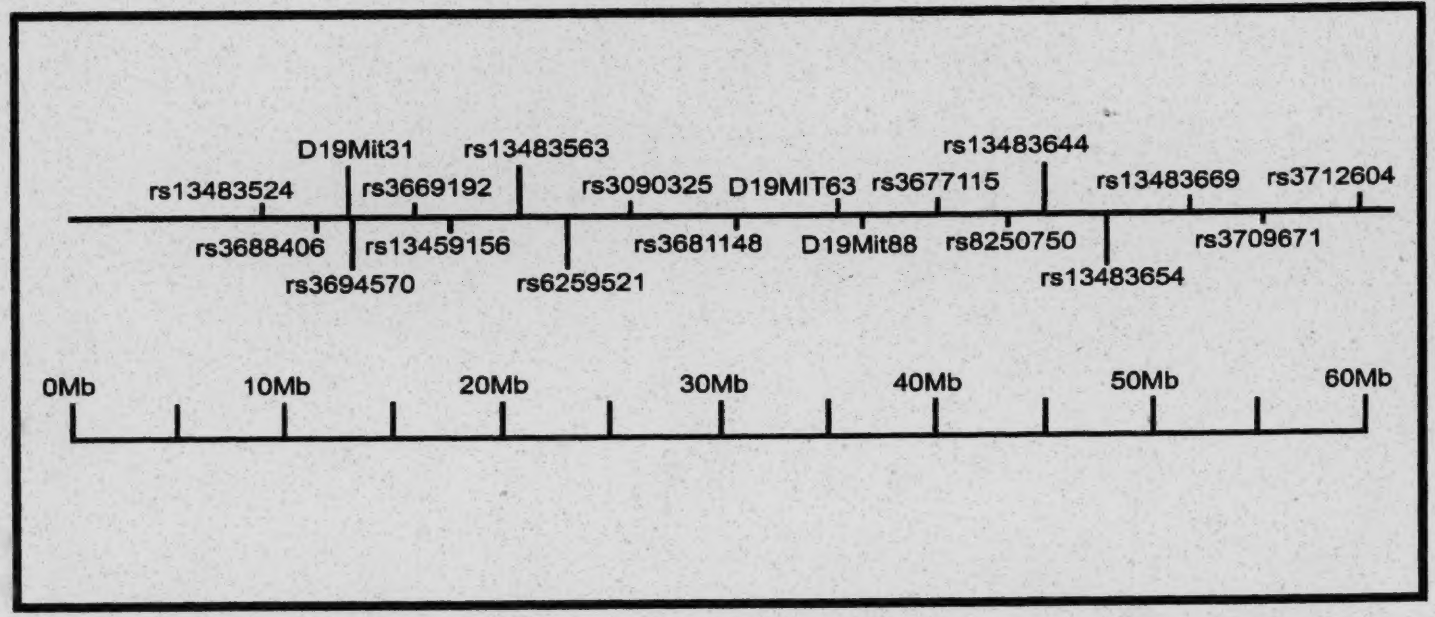
D19Mit31
rs13483563
rs13483644
rs13483524
rs3669192
rs3090325
D19MIT63
rs3677115
rs13483669
rs3712604
rs3688406
rs13459156
rs3681148
D19Mit88
rs8250750
rs3709671
rs3694570
rs6259521
rs13483654
0Mb
10Mb
20Mb
30Mb
40Mb
50Mb
60Mb

Figure 14. Microsatellite and SNP markers used to define the region of a potential modifier on chromosome 19.

All of the exencephalic and non-exencephalic embryos were tested for these markers, which are located ~every 3 Mb.

Table 5. The p values of all the microsatellite and SNP markers on chromosome 19 based on comparing the expected to the unexpected genotypes in the exencephalic and unaffected control groups.

Marker	Exencephaly group		Unaffected control group		p value
	F/B	B/B	F/B	B/B	
rs13483524	39	55	48	46	0.189255519
rs3688406	36	58	50	44	0.041140637
D19Mit31	36	58	49	45	0.057927678
rs3694570	36	58	50	44	0.041140637
rs3669192	36	58	52	42	0.01960411
rs13459156	36	58	54	40	0.008650406
rs13483563	37	57	55	39	0.008650406
rs6259521	35	59	57	37	0.001331837
rs3090325	34	60	58	36	0.000463934
rs3681148	35	59	60	34	0.000265707
D19MIT63	34	60	60	34	0.000149144
D19Mit88	35	59	61	33	0.000149144
rs3677115	34	60	64	30	0.000012090
rs8250750	35	59	64	30	0.000023360
rs13483644	38	56	63	31	0.000265707
rs13483654	37	57	60	34	0.000793952
rs13483669	37	57	59	35	0.001331837
rs3709671	36	58	59	35	0.000793952
rs3712604	36	58	58	36	0.001331837

The "expected genotypes" and "unexpected genotypes" were compared to determine the p values. The markers in red were significantly varied from random ($p \leq 0.001$ level of significance).

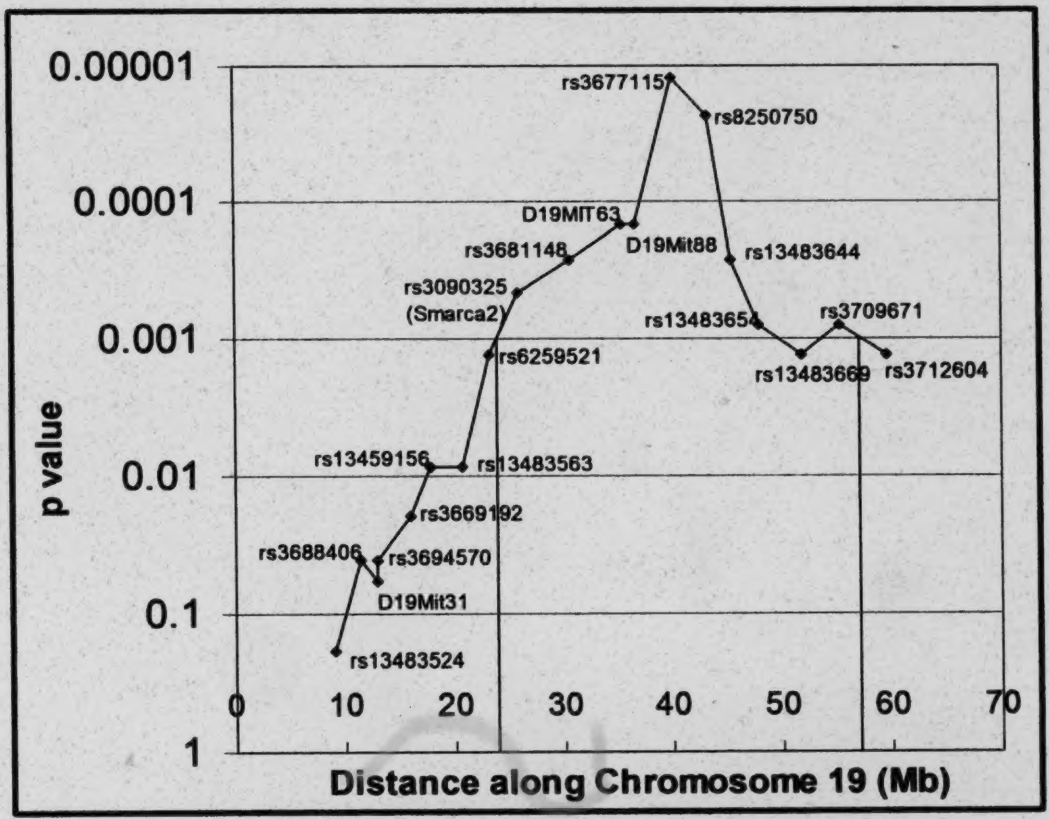

Figure 15. Graphical representation of the p values of all the microsatellite and SNP markers on chromosome 19. The p values, which were determined by comparing the expected to the unexpected genotypes, were plotted against their location along the chromosome in Mb **(Table 4)**. The chromosomal region between the two red lines defines the modifier region, in which the p value is greater than 0.001.

A)

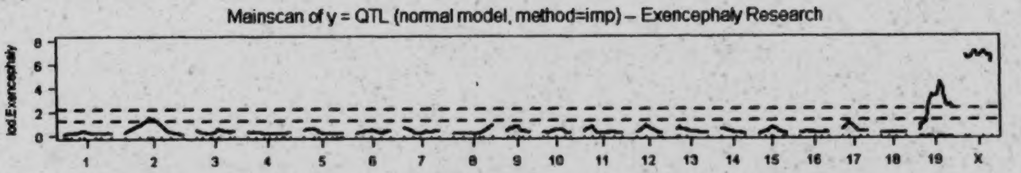

B)

Chromosome	Position	Lod score
2	48 cM (103 Mb), D2Mit249	1.5
19	39 cM (40.1 Mb), rs3677115	4.4

C)

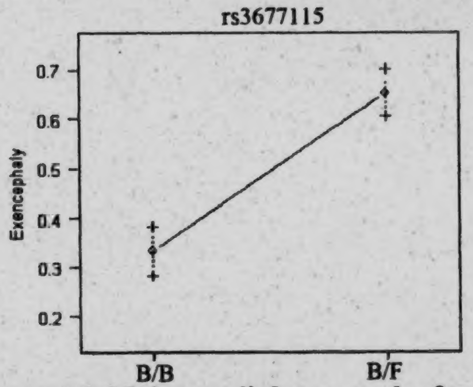

Figure 16. Mainscan linkage results for microsatellite and SNP genotype data and the effect of the major loci on exencephaly frequency. A) Genomic location is plotted against the lod scores for each marker. The red line represents the suggestive threshold of 37% (lod=1.1998) and the blue line represents the 95% significance threshold (lod=2.1129). The X chromosome has multiple artificial peaks because the B/B and B/F genotypes do not segregate randomly based on the inheritance mode of the X chromosome, and therefore is excluded from further analysis. B) The lod scores of the 2 chromosomal locations which are above the suggestive threshold. C) The effect plot of the chromosome 19 rs3677115 marker genotype on the frequency of exencephaly. Individuals with exencephaly were scored as 0 and unaffected individuals were scored as 1. The mean score of each genotype group (B/B and B/F) is plotted.

A)

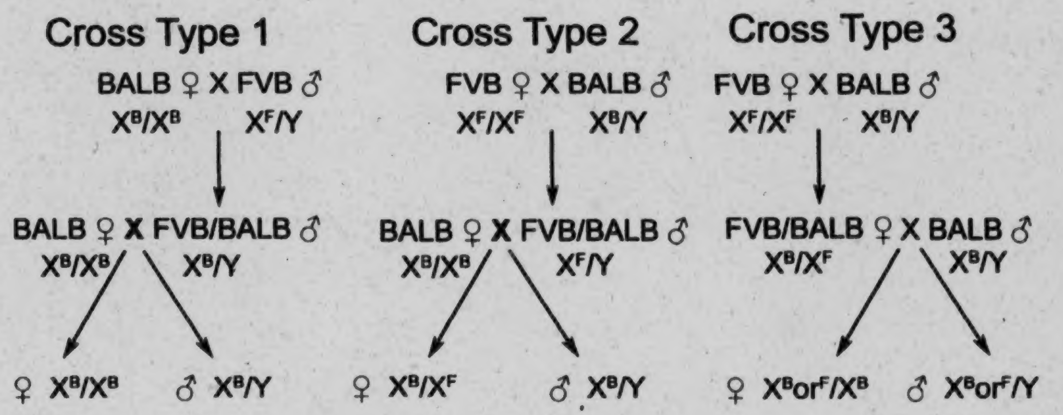
Cross Type 1
BALB ♀ X FVB ♂
X^B/X^B X^F/Y
BALB ♀ X FVB/BALB ♂
X^B/X^B X^B/Y
♀ X^B/X^B
♂ X^B/Y
Cross Type 2
FVB ♀ X BALB ♂
X^F/X^F X^B/Y
BALB ♀ X FVB/BALB ♂
X^B/X^B X^F/Y
♀ X^B/X^F
♂ X^B/Y
Cross Type 3
FVB ♀ X BALB ♂
X^F/X^F X^B/Y
FVB/BALB ♀ X BALB ♂
X^B/X^F X^B/Y
♀ $X^B or^F/X^B$
♂ $X^B or^F/Y$

B)

		Cross Type 1		Cross Type 2		Cross Type 3		Total of 3 Cross Types	
		+/m	m/m	+/m	m/m	+/m	m/m	+/m	m/m
♀	Normal	59	38	44	35	69	41	172	114
	Exencephaly	0	22	0	13	0	32	0	67
	Female Penetrance	**0%**	**36.7%**	**0%**	**27.1%**	**0%**	**43.8%**	**0%**	**37%**
♂	Normal	59	41	41	38	66	66	166	145
	Exencephaly	0	20	0	7	1	7	1	34
	Male Penetrance	**0%**	**32.8%**	**0%**	**16.6%**	**1.5%**	**9.6%**	**0.6%**	**19%**
♀+♂	Normal	118	79	85	73	135	107	338	259
	Exencephaly	0	42	0	20	1	39	1	101
	Combined Penetrance	**0%**	**34.7%**	**0%**	**21.5%**	**0.74%**	**26.7%**	**0.29%**	**28.1%**

Figure 17. The variable penetrance in the backcross population of embryos used for linkage analysis based on the inheritance of the X chromosome, and the sex of the embryo. **A)** The three crossing schemes used and the variable genotypes of the X chromosome which result. **B)** The penetrance of exencephaly in the backcross population, divided into male and female embryos, and then further subdivided based on the cross type. The final column shows the combination of the 3 cross types and the final row shows the combined male and female penetrance.

Table 6. $\chi 2$ results for the four X chromosome markers using linkage results from the subset of 32 embryos from cross type 3. The 32 embryos used [illegible]e are the subset of exencephalic embryos which represent a potential crossover on the maternally derived X chromosome. The results for the DXMit140 marker are near to the $p \leq 0.05$ level of significance which suggests a potential modifier on the X chromosome, though the sample size is too small to confirm this result.

Marker	Location (cM)	$(X^B/X^B+X^B/Y^B)/$ $(X^BX^F+X^FY^B)$ genotypes	Total # embryos analyzed	P value
DXMit140	19	21/11	32	0.077
DXMit46	25	20/12	32	0.16
DXMit79	51	18/14	32	0.48
DXMit121	67	17/15	32	0.72

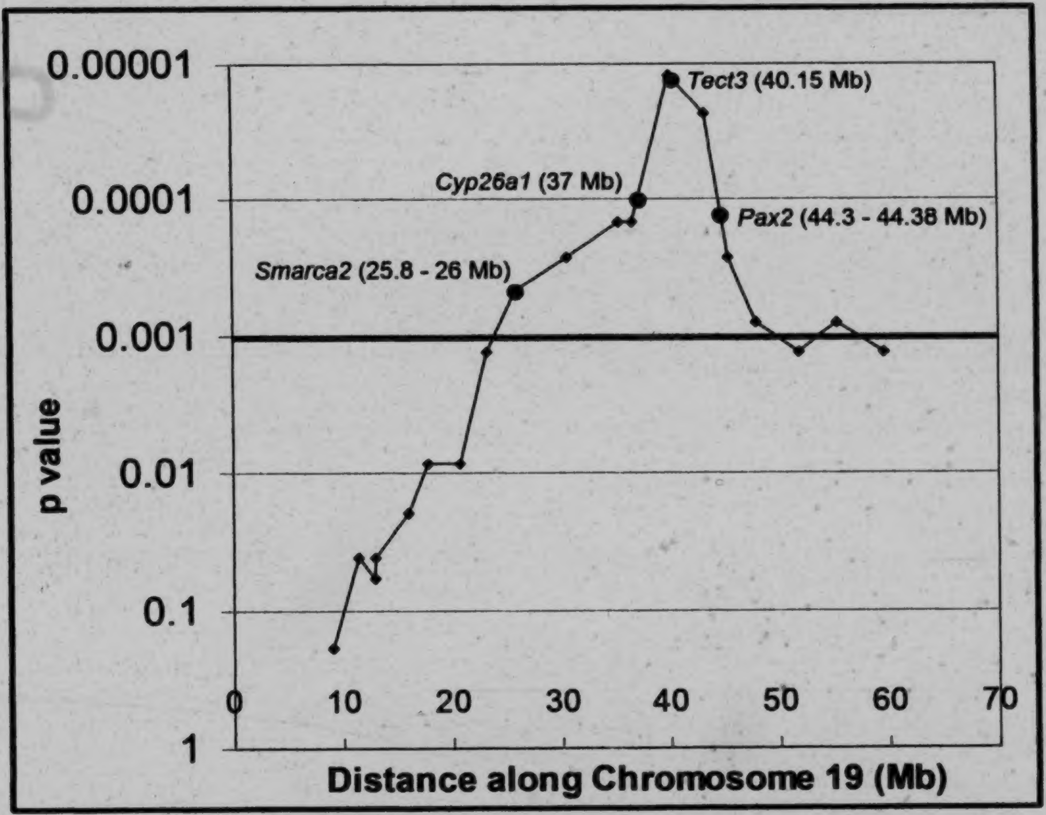

Figure 18. Locations of four modifier candidate genes on chromosome 19 relative to the linkage peak. The locations of the four genes, in Mb, on chromosome 19 are shown. The Mb locations are graphed relative to the p values of various microsatellite and SNP markers.

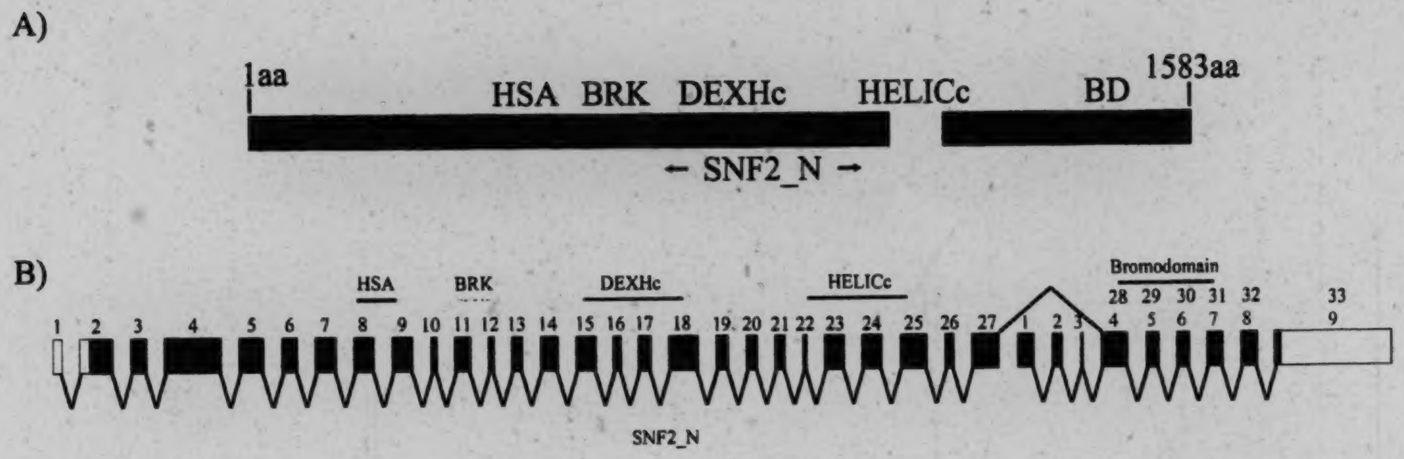
A)
1aa
HSA BRK DEXHc
HELICc
BD
1583aa
← SNF2_N →
B)
HSA
BRK
DEXHc
HELICc
Bromodomain
1 2 3 4 5 6 7 8 9 10 11 12 13 14 15 16 17 18 19 20 21 22 23 24 25 26 27
1 2 3 4 5 6 7 8 9
28 29 30 31 32 33
SNF2_N

Figure 19. Conserved protein motifs and gene structure of *Smarca2*. A) Conserved protein motifs in Smarca2 drawn to scale. B) The gene structure of the *Smarca2* gene, including variant 1 and variant 2. The exons in variant 1 are numbered in black and the variant 2 exons are numbered in red. White exons are untranslated regions of the gene, grey exons are specific to variant 2, black exons are translated exons which have not been sequenced and blue exons have been sequenced in BALB/c and FVB/N. Exons, but not introns, are drawn to scale and the locations of the 6 conserved domains are indicated.

Table 7. The penetrance of exencephaly and spina bifida in *Sp* mutant mice on a pure C57BL/6J background and a predominantly FVB/N mixed genetic background. The penetrance of spina bifida is significantly lower on the FVB/C57 background than on the C57BL/6J, whereas the decrease in the exencephaly frequency on the FVB/C57 background, while suggestive, is not statistically significant due to the small sample size.

	FVB/C57			C57BL/6J		
	$Pax3^{+/+}$	$Pax3^{+/Sp}$	$Pax3^{Sp/Sp}$	$Pax3^{+/+}$	$Pax3^{+/Sp}$	$Pax3^{Sp/Sp}$
Normal	44(100%)	72 (98.6%)	5 (19.2%)	43 (100%)	62 (98.4%)	0 (0%)
Exencephaly	0 (0%)	0 (0%)	3 (11.5%)	0 (0%)	0 (0%)	9 (25.7%)
Spina bifida	0 (0%)	1 (1.4%)	19 (73.1%)	0 (0%)	1 (1.6%)	35 (100%)
Total	44	73	26	43	63	35

Embryos on the FVB/C57 background were collected from an intercross between FVB F2 mice. This background is ~75% FVB/N.

Table 8. The penetrance of exencephaly, facial clefting, ventral closure defects, and spina bifida in *shrm* mutant mice on two genetic backgrounds. The penetrance of exencephaly, craniofacial clefting, and ventral closure defects are not significantly affected by the FVB/N genetic modifiers. The penetrance of spina bifida is significantly lower on the FVB/C57 background than on the C57BL/6J background using the data collected in our laboratory, but does not differ from the penetrance seen on the C57BL/6J background using the data collected by Hildebrand and Soriano (1999).

	FVB/C57			C57Bl/6J			C57Bl/6J (from Hildebrand and Soriano, 1999)
	shrm$^{+/+}$	shrm$^{+/-}$	shrm$^{-/-}$	shrm$^{+/+}$	shrm$^{+/-}$	shrm $^{-/-}$	shrm-/-
Normal	24 (100%)	56 (100%)	0 (0%)	11 (100%)	11 (92%)	0 (0%)	0/93 (0%)
Exencephaly	0 (0%)	0 (0%)	23 (100%)	0	1 (8%)	8 (100%)	93/93 (100%)
Craniofacial clefting	0 (0%)	0 (0%)	23 (100%)	0	0 (0%)	5 (62.5%)	68/78 (87%)
Spina bifida	0 (0%)	0 (0%)	2 (8.7%)	0	0 (0%)	7 (87.5%)	21/93 (23%)
Ventral closure defects	0 (0%)	0 (0%)	3 (13%)	0	0 (0%)	2 (25%)	7/59 (12%)
Total	24	56	23	11	12	8	

Embryos on the FVB/C57 background were collected from an intercross between FVB F2 mice. This background is ~75% FVB/N. The data collected on the C57BL/6J strain in my analysis used mice derived directly from the line used by Hildebrand and Soriano, which had been cryopreserved.

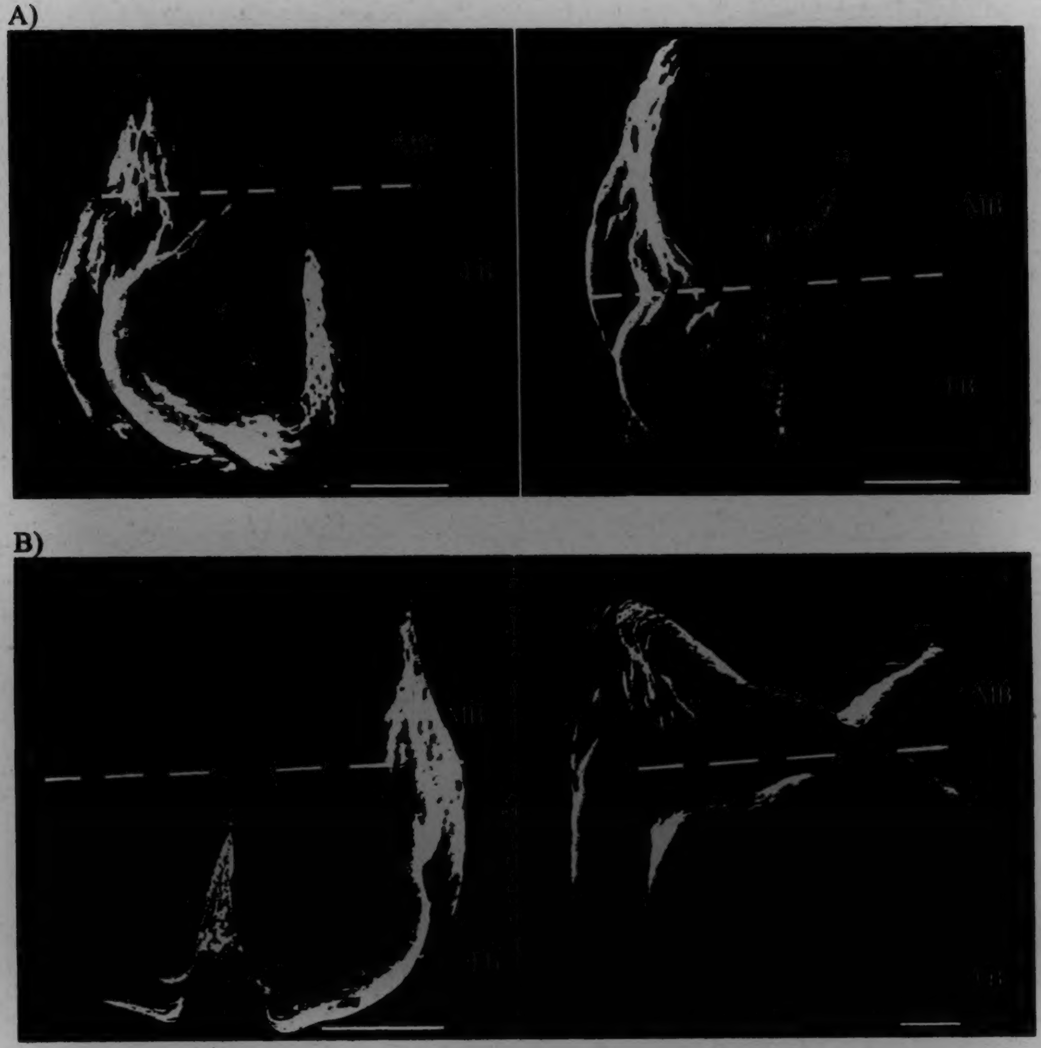

Figure 20. Normal elevation and fusion of cranial neural folds at closure point 2 in BALB/c and FVB/N mouse embryos. A) Rostral SEM photographs of two E9.25 BALB/c mouse embryos at the 9 somite stage and B) two E8.75 FVB/N mouse embryos at the 9 somite stage. The dotted line shows the boundary between the forebrain and the midbrain, at which closure 2 initiated in all of the BALB/c and FVB/N embryos collected. FB represents the forebrain region and MB represents the midbrain region.

Chapter 4. Discussion

4.1 A single strong dominant modifier contributes to the exencephaly penetrance variation in *Cecr2* mutants between BALB/c and FVB/N

4.1.1 Penetrance of exencephaly in intercross embryos resembles FVB/N

The FVB/N modifiers that confer resistance to exencephaly in *Cecr2*$^{m/m}$ mice appear to act in a semidominant manner, based on the observation that exencephaly occurs slightly more frequently in FVB/BALB F1 embryos than in pure FVB/N embryos. In the 42 *Cecr2*$^{m/m}$ embryos examined on the FVB/N background, no exencephaly was seen. This does not necessarily indicate a complete resistance to exencephaly on this background, and examining a greater number of embryos may show that the frequency of exencephaly is just very low, rather than 0. Recently, a single exencephalic embryo has been found in a *Cecr2*$^{m/m}$ embryo on the FVB/N genetic background (Jennifer Pockrant, personal communication).

The penetrance seen on the FVB/BALB F1 background in *Cecr2*$^{m/m}$ embryos was 2.9%, as compared to 0% on the pure FVB/N background, but this difference in penetrance is based on a single exencephalic embryo found on the mixed background. While it appears that the 2.9% represents an increased penetrance in the heterozygous backcross embryos, as compared to the 0% seen in FVB/N embryos, this is not sufficient evidence to distinguish between these 2 backgrounds, as it is a comparison between 1 and 0. This variation could be due to chance, in which case the modifier would be considered dominant. To clarify this difference, a collection of a larger number of embryos on both the FVB/N and FVB/BALB background would be required. These observations do not rule out the possibility that smaller effect modifiers exist which have a different inheritance pattern, though the major effect modifiers are dominant and semidominant.

To specifically characterize the single strong modifier region found on chromosome 19, an examination of an F2 population, rather than just a backcross population, would be an important tool. The genotype in the modifier region of the backcross embryos is either B/B or B/F, but in an F2 population resulting from an intercross of FVB/BALB F1 mice, the genotypes would also include FVB/FVB. In this case, it would be possible to analyze the effect on penetrance of the FVB/FVB genotype as compared to the B/F genotype. If the B/F genotype in the modifier region is more common in the affected population than the FVB/FVB genotype, the modifier is acting in a semidominant manner. Conversely, if the FVB/FVB genotype and B/F genotype occur at the same frequency in the affected population, the modifier is having a dominant effect on the phenotype.

4.1.2 High penetrance in the backcross population suggests one strong modifier

Penetrance analysis can give a preliminary indication of the number of major modifiers which contribute to the exencephaly resistant phenotype in FVB/N mice. While this is a simplified approach to determining the genetic factors which cause the penetrance variation, it is useful for making an initial prediction of the number of major contributing loci. In a backcross population to the susceptible strain, the penetrance is inversely related to the number of major contributing modifiers (Juriloff et al. 2001). This effect occurs because in a backcross population, the modifier regions from the susceptible strain segregate independently from each other, and therefore if there are a small number of modifier regions required to produce the mutant phenotype, a larger number of embryos will inherit the susceptible genotype in all of these regions. For instance, if two necessary loci were involved, 25% of the backcross embryos would be homozygous for the susceptible genotype in both of the areas, as opposed to 50% in the case of a single modifier. The SELH/Bc strain is a multifactorial model of exencephaly, and linkage analysis has been used to map the genes which contribute to the phenotype (Juriloff et al. 2001). The SELH/Bc mice were crossed to the normal LM/Bc strain, which has a very low penetrance of exencephaly (0.1%), and the F1 mice were backcrossed to the SELH/Bc strain. The original SELH/Bc strain developed exencephaly at a penetrance of 17%, and following the backcross, the penetrance was 4.4%. Therefore, the backcross penetrance of exencephaly was reduced to 24% of the original SELH/Bc strain penetrance. This implies that ~25% of embryos inherit the SELH/Bc regions which produce the exencephaly phenotype, predicting that two genes contribute significantly to the exencephaly phenotype. Multiple mapping experiments have implicated 2-3 major loci which contribute to the exencephaly phenotype in the SELH/Bc strain, confirming the predictions made using penetrance analysis (Juriloff et al. 2001; Gunn et al. 1992).

Following the backcross of FVB/BALB F1 mice to the susceptible BALB/c strain, the penetrance was 28.1%, which is 38% of the original BALB/c strain penetrance. This suggests fewer major contributing loci than seen in the SELH/Bc strain, likely 1-2. In the case of a major, dominant modifier, the penetrance in the backcross population should theoretically be halfway between the penetrance of the susceptible strain and the F1 generation, as 50% of embryos should inherit the B/B genotype at this locus. Because the BALB/c *Cecr2*$^{m/m}$ penetrance is 74% and the FVB/BALB F1 penetrance is 2.9%, a single major modifier model predicts a penetrance of 38.45% in the backcross population. The penetrance observed was slightly lower than this, 28.1%, indicating that more than one locus is contributing to the penetrance variation. If there were two major modifiers, the expected penetrance would be only 18.7% in the backcross population (1/4 of the ~71% difference between the BALB/c and F1 penetrance values). Therefore, based on penetrance, the best model predicts 1-2 strong loci. This method is not useful in predicting the number of minor modifier loci, so cannot provide a complete model for the genetic factors which underlie the penetrance variation.

To better estimate the number of major contributing genes, F2 males can be testcrossed to a number of females from the BALB/c susceptible strain. The proportion of males which can produce exencephaly at the level of the susceptible strain, is indicative of the number of modifier loci. There should be an inverse relationship between the number of independently segregating loci involved, and the proportion of F2 mice which genetically resemble the parental strain, in terms of affected progeny (Wright 1934). If ¼ of the F2 males produce a high level of exencephaly resembling the susceptible parent strain, one loci is likely involved, and if 1/16 produce exencephaly within the range of the BALB/c strain, 2 contributing loci are predicted (Juriloff et al. 2001).

The contribution of the FVB/N genetic background to the exencephaly penetrance is likely very complex. This type of penetrance analysis is only capable of making a reasonable prediction of the number of major modifiers. This method is unable to determine the complex genetic contributions of multiple genes, which each make only minor contributions, but may have a significant total effect on the penetrance of exencephaly. The major modifier in the FVB/N background, for example, is only responsible for ~30-35% of the effect on penetrance, and as mapping shows no other regions of strong linkage, a summation of weaker modifier genes likely accounts for the remainder of the effect. The number and strength of these other modifiers cannot be studied using this type of penetrance analysis. Modifier genes in the FVB/N background may be highly variable in terms of strength and mode of inheritance, and this method will only uncover strong, dominant modifiers. This analysis also fails to account for genetic complexity, including epistatic interactions. For instance, the possible linkage on chromosome 2 for which the B/F genotype, rather than the expected B/B genotype, was linked to exencephaly, may interfere with this type of analysis. This simplified analysis has, however, been relatively accurate in predicting the number of major modifiers in the SELH/Bc strain, and in the *Cecr2* mutant line, as determined using linkage analysis.

4.1.3 Single region of significance found using linkage analysis

The original $\chi 2$ analysis of the linkage data, which combined the expected genotypes from unaffected and exencephalic embryos, as well as the unexpected genotypes from both groups, identified a single region of significance at the $p \leq 0.001$ level. This region may contain a single modifier gene or it may contain two or more closely linked modifiers. Nine markers on chromosome 19, between 25.9 Mb and 55 Mb, were above this significance level, which defines a linkage region of ~30-35 Mb with a peak at 40.1 Mb. The p value at the peak of the linkage region is 0.000012, which indicates strong linkage in this area of the genome. This strong linkage confirms that a large enough sample size was used and also indicates that this is likely the major locus which is causing the penetrance difference in exencephaly between FVB/N and BALB/c

Cecr2 mutants. No other regions of linkage were found at this level of significance in the whole genome screen. The model based on the penetrance analysis in the backcross generation predicted one strong modifier, and the linkage results seen here support this and define the location of the modifier. As this major modifier on chromosome 19 is only responsible for ~30-35% of the penetrance variation between the BALB/c and FVB/N strains, several minor modifiers likely contribute to the penetrance. The sample size used here was likely not sufficient to map these smaller effect genes.

The analysis done by the Churchill lab confirmed that chromosome 19, with a lod score of 4.4 which is above the 95% significance threshold, is the only major modifier. This single chromosomal region is responsible for increasing the frequency of exencephaly by 30-35% in embryos with a B/B genotype as compared to embryos with a BALB/FVB genotype, as shown by the effect plot. Approximately 2/3 of exencephalic embryos can be explained by a B/B genotype at this marker. However since 1/3 of exencephalic embryos are F/B at this chromosome 19 locus, it is not necessary for the development of exencephaly. This result suggests that a number of minor effect modifiers likely also exist. It is likely that most modifiers which differ between the strains have only minor effects individually, based on the fact that no other regions show linkage. These minor modifiers are important, as together they are responsible for the majority of the penetrance variation, but the mapping of minor modifiers is difficult because their effects may be masked by the strong modifier, and it requires much larger sample sizes to achieve significance.

The analysis done in the Churchill lab located a second linkage region on chromosome 2 at ~103 Mb, with a lod score of 1.5, which is below the 95% significance threshold but above the suggestive threshold. This region was identified as a possible linkage region in the initial $\chi 2$ analysis, with a p value of 0.0055. A larger sample size could be used to confirm the significance of this linkage region. The effect of this locus on exencephaly, however, indicates that the B/F genotype rather than the B/B genotype in this region predisposes embryos to exencephaly. This opposite effect may be the result of a resistance gene in the BALB/c genome. A similar effect was seen in a linkage study looking for genes that increased methylation of a transgene in BALB/c mice as compared to C57BL/6J mice (Valenza-Schaerly et al. 2001). This study identified a region which increased methylation when it was homozygous for the BALB/c genotype as expected, and a locus at which the B/B genotype was linked to decreased methylation. This study hypothesized that the region contained a demethylating factor, though this has yet to be confirmed. A second study looking at a modifier of XX sex reversal in *Ods* mutant mice also found a genotype distortion in the opposite direction to that expected (Qin et al. 2003). It was suspected that this was an artifact, because the *Ods* mutation was located on the same chromosome as this region and therefore the segregation may be affected. It is possible that a resistance factor does exist on chromosome 2 in the BALB/c strain, though because its linkage is far less significant and because it cannot be as easily explained by previous data for the BALB/c and FVB/N strains, this region will not be the focus of further study at this time. The chromosome 19 region mapped in this linkage study appears to contain the major modifier, which in addition to a number of minor effect genes, leads to an increased risk of exencephaly in the FVB/N strain background. In addition to this, the possibility of a maternal effect or of an X chromosome modifier, have not been ruled out.

4.1.4 Is there a potential modifier on the X chromosome?

The effect of the X chromosome on the penetrance of exencephaly in *Cecr2* mutant embryos is unclear at this point. To analyze the effect of possible X chromosome modifiers, the samples were separated into 3 cross types based on the X chromosome genotype, and also on the sex of the embryo. This allowed the female predominance to be analyzed separately based on the genotype of the X chromosome. A clear overall female predominance of exencephaly was seen in backcross embryos, consistent with observations of the *Cecr2* mutation on other backgrounds (Ames 2006). Using the combined data from the 3 cross types, female embryos develop exencephaly at a penetrance of 37%, and males develop exencephaly at a penetrance of 19%, which is consistent with the male: female ratio of exencephalic embryos seen on the BALB/c and BALB/129P2 backgrounds (~66% of exencephalic embryos are female). This ratio, however, is highly variable based on cross type. Cross type 2 shows the expected male: female ratio of exencephalics, but in cross type 3, female predominance is exaggerated, as about 82% of exencephalic embryos are female, and in cross type 1, there is almost no female predominance, as only 53% of exencephalic embryos are female. As female predominance is not well understood, the reason for this difference in female predominance is difficult to interpret, and may complicate the use of penetrance analysis within the 3 cross types to determine the existence of possible X chromosome modifiers. These observations of variable female predominance between the cross types cannot be explained by X chromosome genotype, as in cross type 1 the X chromosomes are always the BALB/c genotype, and show a different male: female ratio of exencephalics than the pure BALB/c strain. It is possible that if this variable male: female ratio of exencephaly is due to X chromosome modifier(s), that it is dependent on autosomal loci which vary between the two strains. The penetrance for cross type 1 was 34.7%, which is the highest of the 3 cross types. In this group, the X chromosomes in males and females are of the BALB/c genotype. This is consistent with possible X chromosome modifiers, as BALB/c is the susceptible strain. The total penetrance is lowest for cross type 2, in which females are X^F/X^B and males are X^B/Y, which is also consistent with the hypothesis of an X chromosome modifier. This is because females, which are more vulnerable to exencephaly and therefore make up the majority of exencephalic samples, have the resistant genotype on the X chromosome. The penetrance is intermediate in cross type 3, in which the maternal X is a product of recombination between a BALB/c and FVB/N X chromosome, and the other X is BALB/c in females. This analysis, however, is complicated by the variable male: female ratios of exencephalics between the cross types. Because female predominance is a very poorly understood phenomenon at this point, the variable ratios are difficult to interpret and the penetrance analysis between the 3 cross types cannot be considered a reliable method for determining the existence of X chromosome modifiers. This data may prove to be useful in the overall understanding of the effect of the X chromosome, and particularly in the understanding of female predominance of exencephaly, but there is insufficient information available at this point to interpret these results.

The two other methods used to look for possible X chromosome modifier(s) or maternal effects on the penetrance of exencephaly were used in a similar study by Lundberg et al. (2004). First, the penetrance data from cross type 1 was combined with cross type 2 and compared to the penetrance in cross type 3. This separates the data based on maternal effect, as cross type 1 and 2 use a BALB/c mother and cross type 3 uses a FVB/BALB mother. Cross types 1 and 2 combined had a penetrance of 29%, and cross type 3 had a penetrance of 26.7%. This is a fairly small variation and therefore no obvious maternal effect is occurring. The second method analyzed the linkage data for cross type 3 only, as these 32 exencephalic samples were the only samples which represented possible recombination on the maternally derived X chromosome, and had genotype data available. Genotyping of the X chromosome was not done on unaffected samples from cross type 3, so a $\chi 2$ analysis that compared the expected genotype frequencies (1 $X^BX^B + X^BY^B$: 1 $X^BX^F + X^FY^B$) for the X chromosome markers to the observed frequencies, was used. Using this analysis, possible linkage was seen to the DXMit140 marker at 19 cM on the X chromosome, with a p value of 0.077. This result may suggest linkage in this region of the X chromosome, but no conclusions can be made until more embryos are genotyped for markers on the X chromosome, including the unaffected embryos from cross type 3, which would rule out segregation distortion.

A linkage study looking for modifiers of valproic acid induced exencephaly also found a penetrance variation based on X chromosome genotype, though in this case it is likely due to a maternal effect rather than an X chromosome allelic effect and so the causative factor likely differs from that of *Cecr2* mutants (Lundberg et al. 2004). This study used a similar $\chi 2$ analysis on the 49 exencephalic embryos which had a possibly recombinant X chromosome, and found no significant variation, making an allelic effect of the X chromosome unlikely. A number of mutations which cause NTDs do exist on the X, however, including the *ATRX* gene at 43.8 cM, *Nap1l2* at 42.5 cM, *Zic3* at 16.5 cM and *exma* at 34.1 cM. Because only four markers were used on the X chromosome, it is difficult to determine the location of a possible modifier, though the *ATRX*, *Nap1/2* and *exma* genes are all unlikely based on their location. The *Zic3* gene is a possible modifier as it is only ~2.5 cM from the DXMit140 marker which is at 19 cM, and interestingly, the *Snf2l* gene which encodes a protein that interacts with CECR2 in human cell lines, is only ~3 cM away from DXMit140. A finding of X chromosome linkage, followed by a refined map of the area, will be an important future step in understanding Cecr2 and its modifiers.

4.2 Candidate genes in the modifier region

4.2.1 The modifier region and potential types of modifier genes

The modifier was mapped to mouse chromosome 19, between ~23 Mb and ~58 Mb, with a peak at ~40 Mb at the rs3677115 marker. Interestingly, a region on human chromosome 10, which is syntenic to the mouse chromosome 19 region from ~32 Mb to the end of the chromosome, was associated with NTDs in a human linkage study (Rampersaud et al. 2005). The peak of the human linkage region is at nearly the same location as the peak of the mouse chromosome 19 region identified in this study. This is the region showing the strongest linkage to human NTDs after the removal of one large pedigree from the analysis. The human study consisted of 44 multiplex pedigrees, with a total of 292 individuals. The phenotypes in the human study included various NTDs, mainly lumbosacral level myelomeningocele, but also including anencephaly and craniorachischisis. The peak Mlod score for the human linkage region at D10S1731, which is located at 10q25.3, was 2.25, which is strongly suggestive of linkage, but cannot be confirmed with the data available. This may lend support to the idea that modifier genes which differ between mouse strains correspond to human NTD susceptibility factors. It also provides a model for locating the human susceptibility factor in this region, as the only methods to locate a candidate in a human system are mapping and sequencing, and it is difficult to confirm the effects of any polymorphisms found. Assuming that the same gene is causing linkage in the syntenic regions of the two species, the modifier region is narrowed to the overlapping area, ~32 Mb – ~58 Mb, as the 23 Mb to 32 Mb region is not syntenic to chromosome 10 in the human linkage region.

An initial examination of the mouse chromosome 19 region between 23 Mb and 58 Mb focused on genes associated with exencephaly. This is based on the hypothesis that minor effect susceptibility factors, or modifiers of NTDs, are allelic variations of genes which are mutated in highly penetrant NTD mutant mice (reviewed in Harris and Juriloff 1999). Two of these genes, *Cyp26a1* and *Pax2*, were noted for this reason (Abu-Abed et al. 2001; Sakai et al. 2001; Torres et al. 1996). Other potential modifiers could be any gene whose function is related to neural tube closure, such as neural tube patterning, apoptosis or proliferation, NCC emigration or actin localization, or any gene which is expressed before or during neural tube closure in the early embryo (reviewed in Copp 1999). In addition to more general modifiers, possible *Cecr2* specific modifiers were examined. This included any genes which may interact with Cecr2, such as ATPase proteins or other proteins which are found in chromatin remodeling complexes, as it is known that CECR2 interacts with SNF2L in a human cell line (Banting et al. 2005). This led to the focus on a third modifier, *Smarca2*, which is a SWI/SNF family ATPase protein involved in several chromatin remodeling complexes (Reyes et al. 1998). Other potential modifiers may affect the expression of Cecr2, or be downstream genes whose expression is controlled by a Cecr2-remodeling complex, though none of these genes are known at this point. The only other possible modifiers considered were splicing factors, as it is known that alternative splicing occurs for *Cecr2*, though no known genes of this type were located near the peak of the modifier region.

The final method used to locate candidates was the Ensembl SNP database, which allows the examination of polymorphisms between many mouse strains (http://www.ensembl.org/Mus_musculus/transcriptsnpview). While sequence data is not available from the FVB/N and BALB/c strains for many genes in the region, the available SNP data was examined. This analysis revealed a nonsynonymous SNP in the *Tect3* gene that differed between BALB/c and FVB/N. *Tect3* is located directly under the peak of the mouse and human linkage regions. Because a similar gene in the *Tect3* family, *Tectonic*, is known to play a role in neural tube patterning and development, this gene was the fourth candidate noted (Reiter and Skarnes 2006). The function, expression, and any known mutant phenotypes associated with the four genes were considered in order to characterize the likelihood of each as a potential modifier of the *Cecr2* mutant phenotype.

As the linkage region contains more than 500 genes, about half of which have yet to be characterized, it is very early to begin testing candidates. I have speculated on the types of genes which may modify the phenotype, but the modifier may have an unexpected function and therefore would be extremely difficult to predict. For this reason, the major future direction of this project will involve narrowing the modifier region to decrease the number of possible candidates. Because narrowing the region will be a lengthy process, a preliminary candidate gene analysis has begun, and the four candidates which have been noted in this analysis are discussed below.

4.2.2 *Smarca2*

The *Smarca2* gene, which is located at 26 Mb on chromosome 19, encodes an ATPase protein in the SWI/SNF family of chromatin remodelers (Reyes et al. 1998). SWI/SNF complexes contain either Smarca2 or Brg1, and a variable combination of 7-15 other distinct protein subunits (reviewed in Aalfs and Kingston 2000). These SWI/SNF complexes control the transcription of many genes. A mouse line with a mutation in the *Smarca2* gene showed a phenotype that was relatively subtle (Reyes et al. 1998). The *Smarca2* homozygous mutant mice were 15% heavier than wild type mice, suggesting an increase in cell proliferation in adult mice, as this phenotype does not become evident until after weaning. Embryonic fibroblasts from these mutant mice were less able to arrest in G_0/G_1 in conditions of cell confluency or DNA damage. The lack of a more severe phenotype may be due to a partial redundancy with the other SWI/SNF ATPase protein, Brg1, which is upregulated in *Smarca2* mutants. Brg1 is 77% identical to Smarca2 at the aa level, and in *Smarca2* mutant mice Brg1 was able to replace Smarca2 in several complexes (Reyes et al. 1998). *Brg1* has also been knocked out in a mouse line, and although homozygotes die around the time of implantation, heterozygotes are prone to developing exencephaly (Bultman et al. 2000). Smarca2 is expressed in embryo and adult tissues, though Brg1 is expressed at 20-30X higher levels than Smarca2 in the embryo (Reyes et al. 1998). Smarca2 expression is increased in adult mice after birth, and its expression in the early embryo is mainly in the mesodermal tissues involved in heart morphogenesis and vasculogenesis (Dauvillier et al. 2001).

SNF2L, which has been found to interact with CECR2 in human HEK293 cells, is a member of the other major class of chromatin remodeling proteins, the ISWI family

(Banting et al. 2005). The ISWI complexes, like the SWI/SNF complexes, remodel chromatin by changing the accessibility of DNA to factors which bind DNA (reviewed in Aalfs and Kingston 2000). Both families share a similar ATPase domain, and many similar biochemical properties (Aalfs et al. 2001). ISWI complexes, however, also differ in many ways, including the underlying method by which they remodel nucleosomes, and the fact that they consist of only 2-6 protein subunits (reviewed in Aalfs and Kingston 2000). SWI/SNF complexes are thought to loop out DNA on histones to expose it, whereas ISWI complexes slide nucleosomes along the DNA (Aalfs et al. 2001). ISWI complexes, unlike SWI/SNF complexes, cannot be stimulated by naked DNA and require interactions with histone tails to remodel chromatin, (reviewed in Aalfs and Kingston 2000). There is no known protein subunit which participates in both SWI/SNF and ISWI complexes, though this remains a possibility. The two types of complexes are, however, known to play roles in regulating the same genes, and are therefore targeted to some common promoter locations. For example, the Snf2h protein and the SWI/SNF complex are both found at the *hsp70* promoter (Corey et al. 2003). It is thought that Snf2h is constitutively present at this promoter to keep it in a relatively open conformation which allows the gene to quickly respond to heat shock. After heat shock, Hsf1 recruits the SWI/SNF complex to the promoter, and SWI/SNF remodels chromatin downstream of the promoter to allow elongation of transcripts. Both complexes are also thought to be involved in the regulation of hormone responsive genes through nuclear receptors (Dilworth and Chambon 2001). In this case ISWI complexes are required for the nuclear receptors to bind responsive elements in promoters, and SWI/SNF complexes remodel the chromatin at the promoter region to allow binding of the basal transcription machinery.

The ATPase proteins alone can carry out most remodeling functions in vitro, and the additional subunits either enhance the activity of the ATPase protein, or target the protein to a specific promoter (Aalfs et al. 2001). A chimeric Brg1 protein, with the ATPase domain from Snf2h, had chromatin remodeling activity that resembled Snf2h, but was found to interact with subunits of the SWI/SNF complex (Aalfs et al. 2001). The SWI/SNF complexes containing this chimeric protein were able to activate some SWI/SNF controlled genes but not others, though in all cases examined the complex was correctly targeted to the promoters of these genes. This means that both types of remodeling activity are effective at many promoters, and that it is the recruitment of the complex which is specific. Theoretically, if ISWI complexes were targeted to promoters normally remodeled or activated by SWI/SNF complexes, for instance by a common subunit involved in promoter targeting, the ISWI complex could act in a partially redundant manner.

The *Smarca2* gene is a possible modifier of the *Cecr2* exencephaly phenotype for a number of reasons, including the fact that the *Brg1* gene, which is likely partially redundant with *Smarca2*, is associated with exencephaly (Reyes et al. 1998; Bultman et al. 2000). Another SWI/SNF protein, ATRX, is also associated with NTDs in an overexpression mouse line (Berube et al. 2002). Smarca2 is similar in function to SNF2L, which encodes a protein that interacts with CECR2 in human cells (Banting et al. 2005). Smarca2, Snf2l, and Snf2h are all ATPase proteins, though they are members of two different gene families. Though it has not been shown that Smarca2 and Snf2l/Snf2h are redundant in any specific instance, or that any proteins can interact with both types of complexes, the two complexes have been shown to be targeted to similar promoters. It is possible that Cecr2 or some other factor may be involved in the targeting of both ISWI and SWI/SNF complexes to promoters. This would make it possible that *Smarca2* is a direct modifier of the *Cecr2* mutant phenotype, as it may be involved in activating genes which cannot be activated when Cecr2 containing ISWI complexes do not form.

Initial *Smarca2* sequencing of 8 of the 36 exons, which encode some of the conserved domains, has not shown any aa changes. RT-PCR of the *Smarca2* gene was done in wild type BALB/c and FVB/N mice, showing that both strains express *Smarca2* mRNA (Adam Tassone, personal communication). Due to the subtle phenotype, it was possible that a null *Smarca2* allele may sensitize the BALB/c strain to exencephaly in *Cecr2* mutants. This is the only one of the four noted candidates which is not located within the linkage region found on human chromosome 10 (Rampersaud et al. 2005). If the NTD linkage associated with human chromosome 10 and the syntenic region on mouse chromosome 19 are due to the same gene, this rules out *Smarca2* as the causative modifier in the region. It is also the furthest gene from the peak of the modifier region on chromosome 19 mapped in this linkage study. The rs3090325 marker is located within the Smarca2 gene, and the p value of this marker is 0.00046, as opposed to the p value of 0.000012 at the rs3677115 marker, which is at the peak of the linkage region. These findings, along with the expression pattern of the *Smarca2* gene and the lack of any evidence of a redundant function for the ISWI and SWI/SNF complexes in vivo, argues against this gene as a candidate.

4.2.3 *Cyp26a1*

Cyp26a1, which is located at 37 Mb, encodes a retinoic acid metabolizing enzyme. Retinoic acid, a vitamin A metabolite, is an important signaling molecule in the embryonic development of several tissues, including the eye, heart, somites, limbs and the neural tube (reviewed in Chambon 1996). RA acts through a number of nuclear receptors, RARs and RXRs, which bind RAREs (RA responsive elements) to control the expression of target genes (reviewed in Chambon 1996). The distribution of retinoic acid (RA) in the early embryo is carefully regulated by the expression of RA-synthesizing and RA-catabolizing enzymes (Abu-Abed et al. 2003). Throughout gastrulation and neurulation stages Cyp26a1 and Raldh2, which produces RA, are expressed in complementary regions of the embryos (Neiderreither et al. 1997; Fujii et al. 1997). It is believed that certain regions of the embryo require RA, and that it has a teratogenic effect in other regions. These domains are maintained using enzymes like Cyp26a1 and Raldh2. Two independent *Cyp26a1* knockout mice have been produced which developed a number of defects, including exencephaly, spina bifida, caudal agenesis, and vertebral homeotic transformations, and die at midgestation (Abu-Abed et al. 2001; Sakai et al. 2001). Cyp26a1 is expressed in the rostral neuropore and in the tail bud (Fujii et al. 1997).

The effect of exogenous RA on neurulation is highly dependent on the dose and the timing of exposure. RA given on day 8 of gestation can induce NTDs even at a low dose like 5 mg/Kg, possibly by delaying the closure of the neural tube (Tom et al. 1991). This differs significantly from the effect of the same dose given on day 9 of gestation, which can reduce the frequency of NTDs in *ct* and *Sp* mice (Chen et al. 1995; Kapron-Bras and Trasler 1985). Higher RA doses at the same time on day 9 have a teratogenic effect on embryogenesis, leading to NTDs and caudal agenesis (Nobakht et al. 2006). It is therefore likely that there are RA sensitive times in development, and therefore the effects of RA can be unpredictable. The frequency of spina bifida in the *Axd* mutant line is not reduced by 5 mg/Kg RA given on day 9 meaning that the rescuing effect is not completely general (Haviland and Essien 1990).

As exogenous RA is a known modifier of exencephaly in wild type mice, as well as a number of mutant strains, a variation in an enzyme which catabolizes RA is certainly a possible modifier of the exencephaly phenotype between BALB/c and FVB/N *Cecr2*$^{m/m}$ mice. This variation could be a slight change in expression level, or may be a change in the timing or spatial expression pattern of Cyp26a1. A change in the regulation of Cyp26a1 which affects the timing of its expression, may have an unpredictable effect on neurulation. The effect of exogenous RA on the frequency of exencephaly in the *Cecr2*^{Gt45Bic} mutant line is unknown, which makes it more difficult to predict the effect of any Cyp26a1 variation on the phenotype.

4.2.4 *Pax2*

Pax2, which is located at ~44 Mb, is a member of the paired box family of transcription factors. Its expression begins at E7.5 in the prospective boundary between the midbrain and the hindbrain. Pax2 is one of the earliest transcription factors expressed in the MB/HB organizer region (Dressler et al. 1990; Rowitch and McMahon 1995). The MB/HB organizer is a constriction between the midbrain and hindbrain regions which signals the later development of the midbrain and the cerebellum (Wassef and Joyner 1997). Later the *Pax5*, *Wnt-1*, *Fgf-8*, *En1* and *En2* genes are expressed in this region and establish the organizer (Rowitch and McMahon 1995; Kelly and Moon 1995; Krauss et al

1992). Pax2 is also expressed in the developing spinal cord, eye, ear and urogenital system (Dressler et al. 1990). Various *Pax2* mutations exist, though their phenotypes have been highly variable and show a strong dependence on the genetic background. The initial mutant line, on a 129/Sv background, developed exencephaly at 100% penetrance in homozygotes and a low penetrance in heterozygotes (Torres et al. 1996). These mutants did not have patterning defects in the midbrain or cerebellum. This same mutation led to only 30% exencephaly when moved onto a C57BL/6J background, again with no patterning defects or other brain abnormalities. A double mutant for *Pax2* and *Pax5,* on a C57BL/6J background, lacked the organizer and was missing the midbrain and cerebellum (Schwarz et al. 1997). The *Pax5* gene, which is highly similar to *Pax2* and is expressed in a similar spatial region, though at ~E8.25, is likely compensating for the loss of *Pax2*.

A second *Pax2* mutation, which arose from a single base pair insertion, causes a truncated protein lacking the DNA binding regions (Favor et al. 1996). This mutant mouse line was created on a predominantly C3H strain and has a very different phenotype than that of the previous *Pax2* mutation. In this case, 21% of embryos from a cross between two heterozygotes showed a deletion of the cerebellum and posterior midbrain and 5% exhibited exencephaly. The role of *Pax2* in the closure of the neural tube remains unclear, though exencephaly has been seen to some degree on all backgrounds examined, and in two different *Pax2* mutant lines.

A variation in Pax2 levels could modify the NTD phenotype, as Pax2 is known to be dosage-dependent based on the observation of exencephaly at a low level in heterozygotes on the 129/Sv strain (Torres et al. 1996). As well, a variation in the ability to turn on *Pax5* or other genes in the MB/HB organizer region may modify the exencephaly phenotype. Because exencephaly is seen in *Pax2* mutants, and because Pax2 is a transcription factor with embryonic expression in the developing neural tube, it is a possible modifier candidate.

4.2.5 *Tect3*

The *Tect3* gene is located at ~40.15 Mb on mouse chromosome 19, which is directly at the peak of the modifier region. The human *Tect3* homolog is also located directly under the peak of the NTD linkage region on chromosome 10 (Rampersaud et al. 2005). The location of the gene, in addition to the fact that a non-synonymous SNP exists between the BALB/c and FVB/N in the coding region, make it a possible candidate gene even though very little is known about the function of Tect3. Ensembl TranscriptSNP view contains sequence data from several mouse strains, and allows SNPs to be viewed for any strain combination for which sequence data is available. BALB/c and FVB/N sequence is not available for many of the genes in the modifier region, but it does exist for *Tect3* and a single SNP exists between the 2 strains.

In the BALB/c strain, the *Tect3* gene encodes a threonine at position 186, which is a polar, hydrophilic, neutral aa. The FVB/N strain encodes a methionine at this position, which is a hydrophobic, neutral aa (NM_001039153). This change has yet to be confirmed in our mice, and its significance is difficult to predict as the gene is not well characterized and no essential motifs are known, but it is certainly possible that it is significant, particularly as the aa variation is from hydrophobic to hydrophilic. This residue has been examined in several species and mouse strains to determine its conservation, and in doing so to help determine its importance in the function of Tect3.

The human *Tect3*, as well as rat, *Bos Taurus*, *Macaca* and *Canis familaris* all encode a T at this position like the BALB/c strain and other mouse strains including 129S1, A/J, AKR/J, CH3, DBA and NOD (Heather McDermid, personal communication). The C57BL/6J, SWR/J and 129X1 mouse strains all encode a methionine at this position, like the FVB/N strain. The T appears to be fairly well conserved throughout various species, though a subset of mouse strains do encode a methionine, similar to the resistant FVB/N strain. The effect of these other genetic backgrounds on the *Cecr2* exencephaly penetrance would be interesting, and a correlation between the sequence of *Tect3* and exencephaly resistance would offer support to this candidate.

The *Tect3* gene has not been studied in terms of function or expression, and therefore no data is available at this point. It is known that three members of the *Tectonic* gene family exist in mice, *Tectonic*, *Tect2* and *Tect3*, and only *Tectonic* has recently been examined in detail. Tect3 is 58% similar to Tectonic, and Tect2 is 49% similar to Tectonic (Reiter and Skarnes 2006). Tectonic is a secreted protein, whereas Tect2 and Tect3 are predicted to have carboxy terminal transmembrane domains, and are likely integral membrane proteins. The *Tectonic* gene has recently been determined to be involved in patterning of the neural tube via the Sonic hedgehog signaling pathway, making the *Tect3* gene an even more interesting candidate gene for a modifier of exencephaly. A *Tectonic* genetrap mutation, which is presumed to be a null mutant, causes holoprosencephaly which results from a failure of the forebrain to sufficiently divide into two lobes, leading to a single lobed brain as well as skull and facial defects (Reiter and Skarnes 2006). Holoprosencephaly is associated with decreased Hedgehog signaling (Chiang et al. 1996). Shh is a member of the Hedgehog family of secreted proteins, and acts in determining cell fate in the developing neural tube. Shh binds the Patched receptor, which in the absence of Shh, represses downstream signaling through the membrane protein Smoothened (reviewed in Nybakken and Perrimon 2002). When Shh binds Patched, the repression of Smoothened is relieved and the Shh signaling pathway is initiated. The effects of this pathway are, eventually, the activation of Gli transcription factors. Epistasis experiments indicate that Tectonic likely acts downstream of Patched and Smoothened (Reiter and Skarnes 2006). The *Tectonic* mutants lack floor plates, which are thought to be induced by Shh signals, though the notochord forms correctly and expresses Shh. Tectonic, like Shh, is responsible for induction of ventral cell fates in the neural tube (Reiter and Skarnes 2006; Litingtung and Chiang 2000; Wijgerde et al. 2002). Ventral expansion occurs for dorsal neural tube genes in *Tectonic* mutants (Reiter and Skarnes 2006). At this point Tectonic is thought to fully activate the Shh signaling pathway when Shh levels are high, but to repress the pathway when Shh levels are low. This makes Tectonic an interesting component of an important neural signaling pathway which has yet to be completely characterized.

The sequence of the *Tect3* gene should be confirmed in our FVB/N and BALB/c strains, and the expression of Tect3 should be analyzed in the early embryo to confirm that it is expressed in the neural tube or surrounding tissues at the time of neural tube closure, before it can be considered a likely candidate. The location of this gene at the peak of the linkage region, as well as the known SNP, provides initial support for this gene as a modifier candidate. The role of a closely related family member, Tectonic, in the development of the floorplate, which is important in neural fold elevation, make this a very interesting candidate for a modifier of exencephaly.

4.3 Modification of the *Pax3* and *Shrm* mutant phenotypes

4.3.1 The frequency of spina bifida, and possibly exencephaly, is reduced in *Sp* mutant embryos by genes in the FVB/N background

The effect of a ~75% FVB/N background on the *Sp* mutant phenotype was examined, and compared to the phenotype on the C57BL/6J strain. The frequency of spina bifida in *Sp/Sp* mice dropped from 100% on the C57BL/6J background, to 73.1% on the predominantly FVB/N background, which was a significant variation. The frequency of exencephaly also dropped from 25.7% to 11.5%, but because exencephaly is observed less frequently than spina bifida on either background, the sample size was too small to confirm if the deviation was significant.

The effect of the FVB/N background at the F2 generation was not examined for the *Cecr2* mutation, so it is difficult to directly compare the effect of this mixed background on the two mutant lines. The penetrance of the *Cecr2* mutation was analyzed after 5 generations of crosses onto the FVB/N background from a BALB/129ola mixed background, and at this point the penetrance had decreased from 67% to 0% (Banting et al. 2005). The penetrance was also analyzed after a single cross of BALB/c *Cecr2*$^{+/m}$ mice to FVB/N *Cecr2*$^{m/m}$ mice, and this showed that the FVB/N modifiers acted in a dominant or semi-dominant manner, and the penetrance of exencephaly was reduced from 74% to 2.9%. In the FVB/C57 F2 embryos scored for NTD penetrance, only ~1/16 of the loci should be homozygous for the C57BL/6J allele. Therefore, if the FVB/N background was dominantly affecting the *Sp* phenotype in the same manner as for the *Cecr2* mutation, a larger drop would be expected. It is therefore possible that the same chromosome 19 modifier is affecting the penetrance of exencephaly and/or spina bifida, but to a lesser extent or in a recessive manner. It is also possible that some other modifier(s) in the FVB/N background are affecting the frequency of one or both of the NTDs in *Sp* mutants.

It is known that the *Sp* penetrance is highly susceptible to modifier loci present in the genetic background. For example, when the *Sp* mutation was bred onto an In[1]lRk background, the penetrance of exencephaly increased to 100% and the penetrance of spina bifida dropped to 25% (Moase and Trasler 1987). To determine if the chromosome 19 modifier is responsible for the penetrance decreases seen in *Sp* mutants, the *Sp* mutation should be analyzed on a background which is derived completely from the C57BL/6J strain, with the exception of the modifier region on chromosome 19, which would be derived from the FVB/N strain. This experiment would help determine whether the chromosome 19 modifier acts in a more general sense on neural tube closure, or if the modifier acts specifically on the *Cecr2* mutant phenotype, and which regions of the neural tube it is capable of affecting. Knowing that the chromosome 19 modifier also affects caudal neurulation would narrow down the list of candidates to those expressed at the time of neurulation in both the anterior and posterior regions of the neural tube.

4.3.2 Known modifiers of the *Pax3* mutant phenotype

Many gene-gene interactions in the *Sp* mutants have been studied. Through these experiments a number of types of genes have been found to influence the penetrance of NTDs in *Sp* mutants. Several of the genes which affect the *Sp* phenotype are unlikely to function in the Pax3 pathway, but rather have an additive effect on the process of neural tube closure. The genes which are known to affect the *Sp* NTD phenotype include *ct*, *fidgetin*, *neurofibromin* and *p53* (Estibeiro et al. 1993; Konyukhov and Mironova 1979; Lakkis et al. 1999; Pani et al. 2002).

The *neurofibromin (nf1)* gene encodes an intracellular signal transduction protein which acts as a tumor suppressor (reviewed in Gutmann et al. 1997; Ballester et al. 1990). Homozygous mutants for the *nf1* gene develop occasional exencephaly and Nf1 shows a similar expression pattern to *Pax3* (Lakkis et al. 1999; Gutmann et al. 1995). The *Sp/nf1* double heterozygotes develop NTDs at a low level, which is not characteristic of either single heterozygote, and the double homozygous mutant embryos develop severe NTDs in all cases (Lakkis et al. 1999). A Pax3 binding site, which can control Pax3 dependent transcription of a reporter construct, exists in the *nf1* gene. This may indicate a role in modifying expression and therefore be an example of a gene in a common pathway, but no variation in Nf1 levels have been found in *Sp* homozygotes.

Another interacting gene is *p53*. In a *Sp/p53* double mutant, all spinal and cranial NTDs are completely rescued along with the increased apoptosis which occurs in the neuroepithelium of *Sp* homozygous mutants (Pani et al. 2002). This modifier is likely acting at a cellular level to correct an underlying defect in *Sp* mutants.

The *fidgetin* gene encodes an AAA protein, and the fidget mutant line develops ear and eye defects, as well as skeletal abnormalities (Cox et al. 2000; Truslove 1956). The *fidget* mutant line has a two hour increase in the duration of the cell cycle in the midbrain, whereas *Sp* mutants show a decrease in cell cycle length in the developing brain (Konyukhov and Vakhrusheva 1969; Konyukhov and Mironova 1974). The NTD frequency dropped from ~47.2% in the *Sp/Sp* embryos to 3.2% in the double homozygotes (Konyukhov and Mironova 1979). In this case, the two mutants likely have an opposing effect on the proliferation in the neural tube and therefore normalize its development.

The *ct* gene changes the *Sp* penetrance by affecting the end result of a tissue, without affecting any similar pathway or changing the underlying cause of the defect. The *curly tail* line develops spina bifida due to a proliferation defect in the hindgut endoderm and other tissues tethered to the neural tube (reviewed in van Straaten and Copp 2001). This effect, in combination with normal proliferation in the neural tube, causes a curvature defect in the spinal region which delays closure of the posterior neuropore.. The *Sp* mutant shows a reduced curvature in the PNP region, as opposed to the increased curvature in *ct* mice (Estibeiro et al. 1993). The *Sp* heterozygous genotype, however, increases the frequency of spina bifida in ct/ct mice by 13 fold and the frequency of tail flexion defects from 13.7% to 39.8% (Estibeiro et al. 1993). The underlying ventral curvature defect which causes the *ct* phenotype is not worsened in the double mutants, but is actually normalized slightly. This indicates that the two NTD genes can summate to increase the NTD frequency without acting in the same pathway. This is in agreement with the belief that modifiers for NTDs can act on different aspects of neural tube closure, possibly delaying closure beyond the tolerable threshold.

The modification of the *Sp* phenotype by various genetic backgrounds and mutant genes, suggests a high susceptibility of this mutant allele to modifiers. It also illustrates the general susceptibility of NTD mutant mouse lines to modifier genes which may act in the same pathway or just on the same cells or tissues. The idea that several types of genes may modify the phenotype in *Sp* mutant mice makes it more critical to examine the specific effects of the FVB/N chromosome 19 modifier region on NTD penetrance, as the decrease may not result from this modifier.

4.3.3 Which *shrm* mutant phenotypes are affected?

The *shrm* mutant mice develop four types of defects: exencephaly, facial clefting, spina bifida, and ventral closure defects. The original mutation was examined on a C57BL/6J background. This study compares the penetrance of these defects on this original background to the penetrance on a 75% FVB/N and 25% C57BL/6J background. The penetrance of these four defects on the mixed background did not vary significantly from the previously reported penetrance (Hildebrand and Soriano 1999). Interestingly, the spina bifida penetrance found in the small scale penetrance analysis done in our laboratory on the original C57BL/6J strain, which was intended to confirm the penetrance values found by Hildebrand and Soriano, differed from the original frequency reported. Hildebrand and Soriano reported a spina bifida penetrance of 23%, whereas it was found to be 87.5% (7/8) on the same background in my analysis. The penetrance of spina bifida on the predominantly FVB/N background was only 8.7% (2/23), which was lower than that reported by Hildebrand and Soriano, though not significantly. The spina bifida frequency was significantly different between the two backgrounds using the data collected in my analysis. The explanation for a penetrance variation seen in a mutant line on the same genetic background in two different laboratories would most likely be environmental. Environmental variations, like diet, can account for large variations in penetrance. For example, the exencephaly frequency in the SELH/Bc strain can vary 2-8 fold when fed two different commercial diets (Harris and Juriloff 2005).

The study done on the C57BL/6J strain in our lab is more relevant in comparing to the FVB/C57 penetrance collected in our lab, as the common environment eliminates most non-genetic factors. The study, however, lacked sufficient numbers to study the degree of variation in penetrance between the 2 backgrounds. The only other variation between the two backgrounds was a low penetrance of exencephaly, of about 8%, in *shrm* heterozygotes on the C57BL/6J strain, but not on the FVB/C57 strain. This may indicate a slightly increased resistance to exencephaly due to the contribution of the FVB/N strain or a difference in dosage sensitivity between the backgrounds. This effect would also be more easily studied if a larger sample of FVB/C57 mice was used, as the frequency is very low.

4.3.4 How could the modifier candidates affect the *Sp* and *shrm* mutant phenotypes?

The *Pax3* mutant line develops several defects, including two types of NTDs, exencephaly and spina bifida, and several defects in NCC-derived structures (Auerbach 1954). The effect of the FVB/N background was only examined in regards to the NTD phenotypes. As mentioned earlier, the penetrance of spina bifida was decreased on the predominantly FVB/N background, and the frequency of exencephaly was slightly reduced, though this could not be confirmed statistically. The spina bifida penetrance is also reduced in the *shrm* mutant line. It is possible that these phenotypes are modified by the same chromosome 19 loci that modifies exencephaly in *Cecr2* mutants, though this has not been confirmed to date.

If the same modifier gene is responsible for the penetrance variations in the *Sp* and *shrm* mutant lines, the most likely candidate is *Cyp26a1*, though *Pax2* is also a possibility. *Smarca2* was noted as a modifier candidate due to a functional similarity to the ATPase protein SNF2L, which remodels chromatin and is known to complex with CECR2 in humans (Banting et al. 2005). This would most likely be a modifier of *Cecr2* specifically, due to a direct interaction with Cecr2 or a possible functional redundancy with a Cecr2-containing complex. The *Tect3* gene is also not a likely candidate for a modifier in these two mutant lines as the sequence of the *Tect3* mRNA does not differ between the original C57BL/6J strain and the FVB/N strain. Both strains encode a methionine at position 186 of Tect3. The effect of the *Pax2* gene on neurulation in general is not well understood, and the underlying defect which leads to the development of exencephaly is unclear. The role of Pax2 in midbrain-cerebellum formation has been examined to some degree, though the presence of exencephaly in these mutants is not understood. It is therefore difficult to determine how likely Pax2 is to act as a modifier of exencephaly in any of the mutant lines (Torres et al. 1996; Favor et al. 1996). Pax2 is expressed in the developing spinal cord so it is a possible modifier of spina bifida, though its function in this tissue has not been examined (Dressler et al. 1990). The *Cyp26a1* gene encodes a protein which converts retinoic acid to inactive metabolites (Abu-Abed et al. 2001; Sakai et al. 2001). *Cyp26al* mutant mice develop exencephaly and spina bifida, so the gene is known to affect neurulation of both the cranial and caudal regions of the embryo. This makes it a possible modifier of both types of NTDs which show penetrance variations in the *Cecr2*, *Sp*, and *shrm* mutant lines (Abu-Abed et al. 2001; Sakai et al. 2001). Though RA administered at high doses or at E8, is teratogenic and causes increased NTDs, it is known to decrease spina bifida and exencephaly in *Sp* mice when administered at E9 at low doses (Tom et al. 1991; Kapron-Bras and Trasler 1985; Nobakht et al. 2006). The known effect of RA on *Sp* mice increases its likelihood as a modifier gene candidate, and an allele which causes Cyp26a1 expression level or timing to change in a specific manner could possibly decrease exencephaly and spina bifida. Retinoic acid studies have not been done on the *shrm* mutation, so its possible rescuing effect on spina bifida is unknown.

Before further examination is done on the possible candidate genes on chromosome 19, congenic lines should be used to determine whether this region is causing the penetrance decreases in these mutants, as it is in *Cecr2* mutants.

4.3.5 General or specific modifier

Though all three mutant lines examined on the FVB/N background developed exencephaly, the underlying causes for the defects likely differ between the lines. The exencephaly phenotype in the *Sp* mutant line, for instance, differs from the other two lines in that the forebrain region closes normally (Auerbach 1954; Banting et al. 2005; Hildebrand and Soriano 1999). This may be because *Pax3* mutant mice form closure point 2 (Fleming and Copp 2000). Neural tube closure fails in the midbrain region in *Sp* mutants because the neural folds fail to adopt a concave morphology posterior to the initial closure point. This variation between the *Cecr2* and *Sp* mutant phenotypes may reveal an underlying difference which prevents the same modifier from acting on both lines. The exencephaly phenotype in the *shrm* mutants includes the entire brain, as in *Cecr2* mutant embryos, though this does not necessarily mean the same underlying mechanism is affected. Defects in many different pathways and steps in neural tube closure exhibit an identical phenotype. The *Sp* mutation may cause NTDs through a defect in NCC migration, whereas Shrm is presumed to affect the cellular architecture of the closing neural tube such that the neural plate cannot adopt the correct morphology to allow closure to occur (Auerbach 1954; Hildebrand and Soriano 1999). The Cecr2 pathway, and the mechanism by which the *Cecr2* mutation prevents the neural tube from closing, is unknown. The *Sp*, *shrm* and *Cecr2* mutations all cause a different set of NTDs. This observation itself may be evidence that different steps in the neural tube closure pathway are being affected in the different mutant lines, as some processes are specific to certain regions of the neural tube.

The fact that the penetrance of exencephaly was not affected significantly in either the *Sp* or *shrm* lines on a predominantly FVB/N background, suggests that the chromosome 19 modifier is not having a general effect on cranial neural tube closure. The modifier may act specifically on the Cecr2 pathway, or it may modify a subset of mutants which affect the same process involved in neural tube closure. For example if the *Cecr2* mutation results from a defect in fusion of the neural folds in the cranial region, and the FVB/N genome modifies the phenotype so as to allow fusion to occur, this modifier likely would not affect the *Sp* line, as closure 2 fusion does occur in this line. The modifier would likely not affect the *shrm* exencephaly penetrance either because the neural folds may not elevate properly to allow fusion. The FVB/N strain may reduce spina bifida penetrance in a more general manner, as it affects both the *Sp* and *shrm* lines. This effect on spina bifida may or may not be due to the chromosome 19 modifier. The determination of which region modifies the spina bifida penetrance, and the examination of the FVB/N background on other mouse mutants which develop spina bifida, may help determine if the same modifier is causing this effect and whether the effect is common to all mutants which develop spina bifida.

4.4 Closure 2 location

4.4.1 Closure 2 location is not a modifier of the *Cecr2* penetrance between the BALB/c and FVB/N strains

Closure site 2 location variability is a major hypothesis which exists to explain the strain dependent penetrance seen in many mouse models of exencephaly (reviewed in Copp 2005). This led us to examine if the genetic variation between BALB/c and FVB/N strains was affecting this known physiological susceptibility factor. The initiation site of closure point 2, however, did not vary between wild type FVB/N and BALB/c embryos, meaning that the genetic modifier did not act on the location of this closure point.

Exencephaly occurs when the neural folds fail to elevate in the region of the midbrain in nearly all affected mutant lines examined, including *Cart1*, *Opb*, *twist* and SELH/Bc (Zhao et al. 1996; Gunther et al. 1997; Chen and Behringer 1995; Macdonald et al. 1989). In typical exencephaly, the entire region of the brain is open, including the forebrain, midbrain, and hindbrain regions. The existence of closure 2 has not been specifically reported in many cases, but the open forebrain suggests that the failure of closure 2 is occurring in these mutant embryos. Initial examination also shows that the neural folds in *Cecr2*$^{m/m}$ embryos are open throughout the entire region of the forming brain, and exencephaly in *Cecr2*$^{m/m}$ mutants extends from the forebrain to the hindbrain (Ames 2006; Banting et al. 2005).

The only exencephalic mouse mutant which has been shown to be directly affected by closure 2 location is the *Sp*^{2H} mutant line. In this line, moving the mutation from a strain which has a rostral closure 2 location for 4 generations onto the DBA/2 strain, which initiates closure 2 within the midbrain, reduces the penetrance of exencephaly from 75% to 35.7% (Fleming and Copp 2000).

In these Sp^{2H} mutants closure 2 forms even in embryos which go on to develop exencephaly, and neural tube closure fails to zipper up correctly beyond this point (Fleming and Copp 2000). The penetrance reduction in this line which occurred by moving the closure 2 site caudally, is likely because this helps to provide mechanical support for the proper elevation and fusion of the midbrain neural folds. Therefore, the only direct evidence for variable closure 2 location as a susceptibility factor for exencephaly, is in a strain in which exencephalic embryos undergo normal closure 2. It is therefore unclear whether the initiation location of closure 2 will affect the frequency of exencephaly in strains which lack closure 2 in exencephalic mutants. The only other evidence for the role of closure site 2 location as a susceptibility factor is that rostrally closing strains tend to be more sensitive to teratogen induced NTDs, and spontaneous NTDs in the case of the NZW strain (Finnell et al. 1986; Finnell et al. 1988; Vogelweid et al. 1993). A further examination of this effect will clarify the extent of its role as a genetically determined susceptibility factor.

The observation that FVB/N and BALB/c strains both initiate closure 2 at the FB/MB boundary, shows that some other genetic factor plays a role in the strain dependent penetrance. It would be interesting to cross the *Cecr2* mutation onto a rostrally closing strain, and determine whether a change in closure 2 location can have an effect on exencephalic embryos which fail to form closure 2 at all.

4.4.2 The effect of closure 2 timing on penetrance

The BALB/c and FVB/N strains both appear to complete fusion of closure 2 at approximately the 9 somite stage. A more complete analysis of the neurulation process compared to somite number in a larger number of embryos may uncover subtle differences in developmental timing, but no obvious difference was seen in this study. The only difference found between BALB/c and FVB/N was in the timing of closure 2 in relation to gestational age, as FVB/N initiates closure 2 fusion at ~E8.75 as compared to ~E9.25 in BALB/c. The role of closure 2 timing variations in terms of developmental stage or gestational age has not been investigated thoroughly as a susceptibility factor for exencephaly. It is, however, easy to imagine that if closure 2 occurred at a later developmental stage, the delay in neural tube closure may prevent its completion. It is also possible that if closure 2 occurred at an earlier developmental stage there may be a deficiency in the number of cells in the neuroepithelium, or underlying tissues like the cranial mesenchyme, which could prevent correct elevation and fusion.

The effects of a difference in gestational age are more difficult to predict, but it is possible that there may be a difference in relation to the expression of other neurulation genes, or possibly to in utero environmental factors. The relevance of this difference in gestational age at the time of closure 2 between BALB/c and FVB/N is unclear at this point, though it was the only physiological variation in cranial neurulation found in this study. A further examination of the timing of neural tube patterning and closure genes between the two strains may help determine the significance of this finding.

4.4.3 Relevance to human NTD susceptibility

Human neurulation is proposed to occur by a very similar process as it does in the mouse, though the difficulty in studying this relatively short period in the third week of human embryonic development has left some questions unanswered (reviewed in Sadler 2005). Closure points 1 and 3 have been consistently observed in human embryos but there remains a great deal of controversy over the existence of closure 2. Some authors have observed a closure point around the FB/MB boundary, and other groups have postulated its existence based on the types of NTDs which exist in the human population (Nakatsu 2000; van Allen 1993). Others, however, have reported an absence of closure point 2 (Sulik 1998; O'Rahilly and Muller 2002). It is possible that humans are polymorphic for the location of closure site 2, as is the case in mice, and that in some cases closure site 2 is located extremely close to closure site 3 and cannot be distinguished as an independent closure event. This may help explain the variations in NTD frequency seen amongst various ethnic groups, as it has been found that closure site 2 position affects the NTD frequency in mice.

It is also possible that closure point 2 is not required for normal neurulation in human embryos. The brain of a human embryo at the time of neurulation is proportionately smaller than that of a mouse embryo (reviewed in Copp 2005). This may make it possible for the cranial neural tube to close efficiently by a zippering up between closure points 1 and 3, without a requirement for a closure point at the FB/MB boundary. Even in the SELH/Bc strain, which lack closure point 2, the cranial neural tube closes correctly in 83% of embryos through a zippering between closure sites 1 and 3 (Macdonald et al. 1989). If closure 2 is not absolutely necessary in the mouse, the proportionately shorter length of the cranial neural tube that must be fused in human embryos may eliminate the requirement for this closure point.

The modifier loci which causes variation in the penetrance of exencephaly in *Cecr2*$^{m/m}$ mutants between the BALB/c and FVB/N strains is affecting some aspect of cranial neurulation other than the position of closure site 2. Because the variation in closure site 2 is the only known characteristic which varies between normal inbred mouse strains to mediate susceptibility to exencephaly, it is interesting that this is not the variable which is being affected in the case of the *Cecr2* strain dependent penetrance. This is particularly intriguing if closure point 2 does not occur in human neurulation, as this modifier may therefore be a candidate for a susceptibility factor in human NTDs. It also makes it possible that this same modifier gene could affect neurulation in the caudal neural tube as well.

4.5 Future directions

The major future direction of this project is to identify the specific gene on chromosome 19 which is modifying the *Cecr2* exencephaly phenotype. This will involve refining the map to narrow the modifier region, and confirming any candidate genes in the region. A second goal is to confirm and characterize other potential modifier regions, like those on chromosomes 2 and possibly the X chromosome. Characterizing the role of Cecr2 in neurulation will be important not only for understanding the process of neurulation itself and its genetic components, but for determining the type of modifier which may affect its phenotype. Finally, the effect of the modifier on other mutant lines and teratogen induced exencephaly should be further examined. This will show the importance of the modifier to neurulation in general, and determine the underlying causes of exencephaly which can be modified by this locus.

4.5.1 Narrowing the modifier region using congenic lines

The modifier region, based on the linkage results obtained, is ~35 Mb. Although the genes in the peak area of the modifier region, at ~40 Mb, are the most likely candidates for modifier genes, the modifier could potentially be anywhere within this region which contains ~260 known genes, and ~280 predicted genes. One way to narrow the modifier region, and more clearly define the boundaries of the region, is to produce subinterval congenic lines with the *Cecr2* mutation on a BALB/c background with an FVB/N genotype in part of the modifier region on chromosome 19 **(Figure 21)**. Collecting more embryos may increase the difference in p value between the peak area and other regions on the chromosome, strengthening the argument for genes in the peak region, but will never provide clear boundaries for the linkage region. Sub-interval congenic lines can be produced by intercrossing wild type BALB/c and FVB/N mice and backcrossing the progeny to wild type BALB/c mice for ~5 or 6 generations. After each backcross, genotyping for various markers on chromosome 19 will be done , in particular rs3677115 which is at the peak of the linkage region. In this way the FVB/N regions of the genome are separated by recombination and the FVB/N genotype in various portions of the modifier region can be selected for, including small areas directly at the peak of the linkage region. Following the production of these backgrounds, which are more than 95% BALB/c with the exception of the modifier region, the *Cecr2* mutation on the BALB/c background will be mated to these mice, and both *Cecr2* genotyping and chromosome 19 genotyping will be done on the progeny. An intercross will then allow homozygous FVB/N genotypes on chromosome 19 and a heterozygous *Cecr2* genotype to be selected for. These mice will be intercrossed, and penetrance will be examined. The specific chromosomal region which causes the penetrance to be ~35% less than the expected 75% will contain the modifier region. This approach will allow the region to be narrowed such that far fewer candidates will need to be examined. While subinterval congenics may be the best way to narrow the modifier region, which is clearly the next step in this analysis, it is a slow process, and there will still likely be several candidate genes in the refined linkage region.

4.5.2 Sequencing and quantitative RT-PCR of 4 candidate genes

While it is difficult to choose candidate genes before further narrowing the linkage region, the process of producing congenic lines will likely take several years, and testing the preliminary candidate genes noted in this study may be worth pursuing before the completion of the subinterval congenic study. Sequencing should be done to locate any possible SNPs between BALB/c and FVB/N in the 4 genes. Partial sequencing has been done for the *Smarca2* gene but it needs to be completed, and the known SNP in *Tect3* and needs to be confirmed. In addition to looking for amino acid changes by sequencing the cDNA, expression differences in the mRNA using real time RT-PCR and differences in protein levels can also be examined. Any aa changes or differences in expression level provide possible evidence of a candidate gene, though confirmation of this is ultimately required. The likelihood of any candidate gene will be strongly assisted by the location of a variant which is enriched in human NTD cases, as there is known linkage of NTDs to this region in humans (Rampersaud et al. 2005).

4.5.3 Searching for possible X chromosome modifier

One interesting observation based on the mapping data is that the region around DXMit140 on the X chromosome suggests potential linkage to exencephaly penetrance. This could not be fully investigated in this study with the genotype data available, because only 32 samples were tested from the cross type which allowed the production of a recombined X chromosome. This could be investigated by first genotyping the unaffected samples from cross type 3 to discount any segregation distortion, and then by genotyping more exencephalic samples from this type of backcross. This would indicate whether linkage exists in this region. If linkage can be confirmed, a larger number of SNPs could be chosen on the X chromosome to locate the peak of the linkage region, as was done for chromosome 19.

4.5.4 Identify the cause of NTDs in the *Cecr2* mutant line

Several questions remain regarding the role of the *Cecr2* gene in neural tube closure. It is possible that the modifier gene affecting neural tube closure in *Cecr2* mutant mice is specific to this mutant line. One other interesting theory suggested from the data presented here, is that the modifier may be acting on a specific aspect of neural tube closure. In this case, it is possible that only mutations which cause defects in the same underlying process of neurulation can be modified by this gene. The first step in testing this theory is to determine the precise cause of the neurulation defect in *Cecr2* mutants. This will be done by locating differences between *Cecr2* homozygous mutants and wild type littermates at or before the time of neural tube closure. One way to do this is to find variations in the expression of other genes between wild type and mutant embryos at E8-E9.5 using microarray analysis. The types of genes which are directly or indirectly affected by the *Cecr2* mutation will provide a clue as to what role the *Cecr2* gene plays in neural tube closure.

Looking for disruptions in any of the major processes involved in neural tube closure can also be used to characterize the role of Cecr2. For instance, examining the levels of proliferation in the developing neural tube using BrdU staining, would confirm or rule out a proliferation defect similar to defects seen in *RBP-Jκ*, *Hes1* and *Numb* mutants (reviewed in Copp 2005). Misregulation of apoptosis can also lead to exencephaly, as in *Apaf1* and *Caspase 9* mutant mice (reviewed in Copp 2005). Apoptosis levels can be examined in *Cecr2* mutant embryos using TUNEL staining, which labels cells undergoing apoptosis. Several other processes involved in neurulation, such as neural crest migration, actin localization, and fusion of the neural tips, can also be examined in order to determine the specific defect in *Cecr2* mutant mice which results in an open cranial neural tube. As well, in situ hybridization comparisons between wild type and *Cecr2* mutant embryos can be used to find the underlying cause of the NTDs, particularly using genes involved in patterning the neural tube, like *Shh*.

A complete knockout of the *Cecr2* gene may also help identify its role, as the nature of the *Gt45Bic* mutant allele is still unclear. It is possible that the mutant allele is a hypomorph, though the Cecr2-LacZ fusion protein may be acting as a dominant negative if it can form non-functional complexes with Snf2l. This may complicate the understanding of the role of Cecr2, and a null mutation would clarify the role of Cecr2 in embryogenesis.

4.5.5 Examine the effect of a specific FVB/N chromosome 19 region on other NTD mutant lines and teratogens which induce exencephaly

The linkage results all focus on one major modifier region on chromosome 19, so the effect of this specific modifier on various mutations and teratogen induced exencephaly should be examined using congenic lines as explained above. This will eliminate the contribution of minor modifiers elsewhere in the FVB/N genetic background which may complicate the analysis. Looking at whether various teratogens, like valproic acid, hyperthermia, and RA, can induce higher frequencies of exencephaly in wild type BALB/c than in BALB/c mice with an FVB/N derived region on chromosome 19 will show whether exencephaly other than in *Cecr2* mutants can be modified by the same region on chromosome 19 (Nau 1986; Webster and Edwards 1984; Tom et al. 1991). Following this, other exencephaly mutant lines which affect the various processes involved in neural tube closure can also be examined on this congenic background. This will be particularly interesting once the role of *Cecr2* in neurulation has been determined, as other mutant lines affecting the same process can be chosen for this experiment. This will test the theory that the modifier can affect a subset of NTD mutant mice which affect the same underlying process of neural tube closure.

4.6 Significance of this work

In this study I have mapped a genetic modifier of the *Cecr2* mutant phenotype to a 35 Mb region on chromosome 19, and begun characterizing the effect of the modifier and examining candidate genes. I have shown that the modifier(s) which cause *Cecr2* mutant mice to be resistant to exencephaly on the FVB/N background act in a dominant or semidominant manner. The modifier region mapped in my linkage study corresponded to a region of conserved synteny on human chromosome 10 which was mapped in an NTD linkage study (Rampersaud et al. 2005). Though it is not necessarily the same gene which causes linkage in humans and mice, the mouse model system described here may provide a means to locate and test human candidate gene(s). The narrowing of the region mapped to mouse chromosome 19 through genetic methods, like the creation of congenic lines, may be used to reduce the number of human candidates in the syntenic region. Only a single gene, *MTHFR*, has been linked to human NTD susceptibility to date, and this gene does not appear to be involved in a large number of

NTD cases (Whitehead et al. 1995). Mapping a second human susceptibility factor would be a significant step towards understanding human NTDs.

I have also begun to characterize the effect of the FVB/N background, which causes resistance to exencephaly in *Cecr2* mutants, on other NTD mutant lines. This was the initial step taken to determine if the modifier(s) act in a general sense on the closure of the neural tube. I found that exencephaly in two other mutant mouse lines, *Sp* and *shrm*, was not significantly reduced on a background which consisted of 75% FVB/N genetic loci. A slight decrease in exencephaly in *Sp* mice was seen on this new background, though it was difficult to confirm with the sample size used. These results suggest that the modifier acts either specifically in the Cecr2 pathway, or that it is only capable of modifying a subset of neurulation defects, possibly those which result from a defect in a specific process of neural tube closure. I did, however, find that spina bifida was significantly reduced in both *Sp* and *shrm* mutant lines on the predominantly FVB/N background, as compared to their original C57BL/6J backgrounds. Whether the reduction of spina bifida by the FVB/N background is due to the chromosome 19 modifier or a combination of other weaker modifiers has yet to be examined.

I have also characterized normal closure 2 location in wild type BALB/c and FVB/N embryos, and found that the location was consistently at the FB/MB boundary in both strains. This ruled out a variable closure 2 location as the underlying physiological cause of the susceptibility difference. This is a significant observation, as closure 2 location is the only variation between normal mouse strains which is known to affect the penetrance of exencephaly. It may also make the modifier more relevant to human NTDs, as it is still not clear whether closure 2 forms in human embryos. The work completed in this study has identified a chromosomal region, as well as several modifier candidates. This provides the groundwork for future determination of the specific gene which modifies the *Cecr2* mutant phenotype.

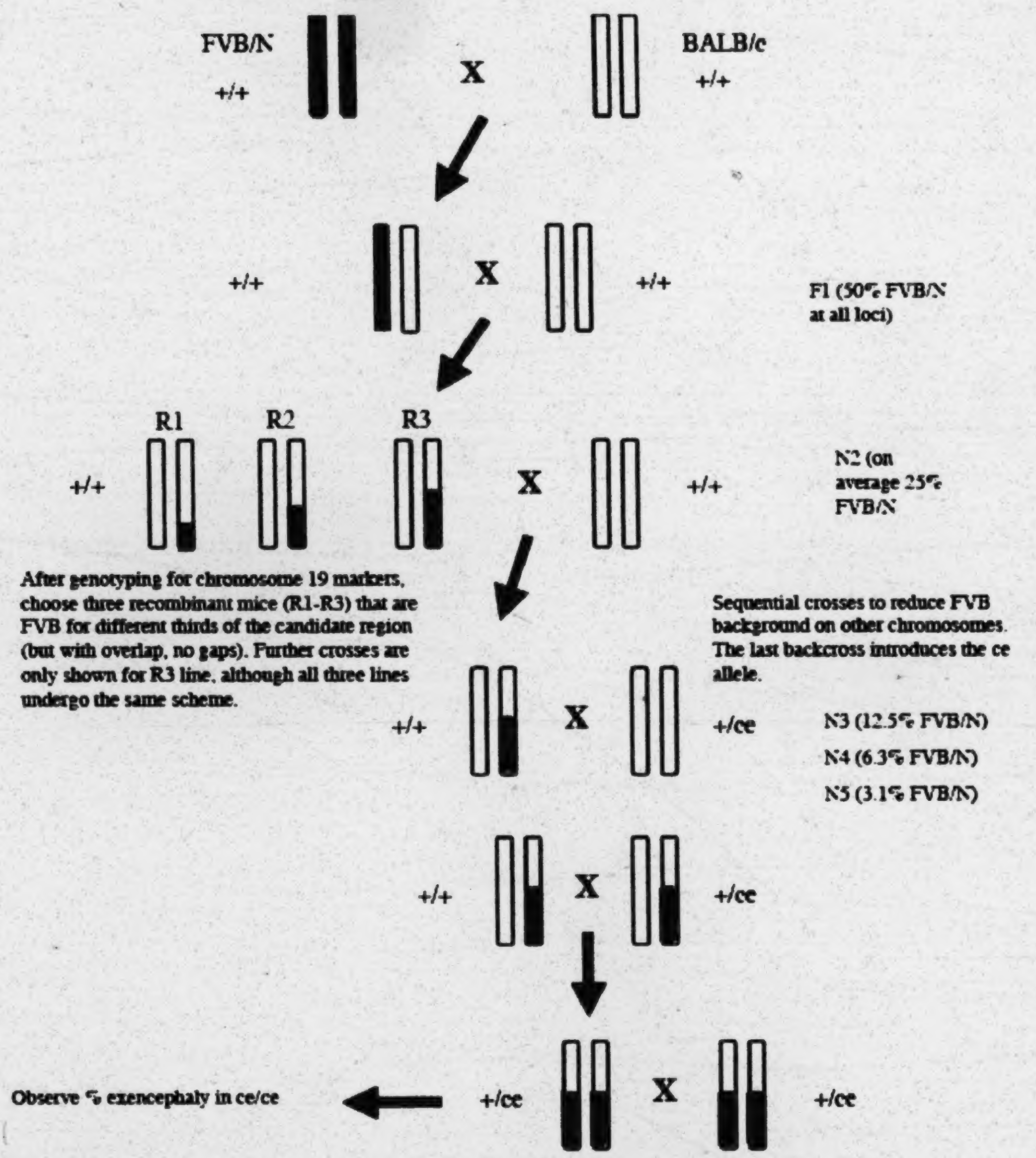
FVB/N
+/+
X
BALB/c
+/+
+/+
X
+/+
F1 (50% FVB/N at all loci)
R1
R2
R3
+/+
X
+/+
N2 (on average 25% FVB/N
+/+
X
+/ce
N3 (12.5% FVB/N)
N4 (6.3% FVB/N)
N5 (3.1% FVB/N)
+/+
X
+/ce
+/ce
X
+/ce
Observe % exencephaly in ce/ce

After genotyping for chromosome 19 markers, choose three recombinant mice (R1-R3) that are FVB for different thirds of the candidate region (but with overlap, no gaps). Further crosses are only shown for R3 line, although all three lines undergo the same scheme.

Sequential crosses to reduce FVB background on other chromosomes. The last backcross introduces the ce allele.

Figure 21. Breeding strategy for producing subinterval-specific congenics to narrow down the modifier region on chromosome 19. Chromosome 19 is depicted in the diagram. Black represents FVB/N and white represents BALB/c. Ce represents the *Cecr2*^{GT45Bic} mutation, + represents the *Cecr2* wild type allele. *Cecr2* is on chromosome 6 (modified from Juriloff et al, 2001). Diagram provided by Heather McDermid.

Chapter 5. References

Aalfs, J.D. and Kingston, R.E. (2000) What does 'chromatin remodeling' mean? *Trends Biochem Sci*, **25**, 548-555.

Aalfs, J.D., Narlikar, G.J. and Kingston, R.E. (2001) Functional differences between the human ATP-dependent nucleosome remodeling proteins BRG1 and SNF2H. *J Biol Chem*, **276**, 34270-34278.

Abu-Abed, S., Dolle, P., Metzger, D., Beckett, B., Chambon, P. and Petkovich, M. (2001) The retinoic acid-metabolizing enzyme, CYP26A1, is essential for normal hindbrain patterning, vertebral identity, and development of posterior structures. *Genes Dev*, **15**, 226-240.

Abu-Abed, S., Dolle, P., Metzger, D., Wood, C., MacLean, G., Chambon, P. and Petkovich, M. (2003) Developing with lethal RA levels: genetic ablation of Rarg can restore the viability of mice lacking Cyp26a1. *Development*, **130**, 1449-1459.

Ames, T.M. (2006) Characterization of *Cecr2* expression and the *Cecr2*^{Gt45Bic} mutation on different mouse genetic backgrounds. In *Biological Sciences*, University of Alberta, Edmonton, Alberta, Canada.

Armstrong, J.F., Kaufman, M.H., Harrison, D.J. and Clarke, A.R. (1995) High-frequency developmental abnormalities in p53-deficient mice. *Curr Biol*, **5**, 931-936.

Auerbach, R. (1954) Analysis of the developmental effects of a lethal mutation in a house mouse. *J. Exp. Zool.* **127**, 305–329.

Baldwin, C.T., Hoth, C.F., Amos, J.A., da-Silva, E.O. and Milunsky, A. (1992) An exonic mutation in the HuP2 paired domain gene causes Waardenburg's syndrome. *Nature*, **355**, 637-638.

Ballester, R., Marchuk, D., Boguski, M., Saulino, A., Letcher, R., Wigler, M. and Collins, F. (1990) The NF1 locus encodes a protein functionally related to mammalian GAP and yeast IRA proteins. *Cell*, **63**, 851-859.

Bamforth, S.D., Braganca, J., Eloranta, J.J., Murdoch, J.N., Marques, F.I., Kranc, K.R., Farza, H., Henderson, D.J., Hurst, H.C. and Bhattacharya, S. (2001) Cardiac malformations, adrenal agenesis, neural crest defects and exencephaly in mice lacking Cited2, a new Tfap2 co-activator. *Nat Genet*, **29**, 469-474.

Banting, G.S. (2003) Characterization of the cat eye syndrome candidate gene CECR2. In *Biological Sciences*, University of Alberta, Edmonton, Alberta, Canada.

Banting, G.S., Barak, O., Ames, T.M., Burnham, A.C., Kardel, M.D., Cooch, N.S., Davidson, C.E., Godbout, R., McDermid, H.E. and Shiekhattar, R. (2005) CECR2, a protein involved in neurulation, forms a novel chromatin remodeling complex with SNF2L. *Hum Mol Genet*, **14**, 513-524.

Barak, O., Lazzaro, M.A., Lane, W.S., Speicher, D.W., Picketts, D.J. and Shiekhattar, R. (2003) Isolation of human NURF: a regulator of Engrailed gene expression. *Embo J*, **22**, 6089-6100.

Bauer, K.A., George, T.M., Enterline, D.S., Stottmann, R.W., Melvin, E.C., Siegel, D., Samal, S., Hauser, M.A., Klingensmith, J., Nye, J.S. and Speer, M.C. (2002) A novel mutation in the gene encoding noggin is not causative in human neural tube defects. *J Neurogenet*, **16**, 65-71.

Benz, L.P., Swift, F.E., Graham, F.L., Enterline, D.S., Melvin, E.C., Hammock, P., Gilbert, J.R., Speer, M.C., Bassuk, A.G., Kessler, J.A. and George, T.M. (2004)

TERC is not a major gene in human neural tube defects. *Birth Defects Res A Clin Mol Teratol*, **70**, 531-533.

Berk, M., Desai, S.Y., Heyman, H.C. and Colmenares, C. (1997) Mice lacking the ski proto-oncogene have defects in neurulation, craniofacial, patterning, and skeletal muscle development. *Genes Dev*, **11**, 2029-2039.

Berube, N.G., Jagla, M., Smeenk, C., De Repentigny, Y., Kothary, R. and Picketts, D.J. (2002) Neurodevelopmental defects resulting from ATRX overexpression in transgenic mice. *Hum Mol Genet*, **11**, 253-261.

Borycki, A.G., Li, J., Jin, F., Emerson, C.P. and Epstein, J.A. (1999) Pax3 functions in cell survival and in pax7 regulation. *Development*, **126**, 1665-1674.

Bouchard, M., Pfeffer, P. and Busslinger, M. (2000) Functional equivalence of the transcription factors Pax2 and Pax5 in mouse development. *Development*, **127**, 3703-3713.

Boyles, A.L., Hammock, P. and Speer, M.C. (2005) Candidate gene analysis in human neural tube defects. *Am J Med Genet C Semin Med Genet*, **135**, 9-23.

Brook, F.A., Estibeiro, J.P. and Copp, A.J. (1994) Female predisposition to cranial neural tube defects is not because of a difference between the sexes in the rate of embryonic growth or development during neurulation. *J Med Genet*, **31**, 383-387.

Bultman, S., Gebuhr, T., Yee, D., La Mantia, C., Nicholson, J., Gilliam, A., Randazzo, F., Metzger, D., Chambon, P., Crabtree, G. and Magnuson, T. (2000) A Brg1 null mutation in the mouse reveals functional differences among mammalian SWI/SNF complexes. *Mol Cell*, **6**, 1287-1295.

Chalepakis, G., Jones, F.S., Edelman, G.M. and Gruss, P. (1994) Pax-3 contains domains for transcription activation and transcription inhibition. *Proc Natl Acad Sci U S A*, **91**, 12745-12749.

Chambon, P. (1996) A decade of molecular biology of retinoic acid receptors. *Faseb J*, **10**, 940-954.

Chen, W.H., Morriss-Kay, G.M. and Copp, A.J. (1995) Genesis and prevention of spinal neural tube defects in the curly tail mutant mouse: involvement of retinoic acid and its nuclear receptors RAR-beta and RAR-gamma. *Development*, **121**, 681-691.

Chen, Z.F. and Behringer, R.R. (1995) twist is required in head mesenchyme for cranial neural tube morphogenesis. *Genes Dev*, **9**, 686-699.

Chiang, C., Litingtung, Y., Lee, E., Young, K.E., Corden, J.L., Westphal, H. and Beachy, P.A. (1996) Cyclopia and defective axial patterning in mice lacking Sonic hedgehog gene function. *Nature*, **383**, 407-413.

Colmenares, C., Heilstedt, H.A., Shaffer, L.G., Schwartz, S., Berk, M., Murray, J.C. and Stavnezer, E. (2002) Loss of the SKI proto-oncogene in individuals affected with 1p36 deletion syndrome is predicted by strain-dependent defects in Ski-/- mice. *Nat Genet*, **30**, 106-109.

Conway, S.J., Henderson, D.J., Kirby, M.L., Anderson, R.H. and Copp, A.J. (1997) Development of a lethal congenital heart defect in the splotch (Pax3) mutant mouse. *Cardiovasc Res*, **36**, 163-173.

Copp, A.J. (2005) Neurulation in the cranial region--normal and abnormal. *J Anat*, **207**, 623-635.

Copp, A.J. and Brook, F.A. (1989) Does lumbosacral spina bifida arise by failure of neural folding or by defective canalisation? *J Med Genet*, **26**, 160-166.

Copp, A.J., Brook, F.A., Estibeiro, J.P., Shum, A.S. and Cockroft, D.L. (1990) The embryonic development of mammalian neural tube defects. *Prog Neurobiol*, **35**, 363-403.

Copp, A.J., Greene, N.D. and Murdoch, J.N. (2003) The genetic basis of mammalian neurulation. *Nat Rev Genet*, **4**, 784-793.

Corey, L.L., Weirich, C.S., Benjamin, I.J. and Kingston, R.E. (2003) Localized recruitment of a chromatin-remodeling activity by an activator in vivo drives transcriptional elongation. *Genes Dev*, **17**, 1392-1401.

Cox, G.A., Mahaffey, C.L., Nystuen, A., Letts, V.A. and Frankel, W.N. (2000) The mouse fidgetin gene defines a new role for AAA family proteins in mammalian development. *Nat Genet*, **26**, 198-202.

Curtin, J.A., Quint, E., Tsipouri, V., Arkell, R.M., Cattanach, B., Copp, A.J., Henderson, D.J., Spurr, N., Stanier, P., Fisher, E.M., Nolan, P.M., Steel, K.P., Brown, S.D., Gray, I.C. and Murdoch, J.N. (2003) Mutation of Celsr1 disrupts planar polarity of inner ear hair cells and causes severe neural tube defects in the mouse. *Curr Biol*, **13**, 1129-1133.

Dauvillier, S., Ott, M.O., Renard, J.P. and Legouy, E. (2001) BRM (SNF2alpha) expression is concomitant to the onset of vasculogenesis in early mouse postimplantation development. *Mech Dev*, **101**, 221-225.

Deak, K.L., Boyles, A.L., Etchevers, H.C., Melvin, E.C., Siegel, D.G., Graham, F.L., Slifer, S.H., Enterline, D.S., George, T.M., Vekemans, M., McClay, D., Bassuk, A.G., Kessler, J.A., Linney, E., Gilbert, J.R. and Speer, M.C. (2005a) SNPs in the neural cell adhesion molecule 1 gene (NCAM1) may be associated with human neural tube defects. *Hum Genet*, **117**, 133-142.

Deak, K.L., Dickerson, M.E., Linney, E., Enterline, D.S., George, T.M., Melvin, E.C., Graham, F.L., Siegel, D.G., Hammock, P., Mehltretter, L., Bassuk, A.G., Kessler, J.A., Gilbert, J.R. and Speer, M.C. (2005b) Analysis of ALDH1A2, CYP26A1, CYP26B1, CRABP1, and CRABP2 in human neural tube defects suggests a possible association with alleles in ALDH1A2. *Birth Defects Res A Clin Mol Teratol*, **73**, 868-875.

Detrait, E.R., George, T.M., Etchevers, H.C., Gilbert, J.R., Vekemans, M. and Speer, M.C. (2005) Human neural tube defects: developmental biology, epidemiology, and genetics. *Neurotoxicol Teratol*, **27**, 515-524.

Dilworth, F.J. and Chambon, P. (2001) Nuclear receptors coordinate the activities of chromatin remodeling complexes and coactivators to facilitate initiation of transcription. *Oncogene*, **20**, 3047-3054.

Dressler, G.R., Deutsch, U., Chowdhury, K., Nornes, H.O. and Gruss, P. (1990) Pax2, a new murine paired-box-containing gene and its expression in the developing excretory system. *Development*, **109**, 787-795.

Eberharter, A. and Becker, P.B. (2004) ATP-dependent nucleosome remodelling: factors and functions. *J Cell Sci*, **117**, 3707-3711.

Echelard, Y., Epstein, D.J., St-Jacques, B., Shen, L., Mohler, J., McMahon, J.A. and McMahon, A.P. (1993) Sonic hedgehog, a member of a family of putative signaling molecules, is implicated in the regulation of CNS polarity. *Cell*, **75**, 1417-1430.

Edelman, G.M. and Jones, F.S. (1995) Developmental control of N-CAM expression by Hox and Pax gene products. *Philos Trans R Soc Lond B Biol Sci*, **349**, 305-312.

Embury, S., Seller, M.J., Adinolfi, M. and Polani, P.E. (1979) Neural tube defects in curly-tail mice. I. Incidence, expression and similarity to the human condition. *Proc R Soc Lond B Biol Sci*, **206**, 85-94.

Epstein, D.J., Vogan, K.J., Trasler, D.G. and Gros, P. (1993) A mutation within intron 3 of the Pax-3 gene produces aberrantly spliced mRNA transcripts in the splotch (Sp) mouse mutant. *Proc Natl Acad Sci U S A*, **90**, 532-536.

Essien, F.B. (1992) Maternal methionine supplementation promotes the remediation of axial defects in Axd mouse neural tube mutants. *Teratology*, **45**, 205-212.

Estibeiro, J.P., Brook, F.A. and Copp, A.J. (1993) Interaction between splotch (Sp) and curly tail (ct) mouse mutants in the embryonic development of neural tube defects. *Development*, **119**, 113-121.

Ewart, J.L., Cohen, M.F., Meyer, R.A., Huang, G.Y., Wessels, A., Gourdie, R.G., Chin, A.J., Park, S.M., Lazatin, B.O., Villabon, S. and Lo, C.W. (1997) Heart and neural tube defects in transgenic mice overexpressing the Cx43 gap junction gene. *Development*, **124**, 1281-1292.

Favor, J., Sandulache, R., Neuhauser-Klaus, A., Pretsch, W., Chatterjee, B., Senft, E., Wurst, W., Blanquet, V., Grimes, P., Sporle, R. and Schughart, K. (1996) The mouse Pax2(1Neu) mutation is identical to a human PAX2 mutation in a family with renal-coloboma syndrome and results in developmental defects of the brain, ear, eye, and kidney. *Proc Natl Acad Sci U S A*, **93**, 13870-13875.

Fazzio, T.G., Gelbart, M.E. and Tsukiyama, T. (2005) Two distinct mechanisms of chromatin interaction by the Isw2 chromatin remodeling complex in vivo. *Mol Cell Biol*, **25**, 9165-9174.

Fazzio, T.G. and Tsukiyama, T. (2003) Chromatin remodeling in vivo: evidence for a nucleosome sliding mechanism. *Mol Cell*, **12**, 1333-1340.

Finnell, R.H., Bennett, G.D., Karras, S.B. and Mohl, V.K. (1988) Common hierarchies of susceptibility to the induction of neural tube defects in mouse embryos by valproic acid and its 4-propyl-4-pentenoic acid metabolite. *Teratology*, **38**, 313-320.

Finnell, R.H., Moon, S.P., Abbott, L.C., Golden, J.A. and Chernoff, G.F. (1986) Strain differences in heat-induced neural tube defects in mice. *Teratology*, **33**, 247-252.

Fleming, A. and Copp, A.J. (2000) A genetic risk factor for mouse neural tube defects: defining the embryonic basis. *Hum Mol Genet*, **9**, 575-581.

Footz, T.K., Brinkman-Mills, P., Banting, G.S., Maier, S.A., Riazi, M.A., Bridgland, L., Hu, S., Birren, B., Minoshima, S., Shimizu, N., Pan, H., Nguyen, T., Fang, F., Fu, Y., Ray, L., Wu, H., Shaull, S., Phan, S., Yao, Z., Chen, F., Huan, A., Hu, P., Wang, Q., Loh, P., Qi, S., Roe, B.A. and McDermid, H.E. (2001) Analysis of the cat eye syndrome critical region in humans and the region of conserved synteny in mice: a search for candidate genes at or near the human chromosome 22 pericentromere. *Genome Res*, **11**, 1053-1070.

Franz, T. (1989) Persistent truncus arteriosus in the Splotch mutant mouse. *Anat Embryol (Berl)*, **180**, 457-464.

Franz, T. (1990) Defective ensheathment of motoric nerves in the Splotch mutant mouse. *Acta Anat (Basel)*, **138**, 246-253.

Fujii, H., Sato, T., Kaneko, S., Gotoh, O., Fujii-Kuriyama, Y., Osawa, K., Kato, S. and Hamada, H. (1997) Metabolic inactivation of retinoic acid by a novel P450 differentially expressed in developing mouse embryos. *Embo J*, **16**, 4163-4173.

Fyodorov, D.V. and Kadonaga, J.T. (2002) Binding of Acf1 to DNA involves a WAC motif and is important for ACF-mediated chromatin assembly. *Mol Cell Biol*, **22**, 6344-6353.

Golden, J.A. and Chernoff, G.F. (1993) Intermittent pattern of neural tube closure in two strains of mice. *Teratology*, **47**, 73-80.

Goulding, M., Sterrer, S., Fleming, J., Balling, R., Nadeau, J., Moore, K.J., Brown, S.D., Steel, K.P. and Gruss, P. (1993) Analysis of the Pax-3 gene in the mouse mutant splotch. *Genomics*, **17**, 355-363.

Gunn, T.M., Juriloff, D.M. and Harris, M.J. (1992) Further genetic studies of the cause of exencephaly in SELH mice. *Teratology*, **45**, 679-686.

Gunther, T., Sporle, R. and Schughart, K. (1997) The open brain (opb) mutation maps to mouse chromosome 1. *Mamm Genome*, **8**, 583-585.

Gutmann, D.H., Aylsworth, A., Carey, J.C., Korf, B., Marks, J., Pyeritz, R.E., Rubenstein, A. and Viskochil, D. (1997) The diagnostic evaluation and multidisciplinary management of neurofibromatosis 1 and neurofibromatosis 2. *Jama*, **278**, 51-57.

Gutmann, D.H., Cole, J.L. and Collins, F.S. (1995) Expression of the neurofibromatosis type 1 (NF1) gene during mouse embryonic development. *Prog Brain Res*, **105**, 327-335.

Haigo, S.L., Hildebrand, J.D., Harland, R.M. and Wallingford, J.B. (2003) Shroom induces apical constriction and is required for hingepoint formation during neural tube closure. *Curr Biol*, **13**, 2125-2137.

Hall, J.G. (1986) Neural tube defects, sex ratios, and X inactivation. *Lancet*, **2**, 1334-1335.

Hamblet, N.S., Lijam, N., Ruiz-Lozano, P., Wang, J., Yang, Y., Luo, Z., Mei, L., Chien, K.R., Sussman, D.J. and Wynshaw-Boris, A. (2002) Dishevelled 2 is essential for cardiac outflow tract development, somite segmentation and neural tube closure. *Development*, **129**, 5827-5838.

Harris, M.J. and Juriloff, D.M. (1997) Genetic landmarks for defects in mouse neural tube closure. *Teratology*, **56**, 177-187.

Harris, M.J. and Juriloff, D.M. (1999) Mini-review: toward understanding mechanisms of genetic neural tube defects in mice. *Teratology*, **60**, 292-305.

Harris, M.J. and Juriloff, D.M. (2005) Maternal diet alters exencephaly frequency in SELH/Bc strain mouse embryos. *Birth Defects Res A Clin Mol Teratol.*, **73**, 532-540.

Haviland, M.B. and Essien, F.B. (1990) Expression of the Axd (axial defects) mutation in the mouse is insensitive to retinoic acid at low dose. *J Exp Zool*, **256**, 342-346.

Henderson, D.J., Ybot-Gonzalez, P. and Copp, A.J. (1997) Over-expression of the chondroitin sulphate proteoglycan versican is associated with defective neural crest migration in the Pax3 mutant mouse (splotch). *Mech Dev*, **69**, 39-51.

Hildebrand, J.D. (2005) Shroom regulates epithelial cell shape via the apical positioning of an actomyosin network. *J Cell Sci*, **118**, 5191-5203.

Hildebrand, J.D. and Soriano, P. (1999) Shroom, a PDZ domain-containing actin-binding protein, is required for neural tube morphogenesis in mice. *Cell*, **99**, 485-497.

Holmberg, J., Clarke, D.L. and Frisen, J. (2000) Regulation of repulsion versus adhesion by different splice forms of an Eph receptor. *Nature*, **408**, 203-206.

Ishibashi, M., Ang, S.L., Shiota, K., Nakanishi, S., Kageyama, R. and Guillemot, F. (1995) Targeted disruption of mammalian hairy and Enhancer of split homolog-1 (HES-1) leads to up-regulation of neural helix-loop-helix factors, premature neurogenesis, and severe neural tube defects. *Genes Dev*, **9**, 3136-3148.

Jones, M.H., Hamana, N., Nezu, J. and Shimane, M. (2000) A novel family of bromodomain genes. *Genomics*, **63**, 40-45.

Juriloff, D.M., Gunn, T.M., Harris, M.J., Mah, D.G., Wu, M.K. and Dewell, S.L. (2001) Multifactorial genetics of exencephaly in SELH/Bc mice. *Teratology*, **64**, 189-200.

Juriloff, D.M. and Harris, M.J. (2000) Mouse models for neural tube closure defects. *Hum Mol Genet*, **9**, 993-1000.

Juriloff, D.M., Harris, M.J., Tom, C. and MacDonald, K.B. (1991) Normal mouse strains differ in the site of initiation of closure of the cranial neural tube. *Teratology*, **44**, 225-233.

Kapron-Bras, C.M. and Trasler, D.G. (1985) Reduction in the frequency of neural tube defects in splotch mice by retinoic acid. *Teratology*, **32**, 87-92.

Kelly, G.M. and Moon, R.T. (1995) Involvement of wnt1 and pax2 in the formation of the midbrain-hindbrain boundary in the zebrafish gastrula. *Dev Genet*, **17**, 129-140.

Konyukhov, B. V. and Mironova, O. V. (1979) Interaction of the mutant genes splotch and fidget in mice. *Sov. Genet.* **15**, 553-562.

Konyukhov, B.V. and Vakhrusheva, M.P. (1969) Abnormal development of eyes in mice homozygous for the fidget gene. *Teratology*, **2**, 147-157.

Krauss, S., Korzh, V., Fjose, A. and Johansen, T. (1992) Expression of four zebrafish wnt-related genes during embryogenesis. *Development*, **116**, 249-259.

Lakkis, M.M., Golden, J.A., O'Shea, K.S. and Epstein, J.A. (1999) Neurofibromin deficiency in mice causes exencephaly and is a modifier for Splotch neural tube defects. *Dev Biol*, **212**, 80-92.

Lander, E., Kruglyak, L. (1995) Genetic dissection of complex. traits: guidelines for interpreting and reporting linkage results. *Nat Genet*, **11**,241–247.

Lazzaro, M.A. and Picketts, D.J. (2001) Cloning and characterization of the murine Imitation Switch (ISWI) genes: differential expression patterns suggest distinct developmental roles for Snf2h and Snf2l. *J Neurochem*, **77**, 1145-1156.

Letts, V.A., Schork, N.J., Copp, A.J., Bernfield, M. and Frankel, W.N. (1995) A curly-tail modifier locus, mct1, on mouse chromosome 17. *Genomics*, **29**, 719-724.

Li, J., Liu, K.C., Jin, F., Lu, M.M. and Epstein, J.A. (1999) Transgenic rescue of congenital heart disease and spina bifida in Splotch mice. *Development*, **126**, 2495-2503.

Litingtung, Y. and Chiang, C. (2000) Specification of ventral neuron types is mediated by an antagonistic interaction between Shh and Gli3. *Nat Neurosci*, **3**, 979-985.

Lundberg, Y.W., Cabrera, R.M., Greer, K.A., Zhao, J., Garg, R. and Finnell, R.H. (2004) Mapping a chromosomal locus for valproic acid-induced exencephaly in mice. *Mamm Genome*, **15**, 361-369.

Macdonald, K.B., Juriloff, D.M. and Harris, M.J. (1989) Developmental study of neural tube closure in a mouse stock with a high incidence of exencephaly. *Teratology*, **39**, 195-213.

Machado, A.F., Martin, L.J. and Collins, M.D. (2001a) Pax3 and the splotch mutations: structure, function, and relationship to teratogenesis, including gene-chemical interactions. *Curr Pharm Des*, **7**, 751-785.

Machado, A.F., Zimmerman, E.F., Hovland, D.N., Jr., Weiss, R. and Collins, M.D. (2001b) Diabetic embryopathy in C57BL/6J mice. Altered fetal sex ratio and impact of the splotch allele. *Diabetes*, **50**, 1193-1199.

Moase, C.E. and Trasler, D.G. (1987) Retinoic acid-induced selective mortality of splotch-delayed mouse neural tube defect mutants. *Teratology*, **36**, 335-343.

Moase, C.E. and Trasler, D.G. (1990) Delayed neural crest cell emigration from Sp and Spd mouse neural tube explants. *Teratology*, **42**, 171-182.

Morriss-Kay, G. and Tuckett, F. (1989) Immunohistochemical localisation of chondroitin sulphate proteoglycans and the effects of chondroitinase ABC in 9- to 11-day rat embryos. *Development*, **106**, 787-798.

Murdoch, J.N., Doudney, K., Paternotte, C., Copp, A.J. and Stanier, P. (2001) Severe neural tube defects in the loop-tail mouse result from mutation of Lpp1, a novel gene involved in floor plate specification. *Hum Mol Genet*, **10**, 2593-2601.

Murdoch, J.N., Henderson, D.J., Doudney, K., Gaston-Massuet, C., Phillips, H.M., Paternotte, C., Arkell, R., Stanier, P. and Copp, A.J. (2003) Disruption of scribble (Scrb1) causes severe neural tube defects in the circletail mouse. *Hum Mol Genet*, **12**, 87-98.

Nadeau, J.H. (2001) Modifier genes in mice and humans. *Nat Rev Genet*, **2**, 165-174.

Nakatsu, T., Uwabe, C. and Shiota, K. (2000) Neural tube closure in humans initiates at multiple sites: evidence from human embryos and implications for the pathogenesis of neural tube defects. *Anat Embryol (Berl)*, **201**, 455-466.

Nau, H. (1986) Transfer of valproic acid and its main active unsaturated metabolite to the gestational tissue: correlation with neural tube defect formation in the mouse. *Teratology*, **33**, 21-27.

Neale, S.A. and Trasler, D.G. (1994) Early sialylation on N-CAM in splotch neural tube defect mouse embryos. *Teratology*, **50**, 118-124.

Neumann, P.E., Frankel, W.N., Letts, V.A., Coffin, J.M., Copp, A.J. and Bernfield, M. (1994) Multifactorial inheritance of neural tube defects: localization of the major gene and recognition of modifiers in ct mutant mice. *Nat Genet*, **6**, 357-362.

Niederreither, K., McCaffery, P., Drager, U.C., Chambon, P. and Dolle, P. (1997) Restricted expression and retinoic acid-induced downregulation of the retinaldehyde dehydrogenase type 2 (RALDH-2) gene during mouse development. *Mech Dev*, **62**, 67-78.

Nobakht, M., Zirak, A., Mehdizadeh, M. and Tabatabaeei, P. (2006) Teratogenic effects of retinoic acid on neurulation in mice embryos. *Pathophysiology*, **13**, 57-61.

Nybakken, K. and Perrimon, N. (2002) Hedgehog signal transduction: recent findings. *Curr Opin Genet Dev*, **12**, 503-511.

O'Rahilly, R. and Muller, F. (2002) The two sites of fusion of the neural folds and the two neuropores in the human embryo. *Teratology*, **65**, 162-170.

Pani, L., Horal, M. and Loeken, M.R. (2002) Rescue of neural tube defects in Pax-3-deficient embryos by p53 loss of function: implications for Pax-3- dependent development and tumorigenesis. *Genes Dev*, **16**, 676-680.

Qin, Y., Poirier, C., Truong, C., Schumacher, A., Agoulnik, A.I. and Bishop, C.E. (2003) A major locus on mouse chromosome 18 controls XX sex reversal in Odd Sex (Ods) mice. *Hum Mol Genet*, **12**, 509-515.

Rampersaud, E., Bassuk, A.G., Enterline, D.S., George, T.M., Siegel, D.G., Melvin, E.C., Aben, J., Allen, J., Aylsworth, A., Brei, T., Bodurtha, J., Buran, C., Floyd, L.E., Hammock, P., Iskandar, B., Ito, J., Kessler, J.A., Lasarsky, N., Mack, P., Mackey, J., McLone, D., Meeropol, E., Mehltretter, L., Mitchell, L.E., Oakes, W.J., Nye, J.S., Powell, C., Sawin, K., Stevenson, R., Walker, M., West, S.G., Worley, G., Gilbert, J.R. and Speer, M.C. (2005) Whole genomewide linkage screen for neural tube defects reveals regions of interest on chromosomes 7 and 10. *J Med Genet*, **42**, 940-946.

Reiter, J.F. and Skarnes, W.C. (2006) Tectonic, a novel regulator of the Hedgehog pathway required for both activation and inhibition. *Genes Dev*, **20**, 22-27.

Reyes, J.C., Barra, J., Muchardt, C., Camus, A., Babinet, C. and Yaniv, M. (1998) Altered control of cellular proliferation in the absence of mammalian brahma (SNF2alpha). *Embo J*, **17**, 6979-6991.

Rowitch, D.H. and McMahon, A.P. (1995) Pax-2 expression in the murine neural plate precedes and encompasses the expression domains of Wnt-1 and En-1. *Mech Dev*, **52**, 3-8.

Sadler, T.W. (2005) Embryology of neural tube development. *Am J Med Genet C Semin Med Genet*, **135**, 2-8.

Sadler, T.W. (1978) Distribution of surface coat material on fusing neural folds of mouse embryos during neurulation. *Anat Rec*, **191**, 345-349.

Sakai, Y., Meno, C., Fujii, H., Nishino, J., Shiratori, H., Saijoh, Y., Rossant, J. and Hamada, H. (2001) The retinoic acid-inactivating enzyme CYP26 is essential for establishing an uneven distribution of retinoic acid along the anterio-posterior axis within the mouse embryo. *Genes Dev*, **15**, 213-225.

Schoenwolf, G.C. (1984) Histological and ultrastructural studies of secondary neurulation in mouse embryos. *Am J Anat*, **169**, 361-376.

Schoenwolf, G.C. and Alvarez, I.S. (1989) Roles of neuroepithelial cell rearrangement and division in shaping of the avian neural plate. *Development*, **106**, 427-439.

Schwarz, M., Alvarez-Bolado, G., Urbanek, P., Busslinger, M. and Gruss, P. (1997) Conserved biological function between Pax-2 and Pax-5 in midbrain and cerebellum development: evidence from targeted mutations. *Proc Natl Acad Sci U S A*, **94**, 14518-14523.

Seller, M.J. (1995) Sex, neural tube defects, and multisite closure of the human neural tube. *Am J Med Genet*, **58**, 332-336.

Serbedzija, G.N. and McMahon, A.P. (1997) Analysis of neural crest cell migration in Splotch mice using a neural crest-specific LacZ reporter. *Dev Biol*, **185**, 139-147.

Shaffer, J.P. (1995) Multiple hypothesis testing. *Ann Rev Psych*, **46**, 561-584.

Smith, J.L. and Schoenwolf, G.C. (1989) Notochordal induction of cell wedging in the chick neural plate and its role in neural tube formation. *J Exp Zool*, **250**, 49-62.

Stopka, T. and Skoultchi, A.I. (2003) The ISWI ATPase Snf2h is required for early mouse development. *Proc Natl Acad Sci U S A*, **100**, 14097-14102.

Stumpo, D.J., Bock, C.B., Tuttle, J.S. and Blackshear, P.J. (1995) MARCKS deficiency in mice leads to abnormal brain development and perinatal death. *Proc Natl Acad Sci U S A*, **92**, 944-948.

Sulik, K.K., Zuker, R.M. and Dehart, D.B. (1998) Normal patterns of neural tube closure differ in the human and the mouse. *Proc Greenwood Genetic Cente,r* **18**, 129–130.

Takada, S., Stark, K.L., Shea, M.J., Vassileva, G., McMahon, J.A. and McMahon, A.P. (1994) Wnt-3a regulates somite and tailbud formation in the mouse embryo. *Genes Dev*, **8**, 174-189.

Takeuchi, T., Kojima, M., Nakajima, K. and Kondo, S. (1999) jumonji gene is essential for the neurulation and cardiac development of mouse embryos with a C3H/He background. *Mech Dev*, **86**, 29-38.

Tassabehji, M., Read, A.P., Newton, V.E., Harris, R., Balling, R., Gruss, P. and Strachan, T. (1992) Waardenburg's syndrome patients have mutations in the human homologue of the Pax-3 paired box gene. *Nature*, **355**, 635-636.

Tom, C., Juriloff, D.M. and Harris, M.J. (1991) Studies of the effect of retinoic acid on anterior neural tube closure in mice genetically liable to exencephaly. *Teratology*, **43**, 27-40.

Torres, M., Gomez-Pardo, E. and Gruss, P. (1996) Pax2 contributes to inner ear patterning and optic nerve trajectory. *Development*, **122**, 3381-3391.

Truslove, G.M. (1956) The anatomy and development of the fidget mouse. *J. Genet*, **54**, 64-86.

Urbanek, P., Wang, Z.Q., Fetka, I., Wagner, E.F. and Busslinger, M. (1994) Complete block of early B cell differentiation and altered patterning of the posterior midbrain in mice lacking Pax5/BSAP. *Cell*, **79**, 901-912.

Valenza-Schaerly, P., Pickard, B., Walter, J., Jung, M., Pourcel, L., Reik, W., Gauguier, D., Vergnaud, G. and Pourcel, C. (2001) A dominant modifier of transgene methylation is mapped by QTL analysis to mouse chromosome 13. *Genome Res*, **11**, 382-388.

Van Allen, M.I., Kalousek, D.K., Chernoff, G.F., Juriloff, D., Harris, M., McGillivray, B.C., Yong, S.L., Langlois, S., MacLeod, P.M., Chitayat, D. and et al. (1993)

Evidence for multi-site closure of the neural tube in humans. *Am J Med Genet*, **47**, 723-743.

van Straaten, H.W. and Copp, A.J. (2001) Curly tail: a 50-year history of the mouse spina bifida model. *Anat Embryol (Berl)*, **203**, 225-237.

van Straaten, H.W., Jaskoll, T., Rousseau, A.M., Terwindt-Rouwenhorst, E.A., Greenberg, G., Shankar, K. and Melnick, M. (1993) Raphe of the posterior neural tube in the chick embryo: its closure and reopening as studied in living embryos with a high definition light microscope. *Dev Dyn*, **198**, 65-76.

Vogelweid, C.M., Vogt, D.W., Besch-Williford, C.L. and Walker, S.E. (1993) New Zealand white mice: an experimental model of exencephaly. *Lab Anim Sci*, **43**, 58-60.

Wallace, M.E., Knights, P.J. and Anderson, J.R. (1978) Inheritance and morphology of exencephaly, a neonatal lethal recessive with partial penetrance, in the house mouse. *Genet Res*, **32**, 135-149.

Wassef, M. and Joyner, A.L. (1997) Early mesencephalon/metencephalon patterning and development of the cerebellum. *Perspect Dev Neurobiol*, **5**, 3-16.

Webster, W.S. and Edwards, M.J. (1984) Hyperthermia and the induction of neural tube defects in mice. *Teratology*, **29**, 417-425.

Whitehead, A.S., Gallagher, P., Mills, J.L., Kirke, P.N., Burke, H., Molloy, A.M., Weir, D.G., Shields, D.C. and Scott, J.M. (1995) A genetic defect in 5,10 methylenetetrahydrofolate reductase in neural tube defects. *Qjm*, **88**, 763-766.

Wijgerde, M., McMahon, J.A., Rule, M. and McMahon, A.P. (2002) A direct requirement for Hedgehog signaling for normal specification of all ventral progenitor domains in the presumptive mammalian spinal cord. *Genes Dev*, **16**, 2849-2864.

Wiley, M.J. (1980) The effects of cytochalasins on the ultrastructure of neurulating hamster embryos in vivo. *Teratology*, **22**, 59-69.

Wilson, D.B. and Finta, L.A. (1979) Gap junctional vesicles in the neural tube of the splotch (Sp) mutant mouse. *Teratology*, **19**, 337-340.

Wright, S. (1934). The results of crosses between inbred strains of guinea pigs, differing in number of digits. *Genetics*, **19**, 537-551.

Xu, W., Baribault, H. and Adamson, E.D. (1998) Vinculin knockout results in heart and brain defects during embryonic development. *Development*, **125**, 327-337.

Ybot-Gonzalez, P., Cogram, P., Gerrelli, D. and Copp, A.J. (2002) Sonic hedgehog and the molecular regulation of mouse neural tube closure. *Development*, **129**, 2507-2517.

Ybot-Gonzalez, P. and Copp, A.J. (1999) Bending of the neural plate during mouse spinal neurulation is independent of actin microfilaments. *Dev Dyn*, **215**, 273-283.

Zhao, Q., Behringer, R.R. and de Crombrugghe, B. (1996) Prenatal folic acid treatment suppresses acrania and meroanencephaly in mice mutant for the Cart1 homeobox gene. *Nat Genet*, **13**, 275-283.

http://www.jax.org/imr/controls.html

http://www.ensembl.org/Mus_musculus/transcriptsnpview

Appendix

23 Mb -24 Mb

- AK020955_B230104FO1Rik (Riken cDNA) MGI (Expression:postnatal adult, corpora quadrigemina
- LOC545284 NCBI, E (discontinued)
- Apba1 (amyloid beta (A4) precursor protein binding, family A, member 1) (Expression: embryonic heart, postnatal)Ko=abnormal dopamine, reduced body size)
- Gm967 (gene model 967) (M/N) (Expression: postnatal thryroid)
- Riken cDNA 1700021P04 (Expression: postnatal testis)
- Tjp2 (tight junction protein 2) (Expression: highly expressed, from 2d embryo-adult)
- Fxn (frataxin) (embryonic (10.5d)-postnatal pancreas) Role in iron ion homeostasis-Ko=lack intramitochondrial iron accumulation-early post implantation lethality)
- Ensembl predicted gene (42071_75232)
- Pip5k1a (phosphatidylinositol-4-phosphate 5-kinase, type 1 alpha) (expression: embryo, retina, thymus KO=immune defect)
- RIKEN cDNA 4930418C01 gene (M)
- RIKEN cDNA 2900009I07 gene (M/N)
- Ensembl predicted gene (51082_50650)- Pseudogene?
- expressed sequence AW742912 (M)
- RIKEN cDNA E030010A14 gene (E/N)
- Pgm5 (phosphoglucomutase 5) (Expression:postnatal, likely function in cell adhesion, cell junctions)

24-25 Mb

- Cycs (cytochrome c, somatic) (Ko=exencephaly?, embryonic lethality)
- Foxd4 (forkhead box D4)
- Cbwd1 (COBW domain containing 1)
- Ensembl predicted gene (64896_82962))
- Dock8 (dedicator of cytokinesis 8)
- Ndufb4 (NADH dehydrogenase (ubiquinone) 1 beta subcomplex 4)
- Ensembl predicted gene (63502_77079)
- expressed sequence AA409025 (m)
- Ankrd15 (ankyrin repeat domain 15)
- Ensembl predicted gene (64843_82909)
- Ensembl predicted gene (42559_49171)
- Dmrt1 (doublesex and mab-3 related transcription factor 1) (KO=Males lack germ cells, seminiferous tubules disorganized)
- Dmrt3 (doublesex and mab-3 related transcription factor 3)

- RIKEN cDNA 2610016A17 gene (m)
- Dmrt2 (doublesex and mab-3 related transcription factor 2) (Ko=somites disorganized, perinatal lethal, breathing defects, skeletal defects)

25-26 Mb
- LOC432542 (similar to Glyceraldehyde-3-phosphate dehydrogenase (GAPDH)
- RIKEN cDNA 1700048O14 gene (m)
- Ensembl predicted gene (65857_83923)
- LOC435592 (similar to ribosomal protein L36)
- Smarca2 (SWI/SNF related, matrix associated, actin dependent regulator of chromatin, subfamily a, member 2)

26-27 Mb
- RIKEN cDNA 4931403E22 gene (M)
- Gm815 (gene model 815) (n/M)
- LOC433234 similar to 40S ribosomal protein S17 (discontinued)
- Vldlr (very low density lipoprotein receptor)
- Kcnv2 (potassium channel, subfamily V, member 2)
- LOC435593 similar to Procollagen (type III) N-endopeptidase (discontinued) (N)
- D19Bwg1357e (DNA segment, Chr 19, Brigham & Women's Genetics 1357 expressed)
- RIKEN cDNA C030016D13 gene
- Ensembl predicted gene (67355_87483)

27-28 Mb
- Ensembl predicted gene (60834_76784)
- Rfx3 (regulatory factor X, 3 (influences HLA class II expression) (KO=left right patterning, cilia formation, embryonic lethal)
- Ensembl predicted gene (67353_87476)
- Ensembl predicted gene (63830_81336)
- LOC433235 peptidylprolyl isomerase A pseudogene chr19_428.1 (n)
- Glis3 (GLIS family zinc finger 3)
- expressed sequence AU042950 (m)
- RIKEN cDNA 4933413C19 gene (m)
- RIKEN cDNA D930032P07 gene (m)
- LOC434460 similar to ribosomal protein S15a

28-29 Mb
- LOC546722 similar to dynein, cytoplasmic, light peptide (discontinued)
- Slc1a1 (solute carrier family 1 (neuronal/epithelial high affinity glutamate transporter, system Xag), member 1) (Ko=reduced movement and increased excretion of glutamate and aspartate)
- Ensembl predicted gene pseudogene (50956_62582)

- Ensembl predicted gene (63205_81992)
- RIKEN cDNA 4430402I18 gene
- Ppapdc2 (phosphatidic acid phosphatase type 2 domain containing 2)
- LOC226086 similar to Tektin-3
- Cdc37l1 (cell division cycle 37 homolog (S. cerevisiae)-like 1)
- Ensembl predicted gene (59150_77729)
- Ak3 (adenylate kinase 3)
- LOC433237 hypothetical gene supported by AK028012
- Rcl1 (RNA terminal phosphate cyclase-like 1)
- Ensembl predicted gene (65556_83622)
- Ensembl predicted gene (52521_64449)
- LOC433238 high mobility group protein 1-like (n)
- Jak2 (Janus kinase 2) (Ko=failure of erythropoieses, die midgestation)
- Insl6 (insulin-like 2)
- Rln1 (relaxin 1) (Ko=abnormal mammary gland development)
- RIKEN cDNA 5033414D02 gene
- RIKEN cDNA A530045L16 gene
- Cd274 (CD274 antigen) (Ko=affects hepatic $CD8^+$ T cells.)
- Pdcd1lg2 (programmed cell death 1 ligand 2) (Ko=Mice homozygous for disruptions in this gene have dendritic cells that display a diminished ability to activate CD4+ T cells)
- RIKEN cDNA A930007I19 gene
- RIKEN cDNA C030046E11 gene
- Wsu12e (DNA segment, Chr 19, Wayne State University 12, expressed)
- Mlana (melan-A)
- 9930021J03Rik RIKEN cDNA 9930021J03 gene
- hypothetical protein LOC545285

29-30 Mb

- Ensembl predicted gene (48936_61906)
- Ranbp6 (RAN binding protein 6)
- Ensembl predicted gene (67327_87425)
- RIKEN cDNA 9230117N10 gene
- Trpd52l3 tumor protein D52-like 3
- Uhrf2 (ubiquitin-like, containing PHD and RING finger domains 2)
- expressed sequence C76533
- Gldc (glycine decarboxylase)
- RIKEN cDNA 9530025L08 gene
- Mbl2 (mannose binding lectin (c))
- RIKEN cDNA 1700048J15 gene
- Ensembl predicted gene (48649_49711)
- LOC546723 similar to protein phosphatase 1, regulatory (inhibitor) subunit 2
- Dkk1 (dickkopf homolog 1 (Xenopus laevis))
- Prkg1 (protein kinase, cGMP-dependent, type I)

30-31Mb

- Cstf2t (cleavage stimulation factor, 3' pre-RNA subunit 2, tau)
- RIKEN cDNA 2900042A17 gene
- RIKEN cDNA 8430431K14 gene
- expressed sequence AI843588
- RIKEN cDNA 9030425L15 gene
- RIKEN cDNA 9330185G11 gene
- D19Ertd200e (DNA segment, Chr 19, ERATO Doi 200, expressed)

31-32 Mb

- RIKEN cDNA 1810073H04 gene
- RIKEN cDNA 9130016M20 gene
- Asah2 (N-acylsphingosine amidohydrolase 2)
- Tmem23 (transmembrane protein 23)
- Drr2 (developmentally regulated repeat element-containing transcript 2)
- EST AF007006
- RIKEN cDNA 2700046G09 gene
- LOC435595 similar to Nuclear transport factor 2 (NTF-2) discontinued
- Ensembl predicted gene (67309_87383)
- Rpl9 (ribosomal protein L9)
- Minpp1 (multiple inositol polyphosphate histidine phosphatase 1)
- Ensembl predicted gene (67308_87382)
- Papss2 (3'-phosphoadenosine 5'-phosphosulfate synthase 2)

32-33 Mb

- Atad1 (ATPase family, AAA domain containing 1)
- Pten (phosphatase and tensin homolog)
- RIKEN cDNA B430203M17 gene
- RIKEN cDNA 6530404N21 gene
- Ensembl predicted gene (67306_87375)
- LOC545286 similar to pregastric esterase (discontinued)
- expressed sequence AI747699
- RIKEN cDNA 1700001A13 gene
- LOC434504 similar to pregastric esterase (discontinued)

33-34 Mb

- LOC546724 similar to lipase-like, ab-hydrolase domain containing (discontinued)
- LOC545287 similar to Gastric triacylglycerol lipase precursor (Gastric lipase) (GL) (discontinued)
- Ensembl predicted gene (37603_42061)
- LOC329055 similar to Gastric triacylglycerol lipase precursor (Gastric lipase) (GL)

- LOC433241 similar to MTH2 protein
- LOC435596 similar to lipase-like, ab-hydrolase domain containing 2
- Ensembl predicted gene (65380_83446)
- Lipf (lipase, gastric)
- Lipl2 (lipase-like, ab-hydrolase domain containing 2)
- LOC383462 similar to 60S ribosomal protein L6 (TAX-responsive enhancer element binding protein 107) (TAXREB107)
- RIKEN cDNA 2210418G03 gene
- Lipl3 (lipase-like, ab-hydrolase domain containing 3)
- Ankrd22 (ankyrin repeat domain 22)
- Stambpl1 (Stam binding protein like 1)
- Acta2 (actin, alpha 2, smooth muscle, aorta)
- Fas (TNF receptor superfamily member)
- Ch25h (cholesterol 25-hydroxylase)
- Lip1 (lysosomal acid lipase 1)
- Ifit2 (interferon-induced protein with tetratricopeptide repeats 2)
- Ensembl predicted gene (67297_87357)
- Ifit3 (interferon-induced protein with tetratricopeptide repeats 3)
- RIKEN cDNA 2010002M12 gene
- Ensembl predicted gene (59021_77734)
- Ifit1 (interferon-induced protein with tetratricopeptide repeats 1)

34-35 Mb

- Slc16a12 (solute carrier family 16 (monocarboxylic acid transporters), member 12)
- Ensembl predicted gene (64479_82545)
- Pank1 (pantothenate kinase 1)
- Ensembl predicted gene (33519_36477)
- Mphosph1 (M-phase phosphoprotein 1)

35-36 Mb

- RIKEN cDNA A830019P07 gene
- Htr7 (5-hydroxytryptamine (serotonin) receptor 7)
- LOC433244 similar to novel protein discontinued
- ribonuclease P/MRP 30 subunit (human)
- ankrd1 (ankyrin repeat domain 1 (cardiac muscle))
- expressed sequence C85546
- Pcgf5 (polycomb group ring finger 5)
- Ensembl predicted gene (45485_57175)
- Hectd2 (HECT domain containing 2)

36-37 Mb

- RIKEN cDNA 1500017E21 gene (Hectd2?)
- Ppp1r3c (protein phosphatase 1, regulatory (inhibitor) subunit 3C)

- Tnks2 (tankyrase, TRF1-interacting ankyrin-related ADP-ribose polymerase 2)
- RIKEN cDNA 2610306H15 gene
- hypothetical LOC381219 discontinued
- Btafl (BTAF1 RNA polymerase II, B-TFIID transcription factor-associated, (Mot1 homolog, S. cerevisiae)
- Cpeb3 (cytoplasmic polyadenylation element binding protein 3)
- RIKEN cDNA A330032B11 gene (cpeb3?)
- RIKEN cDNA 5730499H23 gene
- March5
- RIKEN cDNA 4931408D14 gene
- Ide (insulin degrading enzyme)
- Rpl10 (ribosomal protein 10)
- Kif11 (kinesin family member 11)
- Hhex (hematopoietically expressed homeobox)
- RIKEN cDNA 4933421H12 gene
- RIKEN cDNA 1700122C19 gene
- Exoc6 (exocyst complex component 6)

37-38 Mb

- LOC546726 similar to cytochrome P450, family 26, subfamily C, polypeptide 1
- Cyp26a1 (cytochrome P450, family 26, subfamily a, polypeptide 1)
- Ensembl predicted gene (49227_60445)
- Fer1l3 (fer-1-like 3, myoferlin (C. elegans))
- Cep55 (centrosomal protein 55)
- Gpr120 (G protein-coupled receptor 120)
- Rbp4 (retinol binding protein 4, plasma)
- Pde6c (phosphodiesterase 6C, cGMP specific, cone, alpha prime)
- RIKEN cDNA 5730455O13 gene (e/n)
- Lgi1 (leucine-rich repeat LGI family, member 1)
- Ensembl predicted gene (52663_65022)
- Tmem20 (transmembrane protein 20)
- Plce1 (phospholipase C, epsilon 1)
- Ensembl predicted gene (67239_87246)

38-39 Mb

- Ensembl predicted gene (67237_87245)
- Noc3l (nucleolar complex associated 3 homolog (S. cerevisiae))
- Tbc1d12 (TBC1D12: TBC1 domain family, member 12)
- D19Wsu44e (DNA segment, Chr 19, Wayne State University 44, expressed)
- Ensembl predicted gene (67234_87242)
- Hells (helicase, lymphoid specific)
- Cyp2c55 (cytochrome P450, family 2, subfamily c, polypeptide 55)
- LOC235855 similar to CTD (carboxy-terminal domain, RNA polymerase II, polypeptide A) small phosphatase like 2

- Cyp2c65 (cytochrome P450, family 2, subfamily c, polypeptide 65)
- Cyp2c66 (cytochrome P450, family 2, subfamily c, polypeptide 66)
- Cyp2c29 (cytochrome P450, family 2, subfamily c, polypeptide 29)

39-40 Mb

- Cyp2c38 (cytochrome P450, family 2, subfamily c, polypeptide 38)
- Cyp2c39 (cytochrome P450, family 2, subfamily c, polypeptide 39)
- LOC214362 similar to Cyp2c40 protein discontinued
- LOC433247 similar to Cytochrome P450 2C40 (CYPIIC40)
- Drr2 (developmentally regulated repeat element-containing transcript 2)
- Cyp2c40 (cytochrome P450, family 2, subfamily c, polypeptide 40)
- hypothetical protein LOC545288
- Cyp2c37 (cytochrome P450, family 2. subfamily c, polypeptide 37)
- Cyp2c54 cytochrome P450
- Cyp2c50 (cytochrome P450, family 2, subfamily c, polypeptide 50)
- Cyp2c70 (cytochrome P450, family 2, subfamily c, polypeptide 70)
- expressed sequence AI195470
- LOC545289 similar to Orphan nuclear receptor NR1D2 (Rev-erb-beta) (Orphan nuclear receptor RVR)
- Nr1d2
- LOC434542 similar to Glyceraldehyde-3-phosphate dehydrogenase (GAPDH) discontinued
- Pdlim1 (PDZ and LIM domain 1 (elfin))
- RIKEN cDNA A930028N01 gene
- RIKEN cDNA 9530039L23 gene
- expressed sequence AA416451

40-41 Mb

- RIKEN cDNA 5730409N24 gene
- RIKEN cDNA 9130009M17 gene (same as above?)
- Sorbs1 (sorbin and SH3 domain containing 1)
- Aldh18a1 (aldehyde dehydrogenase 18 family, member A1)
- RIKEN cDNA 4930521E07 gene
- Ptp4a1 (protein tyrosine phosphatase 4a1)
- Entpd1 (ectonucleoside triphosphate diphosphohydrolase 1)
- expressed sequence C79607
- Gm1285 (gene model 1285, (NCBI))
- Ensembl predicted gene (58993_79321)
- Ccnj (cyclin J)
- RIKEN cDNA E030044B06 gene
- RIKEN cDNA E030007J07 gene
- RIKEN cDNA E130314M14 gene
- Zfp518 (zinc finger protein 518)
- Blnk (B-cell linker)
- RIKEN cDNA C330026H20 gene

- RIKEN cDNA A130015J22 gene
- Dntt (deoxynucleotidyltransferase, terminal)
- Tmem10 (transmembrane protein 10)
- Tll2 (tolloid-like 2)
- Smbp (SM-11044 binding protein)
- RIKEN cDNA 1700008F19 gene
- Ensembl predicted gene (54643_67832)
- Pik3ap1 (phosphoinositide-3-kinase adaptor protein 1)

41-42 Mb

- LOC545290 similar to developmental pluripotency-associated 2
- RIKEN cDNA 2010100M03 gene
- Morf4l1 (mortality factor 4 like 1)
- RIKEN cDNA A630025C20 gene
- Gm340 (gene model 340, (NCBI))
- expressed sequence AI606181
- Slit1 (slit homolog 1 (Drosophila))
- Arhgap19 (Rho GTPase activating protein 19)
- Frat1 (frequently rearranged in advanced T-cell lymphomas)
- Frat2 (frequently rearranged in advanced T-cell lymphomas 2)
- expressed sequence AA408556
- Pgam1 (phosphoglycerate mutase 1)
- RIKEN cDNA B130024M06 gene
- Exosc1 (exosome component 1)
- Zdhhc16 (zinc finger, DHHC domain containing 16)
- Ensembl predicted gene (67191_87145)
- Mms19l (MMS19 (MET18 S. cerevisiae)-like)
- RIKEN cDNA B130065D12 gene
- RIKEN cDNA E130107B13 gene
- Ubtd1 (ubiquitin domain containing 1)
- Ankrd2 (ankyrin repeat domain 2 (stretch responsive muscle))
- RIKEN cDNA 0610010D20 gene
- RIKEN cDNA 4933411K16 gene
- cDNA sequence BC023055
- Pi4k2a (phosphatidylinositol 4-kinase type 2 alpha)
- Avpi1 (arginine vasopressin-induced 1)
- Marveld1 (MARVEL (membrane-associating) domain containing 1)
- Q5FWH9_mouse
- hypothetical LOC381225 discontinued
- Zfyve27 (zinc finger, FYVE domain containing 27)
- Sfrp5 (secreted frizzled-related sequence protein 5)
- RIKEN cDNA 4933417O08 gene
- Crtac1 (cartilage acidic protein 1)

42-43 Mb
- D19Ertd386e (DNA segment, Chr 19, ERATO Doi 386, expressed)
- RIKEN cDNA B230214N19 gene
- RIKEN cDNA 2810404I24 gene
- Loxl4 (lysyl oxidase-like 4)
- Ensembl predicted gene (67181_87110)
- LOC546727 similar to Hypothetical protein CBG20455 discontinued
- RIKEN cDNA 4833409A17 gene
- Hps1 (Hermansky-Pudlak syndrome 1 homolog (human))
- LOC545291 similar to heparanase 2
- Ensembl predicted gene (63282_72699)
- LOC546728 similar to leucine zipper transcription factor-like 1 discontinued
- Hpse2 (heparanase 2)
- RIKEN cDNA 8430434A19 gene
- Cnnm1 (cyclin M1)

43-44 Mb
- Got1 (glutamate oxaloacetate transaminase 1, soluble)
- Nkx2-3 (NK2 transcription factor related, locus 3 (Drosophila))
- Slc25a28 (solute carrier family 25, member 28)
- expressed sequence T25620
- cDNA sequence BC037704
- Entpd7 (ectonucleoside triphosphate diphosphohydrolase 7)
- Cox15 (COX15 homolog, cytochrome c oxidase assembly protein (yeast))
- Cutc (cutC copper transporter homolog (E.coli))
- Abcc2 (ATP-binding cassette, sub-family C (CFTR/MRP), member 2)
- Dnmbp (dynamin binding protein)
- RIKEN cDNA 4933403J19 gene
- RIKEN cDNA 1700084K02 gene
- Cpn1 (carboxypeptidase N, polypeptide 1)
- Cyp2c44 (cytochrome P450, family 2, subfamily c, polypeptide 44)
- Spfh1 (SPFH domain family, member 1)
- expressed sequence C80197
- Chuk (conserved helix-loop-helix ubiquitous kinase)
- Cwf19l1 (CWF19-like 1, cell cycle control (S. pombe))
- Bloc1s2 (biogenesis of lysosome-related organelles complex-1, subunit 2)
- Pkd2l1 (polycystic kidney disease 2-like 1)
- Drr2 (developmentally regulated repeat element-containing transcript 2)
- Scd3 (stearoyl-coenzyme A desaturase 3)
- Scd2d (stearoyl-Coenzyme A desaturase 2)
- Scd4 (stearoyl-coenzyme A desaturase 4)
- Scd1 (stearoyl-coenzyme A desaturase 1)

44-45 Mb

- Wnt8b (wingless related MMTV integration site 8b)
- Sec31l2 (SEC31-like 2 (S. cerevisiae))
- Ndufb8 (NADH dehydrogenase (ubiquinone) 1 beta subcomplex 8)
- Hif1an (hypoxia-inducible factor 1, alpha subunit inhibitor)
- Ensembl predicted gene (67157_87052)
- Pax2 (paired box gene 2)
- Ensembl predicted gene (58350_82039)
- RIKEN cDNA 1700039E22 gene
- LOC383450 similar to 3-phosphoglycerate dehydrogenase
- RIKEN cDNA 6030443O07 gene
- Ensembl predicted gene (65159_83225)
- RIKEN cDNA 4930414N06 gene
- Sema4g (sema domain, immunoglobulin domain (Ig), transmembrane domain (TM) and short cytoplasmic domain, (semaphorin) 4G)
- Mrpl43 (mitochondrial ribosomal protein L43)
- Peo1 (progressive external ophthalmoplegia 1 (human))
- Pdzd7 (PDZ domain containing 7)
- Lzts2 (leucine zipper, putative tumor suppressor 2)
- LOC435601 similar to PDZ domain containing 7
- hypothetical protein LOC545293 discontinued
- RIKEN cDNA 9430030N17 gene
- Sfxn3 (sideroflexin 3)
- Kazald1 (Kazal-type serine peptidase inhibitor domain 1)
- RIKEN cDNA 4930557B21 gene
- Tlx1 (T-cell leukemia, homeobox 1)
- Lbx1 (ladybird homeobox homolog 1 (Drosophila))
- RIKEN cDNA 1700016H03 gene
- Ensembl predicted gene (62336_77428)
- Btrc (beta-transducin repeat containing protein)

45-46 Mb

- Poll (polymerase (DNA directed), lambda)
- RIKEN cDNA 5330431N19 gene
- Fbxw4 (F-box and WD-40 domain protein 4)
- Ensembl predicted gene (67145_87017)
- RIKEN cDNA 4933429K18 gene
- Fgf8 (fibroblast growth factor 8)
- Npm3 (nucleoplasmin 3)
- RIKEN cDNA E330018D03 gene
- D19Ertd409e (DNA segment, Chr 19, ERATO Doi 409, expressed)
- Mgea5 (meningioma expressed antigen 5 (hyaluronidase))
- Kcnip2 (Kv channel-interacting protein 2)
- D19Ertd132e (DNA segment, Chr 19, ERATO Doi 132, expressed)

- RIKEN cDNA 9130011E15 gene
- RIKEN cDNA 4930505N22 gene
- Hps6 (Hermansky-Pudlak syndrome 6)
- Ldb1 (LIM domain binding 1)
- Pprc1 (peroxisome proliferative activated receptor, gamma, coactivator-related 1)
- Nolc1 (nucleolar and coiled-body phosphoprotein 1)
- Elovl3 (elongation of very long chain fatty acids (FEN1/Elo2, SUR4/Elo3, yeast)-like 3)
- Pitx3 (paired-like homeodomain transcription factor 3)
- Gbfl (golgi-specific brefeldin A-resistance factor 1)
- Pseudogene (42925_59536)
- RIKEN cDNA D430033H22 gene
- RIKEN cDNA C130013I19 gene
- Nfkb2 (nuclear factor of kappa light polypeptide gene enhancer in B-cells 2, p49/p100)
- Ensembl predicted gene (67130_86982)
- RIKEN cDNA 4833438C02 gene
- Psd pleckstrin and Sec7 domain containing
- Cuedc2 (CUE domain containing 2)
- Fbxl15 (F-box and leucine-rich repeat protein 15)
- hypothetical LOC433250 discontinued
- RIKEN cDNA 2310034G01 gene
- RIKEN cDNA 4930538D17 gene
- Ensembl predicted gene (65204_83270)
- Actr1a (ARP1 actin-related protein 1 homolog A (yeast))
- RIKEN cDNA 9430020M11 gene
- Sufu (suppressor of fused homolog (Drosophila))

46-47 Mb

- expressed sequence AW124847
- Trim8 (tripartite motif protein 8)
- Arl3 (ADP-ribosylation factor-like 3)
- Sfxn2 (sideroflexin 2)
- D19Wsu162e (DNA segment, Chr 19, Wayne State University 162, expressed)
- Cyp17a1 (cytochrome P450, family 17, subfamily a, polypeptide 1)
- Ensembl predicted gene (61949_71544)
- RIKEN cDNA 2010012O05 gene
- As3mt (arsenic (+3 oxidation state) methyltransferase)
- Ensembl predicted gene (65207_83273)
- Cnnm2 (cyclin M2)
- RIKEN cDNA A930026I22 gene
- Ensembl predicted gene (25039_26015)
- Nt5c2 (5'-nucleotidase, cytosolic II)
- Ina (internexin neuronal intermediate filament protein, alpha)

- Pcgf6 (polycomb group ring finger 6)
- Ensembl predicted gene (67122_86960)
- Ensembl predicted gene (64421_82487)
- Taf5 (TAF5 RNA polymerase II, TATA box binding protein (TBP)-associated factor)
- Usmg5 (upregulated during skeletal muscle growth 5)
- Pdcd11 (programmed cell death protein 11)
- RIKEN cDNA 2810048G17 gene
- LOC546729 similar to Protein FAM26C
- LOC240669 similar to Protein FAM26B
- Ensembl predicted gene (61942_75655)
- Neurl (neuralized-like homolog (Drosophila))
- RIKEN cDNA 2310014D11 gene
- expressed sequence AI413738
- hypothetical protein C230050L11

47-48 Mb

- Sh3md1 (SH3 multiple domains 1)
- Obfc1 (oligonucleotide/oligosaccharide-binding fold containing 1)
- RIKEN cDNA 6820402O18 gene
- Slk (STE20-like kinase (yeast))
- Drr2 (developmentally regulated repeat element-containing transcript 2)
- C78505 (expressed sequence C78505)
- Col17a1 (procollagen, type XVII, alpha 1)
- RIKEN cDNA 6330577E15 gene
- D19Ertd652e (DNA segment, Chr 19, ERATO Doi 652, expressed)
- RIKEN cDNA 4930463G05 gene
- Gsto1 (glutathione S-transferase omega 1)
- Gsto2 (glutathione S-transferase omega 2)
- RIKEN cDNA 4833424O12 gene
- cDNA sequence BC063749
- Gm969 (gene model 969, (NCBI))
- hypothetical protein LOC545294 discontinued
- RIKEN cDNA 1700021N20 gene
- Sorcs3 (sortilin-related VPS10 domain containing receptor 3)

48-49 Mb

- RIKEN cDNA 4930535F04 gene

49-50 Mb

- LOC433251 similar to 60S ribosomal protein L13a
- Socrs1 (VPS10 domain receptor protein SORCS 1)

50-51 Mb

- RIKEN cDNA 4933436E20 gene
- Ensembl predicted gene (65143_83209)

51-52 Mb
- Pseudogene (60287_74542)
- Ins1 (insulin I)

52-53 Mb
- Ensembl predicted gene (67098_86907)
- hypothetical LOC433252 discontinued
- Xpnpep1 (X-prolyl aminopeptidase (aminopeptidase P) 1, soluble)
- Ensembl predicted gene (67097_86906)
- RIKEN cDNA 1700054A03 gene
- Add3 (adducin 3 (gamma))
- Ensembl predicted gene (67089_86891)
- RIKEN cDNA 1700001K23 gene
- Mxi1 (Max interacting protein 1)
- expressed sequence AW742986
- Ensembl predicted gene (67086_86888)
- Smndc1 (survival motor neuron domain containing 1)
- RIKEN cDNA 8030456M14 gene

53-54 Mb
- hypothetical protein LOC545295 discontinued
- RIKEN cDNA 5830416P10 gene
- Dusp5 (dual specificity phosphatase 5)
- Ensembl predicted gene (67083_86885)
- LOC433253 similar to Nuclear transport factor 2 (NTF-2) discontinued
- Cspg6 (chondroitin sulfate proteoglycan 6)
- expressed sequence AW492981
- LOC433254 similar to Matrin 3
- hypothetical LOC433255 discontinued
- RIKEN cDNA 1110018J23 gene
- RIKEN cDNA 2310035P21 gene
- Pdcd4 (programmed cell death 4)
- RIKEN cDNA 2310002J21 gene
- Shoc2 (soc-2 (suppressor of clear) homolog (C. elegans))
- RIKEN cDNA 4930484I04 gene
- Adra2a (adrenergic receptor, alpha 2a)

54-55 Mb
- Ensembl predicted gene (67080_86872)
- Ensembl predicted gene (67079_86871)
- Ensembl predicted gene (67078_86870)

- Gpam (glycerol-3-phosphate acyltransferase, mitochondrial)
- LOC435605 similar to GA20650-PA discontinued
- LOC435604 similar to homeobox-containing protein discontinued
- Tectb (tectorin beta)
- Gucy2g (guanylate cyclase 2g)
- Acsl5 (acyl-CoA synthetase long-chain family member 5)
- Zdhhc6 (zinc finger, DHHC domain containing 6)
- Vti1a (vesicle transport through interaction with t-SNAREs homolog 1A (yeast))
- Ensembl predicted gene (67074_86859) Vti1a?

55-56 Mb

- RIKEN cDNA 2310066F23 gene
- RIKEN cDNA 4930552P12 gene
- Tcf7l2 (transcription factor 7-like 2, T-cell specific, HMG-box)
- EST AF007007
- Ensembl predicted gene (54436_15609)
- Ppnr (per-pentamer repeat gene)
- expressed sequence AU021789
- RIKEN cDNA D730002M21 gene
- RIKEN cDNA 1700106J12 gene
- Habp2 (hyaluronic acid binding protein 2)
- Nrap (nebulin-related anchoring protein)
- Casp7 (caspase 7)

56-57 Mb

- RIKEN cDNA 9930023K05 gene
- Dclre1a (DNA cross-link repair 1A, PSO2 homolog (S. cerevisiae))
- Nhlrc2 (NHL repeat containing 2)
- expressed sequence AI835049
- Adrb1 (adrenergic receptor, beta 1)
- Ensembl predicted gene (67063_86830)
- RIKEN cDNA A630007B06 gene
- RIKEN cDNA 1700010L13 gene
- Tdrd1 (tudor domain containing 1)
- Vwa2 (von Willebrand factor A domain containing 2)
- expressed sequence AU041783
- Ablim1 (actin-binding LIM protein 1)
- expressed sequence BB164765
- expressed sequence BB143722
- hypothetical LOC433257 discontinued
- RIKEN cDNA 4930449E18 gene
- RIKEN cDNA B230217O12 gene
- expressed sequence AI450540
- RIKEN cDNA 2600017C09 gene

57-58 Mb
- Trub1 (TruB pseudouridine (psi) synthase homolog 1 (E. coli))
- RIKEN cDNA 6720468P15 gene
- Atrnl1 (attractin like 1)
- Ensembl predicted gene (47387_53730) Artnl1 ?
- RIKEN cDNA E430016L07 gene
- Gfra1 (glial cell line derived neurotrophic factor family receptor alpha 1)
- Q8Vsw1_mouse

58-59 Mb
- Pseudogene (59597_79735)
- RIKEN cDNA 1700011F14 gene
- Gm1726 (gene model 1726, (NCBI))
- RIKEN cDNA 1810007D17 gene
- Pnlip (pancreatic lipase)
- GeneID: 75598 protein coding
- RIKEN cDNA 1810035K13 gene
- RIKEN cDNA 1810018F18 gene
- Pnliprp1 (pancreatic lipase related protein 1)
- RIKEN cDNA 1810073G21 gene
- Pnliprp2 (pancreatic lipase-related protein 2)
- RIKEN cDNA 1700019N19 gene
- Hspa12a (heat shock protein 12A)
- RIKEN cDNA 4930433M22 gene
- RIKEN cDNA 6430537H07 gene
- RIKEN cDNA 4930506M07 gene
- LOC545296 similar to Elongation factor 1-gamma (EF-1-gamma) (eEF-1B gamma)
- Vax1 (ventral anterior homeobox containing gene 1)
- RIKEN cDNA 4930442E04 gene
- Kcnk18 (potassium channel, subfamily K, member 18)
- Slc18a2 (solute carrier family 18 (vesicular monoamine), member 2)
- Pdzd8 (PDZ domain containing 8)
- Rps12 ribosomal protein S12
- RIKEN cDNA 1700022C07 gene
- expressed sequence C87583

59-60 Mb
- Emx2os (empty spiracles homolog 2 (Drosophila) opposite strand)
- Emx2 (empty spiracles homolog 2 (Drosophila))
- RIKEN cDNA 2700089I24 gene
- Ensembl predicted gene (62247_81256)
- gene model 675, (NCBI)

- Ensembl predicted gene (58280_73864)
- expressed sequence W91643
- expressed sequence AW558126
- Rab11fip2 (RAB11 family interacting protein 2 (class I))
- RIKEN cDNA 4930470F04 gene
- LOC433259 similar to colony stimulating factor 3 receptor
- expressed sequence C81543
- hypothetical LOC433260 discontinued
- RIKEN cDNA E330013P04 gene
- D19Ert737e (DNA segment, Chr 19, ERATO Doi 737, expressed)
- RIKEN cDNA 4933412A08 gene
- Pseudogene (43623_61406)

60-60.6 Mb

- Prlhr (prolactin releasing hormone receptor)
- RIKEN cDNA 2700078E11 gene
- RIKEN cDNA 9830127L17 gene
- RIKEN cDNA D130033C15 gene
- Eif3s10 (eukaryotic translation initiation factor 3, subunit 10 (theta))
- Nanos1 (nanos homolog 1 (Drosophila))
- Ensembl predicted gene (65167_83233)
- RIKEN cDNA 1810055E12 gene
- Sfxn4 (sideroflexin 4)
- Prdx3 (peroxiredoxin 3)
- LOC545297 similar to G protein-coupled receptor kinase 5 (G protein-coupled receptor kinase GRK5 discontinued
- Q61875_mouse
- RIKEN cDNA 6030458E02 gene
- Ensembl predicted gene (64803_82869)